



Universiteit
Leiden
The Netherlands

Components and targets of the PINOID signaling complex in *Arabidopsis thaliana*

Zago, Marcelo Kemel

Citation

Zago, M. K. (2006, June 15). *Components and targets of the PINOID signaling complex in Arabidopsis thaliana*. Retrieved from <https://hdl.handle.net/1887/4436>

Version: Corrected Publisher's Version

License: [Licence agreement concerning inclusion of doctoral thesis in the Institutional Repository of the University of Leiden](#)

Downloaded from: <https://hdl.handle.net/1887/4436>

Note: To cite this publication please use the final published version (if applicable).

Components and targets of the PINOID signaling complex in *Arabidopsis thaliana*

Marcelo Kemel Zago

Cover: *Arabidopsis thaliana* protoplasts overexpressing GFP-tagged
PID, PBP2 and PBP2IPs.

Printed by: Optima Grafische Communicatie, Rotterdam, The Netherlands

ISBN: 90-8559-188-0

Components and targets of the PINOID signaling complex in *Arabidopsis thaliana*

Proefschrift

ter verkrijging van
de graad van Doctor aan de Universiteit Leiden,
op gezag van de Rector Magnificus Dr. D. D. Breimer,
hoogleraar in de faculteit der Wiskunde en
Natuurwetenschappen en die der Geneeskunde,
volgens besluit van het College voor Promoties
te verdedigen op donderdag 15 juni 2006
klokke 15.15 uur

door

Marcelo Kemel Zago

geboren te Porto Alegre (Brazilië) in 1976

Promotiecommissie

Promotor:	Prof. dr. P. J. J. Hooykaas
Co-promotor:	dr. R. Offringa
Referent:	dr. J. Friml (University of Tübingen, Germany)
Overige leden:	Prof. dr. M. H. M. Noteborn Prof. dr. H. P. Spaink

This work was financially supported by CAPES (Brazilian Federal Agency for Post-Graduate Education)

À minha esposa Sheila, meus pais e meus irmãos

CONTENTS	Page
Chapter 1	Auxin distribution and signaling act to shape the plant 9
Chapter 2	The multi-functional scaffold PINOID Binding Protein 2 interacts with both cytoskeletal proteins and transcriptional regulators 29
Chapter 3	A BTB/POZ domain protein-kinesin complex is likely to provide polarity to PINOID kinase signaling 59
Chapter 4	PINOID phosphorylates the PIN cytoplasmic loop at multiple conserved serine residues 81
Chapter 5	PINOID is a potential COP9 signalosome-associated kinase that modulates auxin response 101
Summary	123
Samenvatting	131
<i>Curriculum vitae</i>	137
Publications	139
Acknowledgements	141

Chapter 1

Auxin distribution and signaling act to shape the plant

Marcelo Kemel Zago and Remko Offringa

INTRODUCTION

The phytohormone auxin, or indole-3-acetic acid (IAA), is a central regulator of plant development that controls elementary processes such as cell division and -elongation and also directs complex developmental and patterning processes such as embryogenesis, vascular differentiation, phyllotaxis and fruit development (1, 2). More than a century ago, Darwin's observations on the bending of canary grass coleoptiles to unidirectional light led him to conclude that some matter in the upper part of the coleoptile is acted on by light, and then transmits its effects to the lower part of this tissue (3). Around 1930 this matter was identified as indole-3-acetic acid (IAA) and named after the greek word for "to grow" (auxein) (4, 5). More detailed observations by Went and Cholodny on the auxin-mediated orientation of plant growth to unidirectional light (phototropism) or gravity (gravitropism) led to the Cholodny and Went hypothesis (4, 6, 7). This model states that tropic growth is the result of predominant distribution of auxin to the dark or lower side upon light or gravity stimulation, respectively, and that due to differences in sensitivity to auxin, shoot growth is enhanced, whereas root growth is inhibited by the elevated auxin concentrations, ultimately leading to bending of the shoot or the root. In support of this hypothesis, more recent experiments demonstrated asymmetric expression of auxin responsive genes in light and gravity-induced shoots (8-10) and roots (11-13). The early tropic growth experiments clearly demonstrate that auxin action is a result of the interplay between the local auxin concentration – which is determined by biosynthesis, transport, and inactivation - and the sensitivity or responsiveness of cells to this plant hormone.

Below we will review what is known on auxin-mediated plant development with an emphasis on auxin signaling and -transport and the role of the PINOID protein kinase in these processes. The biosynthesis of auxin and its inactivation through catabolism and conjugation, although important, are beyond the scope of this thesis, and for these subjects we refer to recent reviews (14).

Abbreviations: 1-NAA, 1-naphthaleneacetic acid; 2,4-D, 2,4-dichlorophenoxyacetic acid; ABC/MDR/PGP, ATP binding cassette/multidrug resistance type/P-glycoprotein protein; AEC, auxin efflux carrier; AIC, auxin influx carrier; ARF, auxin response factor; ARF-GEF, ADP-ribosylation factor-GTP exchange factor; AuxRe, auxin responsive element; AXR, auxin resistant; BDL/IAA12, Bodenlos/IAA12 protein; BFA, Brefeldin A; COP, constitutive photomorphogenesis; CSN, COP9 Signalosome; IAA, indole-3-acetic acid; MP, ARF5/Monopteros; NPA, 1-N-naphthylphthalamic acid; NPH4, ARF7/Nonphototropic hypocotyl 4; PAT, polar auxin transport; PBK, PBP2 binding kinesin; PBP, pinoid binding protein; PID, pinoid; PM, plasma membrane; SCF, SKP1/Cullin/F-box

AUXIN SIGNALING

The term auxin signaling is often used to describe the role of proteins that are by default part of a signaling pathway - such as protein kinases - and are known to regulate auxin-action. In this chapter we will use signaling in the strictest meaning of the word, aiming at canonical signaling pathways that perceive the hormone signal, and based on its concentration – the net result of biosynthesis, transport and inactivation – induce primary cellular responses.

Several processes are known to occur within a few minutes after auxin application. These vary from changes in enzymatic activities (15-17) and gene expression (18-20) to changes in transporter activities, leading to increase of the membrane potential (21), rapid increase of the cytosolic calcium levels (22) and acidification of the cell wall (23). For most of these primary responses the signaling pathways are yet unknown, but in the last few years the signaling processes leading to auxin responsive gene expression have been elucidated.

Auxin responsive gene expression: a balance between activators and repressors

Differential screens of cDNA libraries in the 1980s led to the identification of the first auxin responsive genes (24-27). Most of these genes were activated within minutes after auxin stimulation in a process independent of *de novo* synthesis of proteins. Several auxin responsive elements (AuxREs) have been identified in the promoters of these primary auxin response genes (28-30), and Auxin Response Factors (ARFs) were shown to bind to these elements and to activate or to repress transcription (31).

ARFs in general contain four well defined domains: a DNA binding domain (DBD) that binds AuxREs, a middle region domain and domains III and IV (31). Whether an ARF is an activator or repressor depends on the structure of its middle region domain. For example, ARFs with Q-rich middle regions activate transcription, while ARFs with P/S/T-rich middle region repress transcription (31). Domains III and IV were found to mediate homo- or heterodimerization (28).

Some of the primary auxin response genes were found to encode small short-lived proteins, named Aux/IAA proteins, that resemble bacterial repressors (20, 32). Aux/IAA proteins contain four distinct domains, of which domain I has been shown to have transcription repression activity (33), domain II is involved in destabilization of Aux/IAA proteins, and may be target for ubiquitination (34), and domains III and IV have protein-protein interaction properties, allowing Aux/IAA proteins to homodimerize or to heterodimerize with ARFs or other Aux/IAA proteins (35).

Apart from being identified in screens for auxin responsive genes, the Aux/IAA encoding genes have also been identified through gain-of-function mutations that

lead to auxin insensitivity. Aux/IAA proteins are generally short lived, and all gain-of-function mutations in the *Aux/IAA* genes led to specific amino acid changes in domain II that stabilize the encoded protein, and thus lead to phenotypes that relate to auxin insensitivity (36).

Surprisingly, *aux/iaa* loss-of-function mutants provide very little information compared to gain-of-function ones. In fact, all of these knock-out mutant plant lines analyzed to present display very subtle phenotypes, indicating that there is functional redundancy between Aux/IAAs. By contrast, loss-of-function mutations have been informative for three ARFs: ARF3/ETTIN, ARF5/MONOPTEROS (MP) and ARF7/NONPHOTOTROPIC HYPOCOTYL 4 (NPH4). ARF3/ETTIN was characterized for playing a role in floral organ development since the *arf3/ettin* mutant displays abnormal apical-basal gynoecium development (37). Mutations in the gene *ARF5/MP* interfere with the formation of vascular strands at all stages and also with the initiation of the body axis in the early embryo (38). The mutant *arf7/nph4* shows non-phototropic response, resistance to the auxin transport inhibitor 1-*N*-naphthylphthalamic acid (NPA), impaired hypocotyls gravitropism, altered apical hook maintenance, and epinastic or hyponastic leaves. In general terms, *arf7/nph4* is impaired in differential growth responses in aerial tissues (36, 39).

The Arabidopsis genome encodes 29 AUX/IAA proteins and 23 ARFs, which can combine to translate the auxin signal into a gene expression response. For example, it has been shown in yeast two-hybrid assays that specific combinations of ARFs and Aux/IAAs are preferred interaction partners (40, 41). Expression and functional specificity has been demonstrated for several ARFs and Aux/IAAs, further demonstrating that specific interactions between such proteins should occur (42, 43). The specificity in these interactions seems essential to differentiate auxin responses in different cell types.

Auxin perception leads to enhanced degradation of the Aux/IAA repressors

The identification of Aux/IAAs as primary response proteins (20) and the observation that they are unstable, especially, undergoing rapid degradation upon auxin stimulation (44), placed the proteolysis machinery as key player in auxin signaling. More specifically, the proteolysis components are an E1 ubiquitin-activating enzyme, which transfers the ubiquitin component to an E2 ubiquitin conjugating protein. The E2-ubiquitin complex then binds to an E3 ubiquitin ligase complex, which mediates transfer of ubiquitin to the target protein. Ubiquitination is generally thought to label these target proteins for degradation by the 26S proteasome (Figure 1A), but strangely enough, auxin-induced ubiquitination of Aux/IAA proteins has not yet been demonstrated. The E3 ligase complex that

participates in auxin signaling is the SCF (SKP1/Cullin/F-box) complex comprising ASK1 (the Arabidopsis SKP1-like protein), CUL1 (Cullin 1) the F-Box protein TIR1 (Transport Inhibitor Response 1), and the E2-interacting RING domain protein RBX1 (Figure 1A) (45). Interestingly, three of the components of the SCF^{TIR1} complex have been identified through Arabidopsis mutants with a defective auxin response (46-49). Aux/IAA proteins were shown to interact with the F-box protein TIR1 (44), and the recent finding that auxin-binding to TIR1 enhances this interaction with and thus leads to enhanced degradation of Aux/IAAs, uncovered TIR1 as the long sought auxin receptor (Figure 1A) (50, 51).

Several regulatory components of SCF E3 ligases have been identified. For example, it has been found that the CUL1 subunit of the SCF complex is modified by the addition of the ubiquitin-like protein RUB1/NEDD8 in a process mediated by the regulatory protein RCE1 which binds to RBX1 (49, 52). Prior to that process, RUB1/NEDD8 is activated by the subcomplex AXR1-ECR1, which catalyzes the transfer of RUB1 to RCE1 (Figure 1A) (53). Knock-out mutations in most of these regulatory components lead to auxin resistant phenotypes, and the double mutant *axr1/rce1* causes embryonic defects similar to *mp*, leading to the hypothesis that RUB modification positively regulates SCF activity (53-56). The RUB-conjugated state of the SCF complex is regulated by the COP9 Signalosome (CSN), a protein complex that shares reasonable similarity to the lid of the 26S proteasome (57). CSN action has been demonstrated to be necessary for both auxin response and RUB1 removal from CUL1 (58), which probably destabilizes the SCF complex after its function so that new complexes can be formed (Figure 1) (59, 60). The CSN is also known to interact with other types of E3 ligases, such as the photomorphogenesis related COP1, and to be required for the nuclear import of this RING finger protein (61-63). COP1 and the CSN have been shown to promote degradation of HY5 (64, 65), a transcription factor that positively regulates photomorphogenesis, and loss-of-function mutations in *COP1* or in the single CSN-subunit encoding genes causes a constitutive photomorphogenesis (*cop*) phenotype (66). Finally, the protein CAND1 has been demonstrated to specifically bind the CUL1/RBX1 core complex and to dissociate from it upon RUB modification of CUL1, allowing the F-Box/ASK1 substrate receptor to interact. It is therefore hypothesized that CAND1 regulates SCF complex assembly by making the interaction of CUL1 with F-Box/ASK1 dependent on RUB modification (Figure 1B) (67). The role for CAND1 in auxin signaling is apparent, since *cand1* loss-of-function mutants display clear auxin resistant features (67).

An integrative role of protein kinases in auxin signaling

With the molecular basis of auxin signaling - from the perception of this hormone to the induction of auxin responsive gene expression - largely uncovered, it is

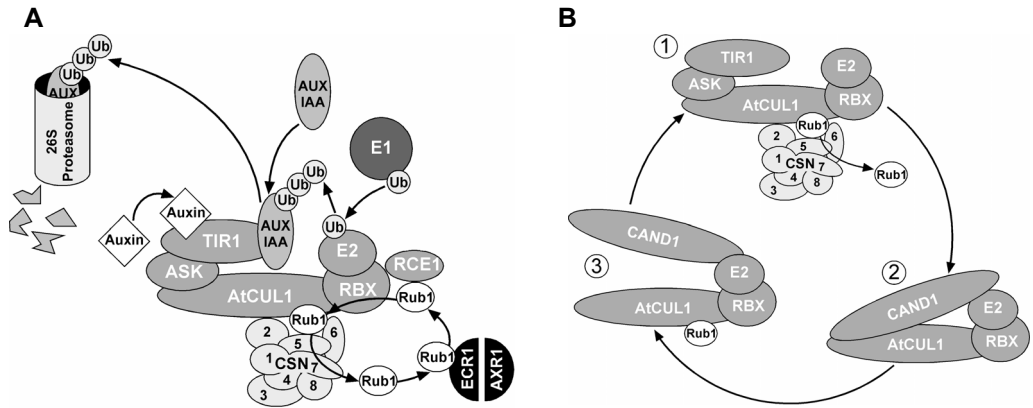


Figure 1. The SCF^{TIR1} E3 ubiquitin ligase is the core of the protein degradation machinery that regulates auxin responses in *Arabidopsis thaliana*. (A) Target proteins are labeled for proteolysis by ubiquitination. This process is mediated by the ubiquitin activating enzyme E1, the ubiquitin conjugating enzyme E2 and the ubiquitin ligase E3. E1 transfers the ubiquitin component to E2, that in turn binds to and acts in concert with E3 to ubiquitinate the substrate protein. Once targets are ubiquitinated, they are degraded by the 26S proteasome. SCF^{TIR1}, the E3 ligase complex that participates in auxin signaling, consists of CULLIN1 (CUL1), the Arabidopsis SKP1 homolog ASK1, and the F-box protein TIR1. Auxin-binding to TIR1 enhances its interaction with the AUX/IAAs which leads to enhanced degradation of these proteins. Regulatory subunits of SCF^{TIR1} include RCE1, which modifies CUL1 by adding RUB1 that is previously activated by the AXR1-ECR1 subcomplex. The COP9 signalosome (CSN) removes RUB1 from CUL1, leading to subsequent dissociation of the SCF^{TIR1} complex. (B) CAND1 and CSN are modulators of the cyclic assembly and dissociation of the SCF complex. The active SCF complex recruits CSN, which cleaves RUB1 from CUL1 (1). This enables CAND1 to bind CUL1 and eventually strip away ASK1 and the F-Box protein TIR1, thereby sequestering CUL1 in an inactive state (2). RUB1 modification of CUL1 weakens the affinity of CAND1 for the CUL1-complex (3), and an incoming ASK1-F-Box heterodimer is able to displace CAND1 to yield an active SCF complex (1) (Cope *et al.*, 2003).

intriguing to note that there is limited evidence for the involvement of canonical signaling pathways, comprising a membrane bound receptor and a protein kinase cascade. Phosphorylation events have occasionally been reported to be involved in auxin signaling. Aux/IAA proteins have been shown to be phosphorylated by phytochromes *in vitro*, suggesting that light signaling acts on auxin responsive gene expression by influencing the stability of Aux/IAA proteins (68). Also the Mitogen Activated Protein Kinase (MAPK) cascade has been implied in the modulation of auxin response. Roots of *Arabidopsis* seedlings treated with auxin showed an increase in MAPK activity and this activation was inhibited in the auxin resistant *axr4* mutant (69). It has also been shown that the MAPKKK NPK1 that activates stress responses, represses auxin induced gene expression (70). For now we conclude that phosphorylation events are important modulators of the auxin

response pathway, that serve to integrate other signals, such as light or stress, with auxin signaling (71).

AUXIN TRANSPORT

The initial observations by Darwin on tropisms (3) and subsequent more detailed experiments by plant biologists such as Went (7) not only led to the identification of auxin, but also revealed that this hormone is transported to sites of action. Based on transport measurements using radio-labeled auxin, two types of auxin transport are distinguished: a fast and non-directional one occurring through the phloem, and a slow and directional cell-to-cell transport that is referred to as polar auxin transport (PAT). The transport through the phloem was first detected by Morris and Thomas (72) and occurs in both basi- and acropetal directions at approximately 5-20cm/h (73). Experiments performed by Baker (74) indeed revealed significant presence of IAA in the phloem. A connection between the fast transport of auxin and PAT was demonstrated in experiments performed in pea, in which radio-labeled IAA initially present in the phloem was detected later in the polar transport system (75).

In contrast to the phloem-mediated auxin transport, PAT is restricted to free IAA, is unidirectional and occurs in a cell-to-cell manner only. The velocity is much slower, and has been estimated to occur at approximately 5-20mm/h. PAT is initiated in the young growing organs at the plant shoot apex and runs via the plant base down to the root tip (76). At the root tip, PAT is redirected upwards, proceeding basipetally through the root epidermis towards the root elongation zone (77). In the shoot, PAT is believed to also occur laterally for shoot elongation and to inhibit lateral bud outgrowth (72).

Polar auxin transport: the chemiosmotic model

Initial evidence that PAT requires energy, is saturable and sensitive to protein synthesis inhibitors led to the formulation in the 1970s of the chemiosmotic hypothesis for the mechanism behind PAT (78, 79). It was postulated that, due to the acidic extracellular pH of approximately 5.5, part of the IAA molecules in the apoplast is protonated (IAAH) and can easily pass through the plasma membrane by diffusion; once in the more basic cytoplasmic environment (pH close to 7.0), IAAH becomes de-protonated, assuming an anionic form (IAA⁻) that becomes trapped inside the cell. Due to this ion trap, the IAA⁻ anion can only exit the cell via the activity of auxin efflux carriers (AECs), whose asymmetric subcellular distribution determines the direction of PAT. An addition to this model was elaborated in which the presence of auxin influx carriers (AICs) was considered (80). The presence of AICs was later demonstrated to be viable based on experiments showing that the auxin influx capacity of cells is saturable (81, 82). Interestingly,

mathematical modeling of PAT predicts that polar transport can only lead to the observed local auxin accumulation when AICs and AECs act in concert (83).

In *Arabidopsis*, the AUX1/LAX amino-acid permease-like proteins have been identified as candidates for the AICs (84). The *aux1* mutants show a reduced response of the root to gravity, a reduced number of lateral roots and altered IAA distribution in young leaf and root tissues (85). The *aux1* root phenotypes can be rescued by germinating mutant seedlings on the lipophilic and highly diffusible auxin 1-naphthaleneacetic acid (1-NAA), but not with the impermeable auxin analog 2,4-dichlorophenoxyacetic acid (2,4-D), nor with the natural auxin IAA (86). It has also been demonstrated that AUX1 facilitates IAA loading into the vascular transport system (85). Interestingly, *aux1* phenotypes can be mimicked by application of the auxin influx inhibitors 1-naphthoxyacetic acid (1-NOA) and 3-chloro-4-hydroxyphenylacetic acid (CHPAA). Again, rescue is possible by 1-NAA but not by 2,4-D (87). Finally, AUX1 shows an asymmetrical subcellular localization (88, 89), which is in line with the chemiosmotic model for PAT and further supports the role of AUX1 as AIC.

Direction in polar auxin transport through the auxin efflux carriers (AECs)

The most important components for PAT, according to the chemiosmotic model, that provide both the driving force and the direction, are the AECs. To date two families of putative AECs have been identified: the PIN proteins and the ATP binding cassette (ABC), multidrug resistance (MDR)-type, P-glycoprotein (PGP) proteins (90-92).

The *Arabidopsis* PIN family is best characterized and includes the proteins PIN1 to PIN8. The main characteristic of the PIN proteins is the presence of several highly conserved transmembrane domains that, with the exception of PIN5 and PIN8, flank a less conserved central large cytoplasmic loop (93, 94). As predicted for the AECs, PINs mostly localize polarly in the plasma membrane (PM) of the cells in positions that are perfectly correlated with the actual directionality of the efflux of auxin (89, 91, 95, 96). The placement of PINs in cells differs per PIN protein and tissue of expression, and in this chapter the words apical and basal are used to indicate their localization at respectively the upper or lower cell membrane. As each PIN has a particular expression domain, loss-of-function mutations in their corresponding genes results in tissue-specific defects related to the directional transport of auxin (97).

PIN1, for example, is present in the apical pole of epidermal, and basal pole of provascular strand, cells of the shoot apex and in the basal pole of vascular and cortical root cells, therefore it is believed that this protein is essential for IAA transport in shoot and root tissues (89, 94, 98, 99). *pin1* mutants display pin-formed

inflorescences and reduced basipetal PAT in inflorescences (100), although no root defects were observed in such plants, probably implying functional redundancy in this organ.

PIN2 is present at the basal cell pole in cortical cells and in the apical pole in epidermal cells of the root and functions primarily in the redistribution of auxin involved in root gravitropism (93, 101, 102). Accordingly, *pin2* mutants show agravitropic root response as a result of the reduced basipetal PAT in this organ (93, 101, 102).

PIN3 is mainly present at the apical hook, around the hypocotyl vasculature, where it seems to be baso-laterally localized, and in the root pericycle and columella, where it is apolarly localized and appears to function in the lateral redistribution of auxin upon gravistimulation (8). *pin3* mutants are defective in tropic growth responses (8).

PIN4 is localized in the root meristem cells surrounding the quiescent center, where its subcellular localization is responsible for the establishment of an auxin sink below the quiescent center (QC) of the root apical meristem (103). *pin4* mutants are defective in establishment and maintenance of endogenous auxin gradients, fail to canalize externally applied auxin, and display slight patterning defects in both embryonic and seedling roots (103).

Finally, PIN7 localizes polarly in embryonic cells and plays a role in forming and maintaining apical–basal auxin gradients that are essential for the establishment of embryonic polarity. PIN7 also functions in root acropetal auxin transport (104). In *pin7* mutants, specification of the apical daughter cell of the zygote is compromised and occasionally *pin7* embryos fail to establish the pro-embryo (104).

Despite the specific roles of each PIN in auxin distribution throughout the plant, their functions have been shown to be overlapping. For example, PIN1 is localized at the basal cell pole in vascular root tip cells, but the *pin1* loss-of-function mutant does not show a clear root phenotype. In addition, the phenotypic defects of the *pin4* loss-of-function mutant are very weak, and loss of QC establishment is only found in triple and quadruple mutant background with *pin1*, *pin3* and *pin7* (98, 103, 104). It has been demonstrated that some PINs have their expression either enhanced and/or broadened to different cell files in the root tip in other *pin* loss-of-function backgrounds (105). This explains in part the observed functional redundancy among the different *PIN* genes (91, 98, 106).

Evidence that PINs really are AECs is accumulating. Initially, the activity of PIN2 was tested in a heterologous yeast system and this showed that yeast cells expressing this protein become more resistant to the toxic IAA-derivative 5-fluoro-IAA (12, 107). Only recently, a more extensive study in both plant, animal and yeast cells confirmed the direct involvement of PIN proteins in catalyzing cellular auxin efflux (108). This together with the strong correlation between their subcellular

localization and the direction of auxin transport (95, 96, 104) assigns to these proteins the status of AECs.

On the other hand, there is also substantial evidence that proteins of the MDR/PGP family of ABC transporters function as auxin transporters. Initially, loss-of-function mutants of two of these proteins, AtMDR1 and AtPGP1, which were originally identified as being functionally related to anion channels, have been characterized for their reduced auxin transport capabilities (109). The finding that AtMDR1 and AtPGP1 are able to bind NPA reinforces their role as auxin transporters (109, 110). The most striking evidence supporting the participation of such proteins in the transport of auxin, however, comes from experiments showing that AtPGP1, a protein localized apolarly in the cells of shoot and root apices, catalyzes auxin efflux from Arabidopsis protoplasts and in yeast and human cells (111). Interestingly, transport assays have indicated that the MDR/PGP family member PGP4 enhances auxin uptake of plant cells (112). The MDR/PGP proteins should therefore be classified as auxin transporters, rather than AECs.

Recently, it has been reported that PINs co-purify with MDR/PGP proteins (97). These data point to a scenario where the PIN and MDR/PGP proteins represent two PAT pathways, and that the PIN and MDR proteins interact in cells and tissues where both pathways overlap to mediate and direct PAT (97).

PIN polarity is maintained through GNOM ARF GEF-controlled vesicle trafficking

The polarity of PINs is determining the direction of polar auxin transport (95), and the polar localization of PIN1 appears to depend on the cytoskeleton. Treatment with the microtubule depolymerizing agent oryzalin suggested the presence of a microtubule-dependent cytokinesis pathway that localizes PIN1 at the cell plate of dividing cells (99). In interphase cells, however, asymmetric localization of PIN1 at the PM is reduced in response to treatment with actin depolymerizing drugs. Interestingly, this treatment impairs PAT, corroborating the importance of F-actin and polar localization of PIN1 for this process (113). Actin depolymerization also prevents the internalization of PIN1 to endosomal compartments upon treatment with the vesicle trafficking inhibitor Brefeldin A (BFA), and the restoration of PIN1 localization after BFA wash-out, indicating that F-actin provides tracks for vesicle movement between the endosomal compartments and the PM (99). In support of these data, it has been shown that the ADP-Ribosylation Factor-GTP Exchange Factor (ARF-GEF) GNOM is the BFA sensitive component that is required for recycling of PIN1 to the PM (114, 115). It remains to be established, however, whether GNOM is the polarity determinant in the recycling of PIN vesicles.

Based on the current data, two different functions for the PIN cycling could be hypothesized: i) to maintain PIN polarity and thus keep the directionality of auxin

efflux, as blocking of the cycling seems to suppress this characteristic; ii) to allow rapid changes in cell polarity, as the cycling of auxin efflux complexes would provide important flexibility for rapid changes in polarity of PM localization and thereby for the redirection of auxin efflux.

Recently, Paciorek and co-workers (116) demonstrated that auxin itself is an important component in the regulation of PIN cycling, since this hormone appears to inhibit PIN endocytosis. By performing this task, auxin increases PIN levels at the PM, thereby stimulating its own efflux by a vesicle-trafficking dependent mechanism.

PIN polarity is controlled by protein kinase activity

How is the directionality of PAT regulated or, in other words, what determines the asymmetric sub-cellular localization of PIN proteins? A key component in PIN polar targeting was identified through the *pinoid* loss-of-function mutant, that phenocopies the pin-like inflorescences of the *pin formed/pin1* mutant (117). Cloning of the *PINOID* gene revealed that it encodes a plant specific protein kinase (118), overexpression of which results in phenotypes such as agravitropic growth and collapse of the main root meristem. The root meristem collapse could be rescued by PAT inhibitors, suggesting that the PINOID (PID) protein kinase is a regulator of PAT (119). Recently, it was shown that the apico-basal subcellular polarity of PIN proteins is determined by threshold levels of PID. PID overexpression in the root tip, an organ where PID is not expressed, causes basally localized PINs (PIN1, 2 and 4) to be re-localized apically. Conversely, reduced PID activity in the epidermis of the inflorescence apex, an organ where PID activity is normally high, causes apically localized PIN1 to be re-localized to the basal PM (120). These data imply that regular levels of cellular PID are required in order to maintain proper PIN and PAT polarity.

Interestingly, a mutant has been identified in a gene encoding the regulatory A subunit of a trimeric protein phosphatase 2A, that displays root curling in response to NPA (*rcn1*) (121). The *rcn1* mutant displays increased root basipetal auxin transport, reduced gravitropic response and a delay in the establishment of differential auxin-induced gene expression across a gravity-stimulated root tip, aspects that were restored to normal upon NPA treatment (13). Although a direct link between RCN1 and PID has not been established yet, it is tempting to speculate that 2A-type protein phosphatases are involved in directing PAT, by counteracting the activity of the PID protein kinase.

Recently, Dai and co-workers (122) provided a first indication that PAT is also regulated by a MAPK cascade. Overexpression of the MAPKK BUD1/MKK7 resulted in defective auxin response and transport, while MKK7 repression caused enhanced PAT, indicating that this protein is a negative regulator of PAT (122).

Unraveling the PINOID signaling pathway

The demonstration that overexpression of the wild type PID kinase (35S::PID), but not of the negative kinase mutant MPID, leads to severe phenotypes that are the result of defective PIN localization, corroborate that PID-mediated phosphorylation is an important factor in the regulation of PAT (119, 120).

In an effort to unravel the phosphorylation targets of PID, and consequently the link between PID, PINs and PAT, several PID interactors were identified. Two of them, PINOID Binding Protein 1 (PBP1) and TOUCH3 (TCH3), are calmodulins which *in vitro* seem to up- or downregulate PID activity in the presence of Ca^{2+} , respectively. This result is corroborated by assays in which 35S::PID seedlings treated with calcium influx and calmodulin inhibitors were found to have enhanced PID activity, and by the fact that neither PBP1 nor TCH3 seem to be PID phosphorylation targets (123).

A third interactor of PID is the PINOID Binding Protein 2 (PBP2). PBP2 contains two protein-protein interaction domains, the BTB/POZ- ('Bric-a-brac, Tramtrack and Broad Complex/Pox virus and Zinc finger) and the TAZ (Transcriptional Adaptor putative Zinc Finger) domain. PBP2 has previously been identified as a calmodulin binding transcriptional regulator AtBT1 (124). Moreover, BTB domain proteins have been implicated in proteolysis processes, as several of them were shown to interact with CULLIN3 (CUL3) and to recruit target proteins for degradation. Although PBP2 was not found to interact with CUL3 in the yeast two-hybrid system (124, 125), *in vitro* pull down with CUL3 has been reported (126). Our observations suggest, however, that PBP2 acts as a regulator of PID activity. PBP2 has a repressive effect on PID auto-phosphorylation activity *in vitro* (127). Moreover, the fact that the GFP-PBP2 fusion protein shows a cytoskeleton-like localization in onion cells (127), suggests that PBP2 provides a possible link between the established roles of PID and the cytoskeleton in regulating PAT.

The fourth identified PID binding protein is COP9/CSN8, one of the subunits of the COP9 Signalosome (CSN) (127). Considering the role of COP9 in proteolysis, the finding that PID interacts with the CSN suggests that PID plays a role in the protein degradation machinery, possibly by regulating the activity of CSN itself. Recent work by Abas and co-workers (128) indicated that PIN2 levels and localization are modulated by proteasome-dependent degradation. This finding also suggests that an hypothetical association of PID with proteolysis could influence the regulation of some PINs.

Although the PID interactors are very interesting proteins that unravel unexpected facets of PID action, none of them is a substrate for PID-mediated phosphorylation (127). The identification of substrates of the PID kinase will be a crucial step in unraveling the signaling pathways that lead to the asymmetry in PIN localization and thus determine the direction of auxin flow.

Thesis outline

The role of PID in the regulation of PAT has now been elucidated (120), but the signaling components downstream of this kinase are still elusive. The effort to unravel such PID-signaling related proteins began with the identification of several PID interactors, namely PBP1, PBP2, TCH3 and COP9 (127). Although the interaction of PID with PBP2 and COP9 revealed unexpected aspects of the functionality of this kinase, their role as part the PID-signaling complex remained unclear. The research described in this thesis therefore focused on uncovering the function of PBP2 and COP9, and on the identification of PID phosphor-targets through an 'estimated-guess' approach.

The PID partner PBP2 was characterized for being a putative protein complex organizer, an observation that opened great possibilities for putative complexes eventually formed between PID, PBP2 and PBP2 binding proteins. Consequently, the research described in this thesis starts with a detailed characterization of the interaction between PID and PBP2 and the identification of PBP2 interactors (Chapter 2). The data indicate that PBP2 is a scaffold protein with multiple functions, one of which is to be recruited to the PID signaling complex to regulate PIN polar targeting.

Chapter 3 addresses in more detail the interaction between PBP2 and two paralogous microtubule motor proteins PBP2 Binding Kinesin 1 and 2 (PBK1 and 2, respectively), and their possible relationship with PID. The analyses provide evidence that PBK1 and 2 may be involved in the PBP2-mediated repression of PID, possibly by transporting PBP2 to specific sub-cellular locations.

In the view of the clear relationship between PID and PINs, we performed *in vitro* phosphorylation assays involving PID and the large cytoplasmic loops of several PIN proteins, to test whether these cytosolic domains can be phosphorylated by PID (Chapter 4). The results suggest that PID regulates the trafficking and subcellular localization of PIN proteins by direct modification of these auxin transporters at conserved serine residues in their large cytoplasmic domains.

Finally, Chapter 5 describes the interaction between PID and components of auxin signaling such as subunits of the CSN and the AUX/IAA protein BDL/IAA12. The analyses show that, although PID interacts with one subunit of the CSN, the COP9/CSN8, it phosphorylates a second CSN subunit, the COP15/CSN7. Further observations that PID phosphorylates BDL/IAA12 *in vitro* and that both proteins functionally interact *in vivo* open the possibility that PID controls auxin signaling by affecting proteolysis processes.

REFERENCE LIST

1. Davies, P. J. (1995) in *Plant Hormones: Physiology, Biochemistry and Molecular Biology*, ed. Davies, P. J. (Kluwer, Boston), pp. 13-38.
2. Leyser, O. (2005) *Cell* **121**, 819-822.
3. Darwin, C. & Darwin, F. (1881) *The Power of Movement in Plants* (London).
4. Went, F. W. (1926) *Proc K Akad Wet Amsterdam* **30**, 10-19.
5. Kogl, F. & Haagen-Smit, A. (1931) *Proc. Sect. Sci.* **34**, 1411-1416.
6. Cholodny, N. (1927) *Biol Zent* **47**, 604-626.
7. Went F. & Thimann, K. (1937) *Phytohormones* (MacMillan, New York).
8. Friml, J., Wisniewska, J., Benkova, E., Mendgen, K. & Palme, K. (2002) *Nature* **415**, 806-809.
9. Li, Y., Hagen, G. & Guilfoyle, T. J. (1991) *Plant Cell* **3**, 1167-1175.
10. Esmon, C. A., Tinsley, A. G., Ljung, K., Sandberg, G., Hearne, L. B. & Liscum, E. (2006) *Proc Natl. Acad. Sci. U S A* **103**, 236-241.
11. Larkin, P. J., Gibson, J. M., Mathesius, U., Weinman, J. J., Gartner, E., Hall, E., Tanner, G. J., Rolfe, B. G. & Djordjevic, M. A. (1996) *Transgenic Res.* **5**, 325-335.
12. Luschnig, C., Gaxiola, R. A., Grisafi, P. & Fink, G. R. (1998) *Genes Dev.* **12**, 2175-2187.
13. Rashotte, A. M., DeLong, A. & Muday, G. K. (2001) *Plant Cell* **13**, 1683-1697.
14. Woodward, A. W. & Bartel, B. (2005) *Ann. Bot. (Lond)* **95**, 707-735.
15. Morre, D. J., Morre, D. M. & Ternes, P. (2003) *In Vitro Cell Dev. Biol Plant* **39**, 368-376.
16. Droog, F., Hooykaas, P. & van der Zaal, B. J. (1995) *Plant Physiol* **107**, 1139-1146.
17. Bilang, J. & Sturm, A. (1995) *Plant Physiol* **109**, 253-260.
18. Theologis, A. (1986) *Ann. Rev. Plant Physiol.* **37**, 407-438.
19. Guilfoyle, T. (1986) *CRC Crit Rev Plant Sci* **4**, 247-276.
20. Abel, S. & Theologis, A. (1996) *Plant Physiol* **111**, 9-17.
21. Karcz, W. & Burdach, Z. (2002) *J Exp. Bot* **53**, 1089-1098.
22. Gehring, C. A., Irving, H. R. & Parish, R. W. (1990) *Proc Natl. Acad. Sci. U S A* **87**, 9645-9649.
23. Grebe, M. (2005) *Science* **310**, 60-61.
24. Theologis, A., Huynh, T. V. & Davis, R. W. (1985) *J Mol. Biol* **183**, 53-68.

25. Hagen, G. & Guilfoyle, T. J. (1985) *Mol. Cell Biol* **5**, 1197-1203.
26. Key, J. L., Kroner, P., Walker, J., Hong, J. C., Ulrich, T. H., Ainley, W. M., Gantt, J. S. & Nagao, R. T. (1986) *Philos. Trans. R. Soc. Lond B Biol Sci.* **314**, 427-440.
27. van der Zaal E., Memelink, J., Mennes, A., Quint, A. & Libbenga, K. (1987) *Plant Mol Biol.* **10**, 145-157.
28. Ulmasov, T., Murfett, J., Hagen, G. & Guilfoyle, T. J. (1997) *Plant Cell* **9**, 1963-1971.
29. Guilfoyle, T., Hagen, G., Ulmasov, T. & Murfett, J. (1998) *Plant Physiol* **118**, 341-347.
30. Guilfoyle, T. J., Ulmasov, T. & Hagen, G. (1998) *Cell Mol. Life Sci.* **54**, 619-627.
31. Ulmasov, T., Hagen, G. & Guilfoyle, T. J. (1999) *Proc. Natl. Acad. Sci. U S A* **96**, 5844-5849.
32. Abel, S., Oeller, P. W. & Theologis, A. (1994) *Proc Natl. Acad. Sci. U S A* **91**, 326-330.
33. Tiwari, S. B., Hagen, G. & Guilfoyle, T. J. (2004) *Plant Cell* **16**, 533-543.
34. Ramos, J. A., Zenser, N., Leyser, O. & Callis, J. (2001) *Plant Cell* **13**, 2349-2360.
35. Ulmasov, T., Hagen, G. & Guilfoyle, T. J. (1999) *Plant J.* **19**, 309-319.
36. Liscum, E. & Reed, J. W. (2002) *Plant Mol. Biol.* **49**, 387-400.
37. Sessions, A., Nemhauser, J. L., McColl, A., Roe, J. L., Feldmann, K. A. & Zambryski, P. C. (1997) *Development* **124**, 4481-4491.
38. Hardtke, C. S. & Berleth, T. (1998) *EMBO J.* **17**, 1405-1411.
39. Liscum, E. & Briggs, W. R. (1995) *Plant Cell* **7**, 473-485.
40. Kim, J., Harter, K. & Theologis, A. (1997) *Proc. Natl. Acad. Sci. U S A* **94**, 11786-11791.
41. Hardtke, C. S., Kukurshumova, W., Vidaurre, D. P., Singh, S. A., Stamatiou, G., Tiwari, S. B., Hagen, G., Guilfoyle, T. J. & Berleth, T. (2004) *Development* **131**, 1089-1100.
42. Weijers, D. & Jurgens, G. (2004) *Curr. Opin. Plant Biol.* **7**, 687-693.
43. Weijers, D., Benkova, E., Jager, K. E., Schlereth, A., Hamann, T., Kientz, M., Wilmoth, J. C., Reed, J. W. & Jurgens, G. (2005) *EMBO J.* **24**, 1874-1885.
44. Gray, W. M., Kepinski, S., Rouse, D., Leyser, O. & Estelle, M. (2001) *Nature* **414**, 271-276.
45. Schwechheimer, C. & Deng, X. W. (2001) *Trends Cell Biol.* **11**, 420-426.
46. Hellmann, H., Hobbie, L., Chapman, A., Dharmasiri, S., Dharmasiri, N., del Pozo, C., Reinhardt, D. & Estelle, M. (2003) *EMBO J.* **22**, 3314-3325.
47. Gray, W. M., del Pozo, J. C., Walker, L., Hobbie, L., Risseuw, E., Banks, T., Crosby, W. L., Yang, M., Ma, H. & Estelle, M. (1999) *Genes Dev.* **13**, 1678-1691.

48. Ruegger, M., Dewey, E., Gray, W. M., Hobbie, L., Turner, J. & Estelle, M. (1998) *Genes Dev.* **12**, 198-207.
49. Gray, W. M., Hellmann, H., Dharmasiri, S. & Estelle, M. (2002) *Plant Cell* **14**, 2137-2144.
50. Kepinski, S. & Leyser, O. (2005) *Nature* **435**, 446-451.
51. Dharmasiri, N., Dharmasiri, S. & Estelle, M. (2005) *Nature* **435**, 441-445.
52. del Pozo, J. C. & Estelle, M. (1999) *Proc Natl. Acad. Sci. U S. A* **96**, 15342-15347.
53. Dharmasiri, S., Dharmasiri, N., Hellmann, H. & Estelle, M. (2003) *EMBO J* **22**, 1762-1770.
54. Lincoln, C., Britton, J. H. & Estelle, M. (1990) *Plant Cell* **2**, 1071-1080.
55. Bostick, M., Lochhead, S. R., Honda, A., Palmer, S. & Callis, J. (2004) *Plant Cell* **16**, 2418-2432.
56. Larsen, P. B. & Cancel, J. D. (2004) *Plant J* **38**, 626-638.
57. Fu, H., Reis, N., Lee, Y., Glickman, M. H. & Vierstra, R. D. (2001) *EMBO J.* **20**, 7096-7107.
58. Schwechheimer, C., Serino, G., Callis, J., Crosby, W. L., Lyapina, S., Deshaies, R. J., Gray, W. M., Estelle, M. & Deng, X. W. (2001) *Science* **292**, 1379-1382.
59. Schwechheimer, C. (2004) *Biochim. Biophys. Acta* **1695**, 45-54.
60. Cope, G. A. & Deshaies, R. J. (2003) *Cell* **114**, 663-671.
61. Chamovitz, D. A., Wei, N., Osterlund, M. T., von Arnim, A. G., Staub, J. M., Matsui, M. & Deng, X. W. (1996) *Cell* **86**, 115-121.
62. von Arnim, A. G., Osterlund, M. T., Kwok, S. F. & Deng, X. W. (1997) *Plant Physiol* **114**, 779-788.
63. Seo, H. S., Yang, J. Y., Ishikawa, M., Bolle, C., Ballesteros, M. L. & Chua, N. H. (2003) *Nature* **423**, 995-999.
64. Osterlund, M. T., Wei, N. & Deng, X. W. (2000) *Plant Physiol* **124**, 1520-1524.
65. Osterlund, M. T., Hardtke, C. S., Wei, N. & Deng, X. W. (2000) *Nature* **405**, 462-466.
66. Schwechheimer, C. & Deng, X. W. (2000) *Semin. Cell Dev. Biol.* **11**, 495-503.
67. Cheng, Y., Dai, X. & Zhao, Y. (2004) *Plant Physiol* **135**, 1020-1026.
68. Colon-Carmona, A., Chen, D. L., Yeh, K. C. & Abel, S. (2000) *Plant Physiology* **Vol. 124**, 1728-1738.
69. Mockaitis, K. & Howell, S. H. (2000) *Plant J* **24**, 785-796.
70. Kovtun, Y., Chiu, W. L., Zeng, W. & Sheen, J. (1998) *Nature* **395**, 716-720.
71. DeLong, A., Mockaitis, K. & Christensen, S. (2002) *Plant Mol Biol* **49**, 285-303.

72. Morris, D. A. & Thomas (1978) *J. Exp. Bot.* **29**, 147-157.
73. Nowacki, J. & Bandurski, R. S. (1980) *Plant Physiol.* **65**, 422-427.
74. Baker, D. A. (2000) *Israel J. Plant Sci.* **48**, 199-203.
75. Cambridge, A. P. & Morris, D. A. (1996) *Planta* **199**, 583-588.
76. Lomax, T. L., Muday, G. K. & Rubery, P. H. (1995) in *Plant Hormones: Physiology, Biochemistry and Molecular Biology*, ed. Davies, P. J. (Kluwer, Boston), pp. 509-530.
77. Rashotte, A. M., Brady, S. R., Reed, R. C., Ante, S. J. & Muday, G. K. (2000) *Plant Physiol* **122**, 481-490.
78. Rubery, P. H. & Sheldrake, A. R. (1974) *Planta* **118**, 101-121.
79. Raven, J. (1975) *New Phytologist* **74**, 163-172.
80. Goldsmith, M. H. M. (1977) *Annu. Rev. Plant. Physiol.* **28**, 439-478.
81. Lomax, T. L., Mehlhorn, R. J. & Briggs, W. R. (1985) *Proc Natl. Acad. Sci. U S A* **82**, 6541-6545.
82. Benning, C. (1986) *Planta* **169**, 228-237.
83. Kramer, E. M. (2004) *Trends Plant Sci.* **9**, 578-582.
84. Parry, G., Marchant, A., May, S., Swarup, R., Swarup, K., James, N., Graham, N., Allen, T., Martucci, T., Yemm, A. *et al.* (2001) *J Plant Growth Regul* **20**, 217-225.
85. Marchant, A., Bhalerao, R., Casimiro, I., Eklof, J., Casero, P. J., Bennett, M. & Sandberg, G. (2002) *Plant Cell* **14**, 589-597.
86. Marchant, A., Kargul, J., May, S. T., Muller, P., Delbarre, A., Perrot-Rechenmann, C. & Bennett, M. J. (1999) *EMBO J* **18**, 2066-2073.
87. Parry, G., Delbarre, A., Marchant, A., Swarup, R., Napier, R., Perrot-Rechenmann, C. & Bennett, M. J. (2001) *Plant J* **25**, 399-406.
88. Swarup, R., Friml, J., Marchant, A., Ljung, K., Sandberg, G., Palme, K. & Bennett, M. (2001) *Genes Dev.* **15**, 2648-2653.
89. Reinhardt, D., Pesce, E. R., Stieger, P., Mandel, T., Baltensperger, K., Bennett, M., Traas, J., Friml, J. & Kuhlemeier, C. (2003) *Nature* **426**, 255-260.
90. Friml, J. & Palme, K. (2002) *Plant Mol. Biol.* **49**, 273-284.
91. Friml, J. (2003) *Curr. Opin. Plant Biol.* **6**, 7-12.
92. Geisler, M. & Murphy, A. S. (2006) *FEBS Lett.* **580**, 1094-1102.
93. Muller, A., Guan, C., Galweiler, L., Tanzler, P., Huijser, P., Marchant, A., Parry, G., Bennett, M., Wisman, E. & Palme, K. (1998) *EMBO J.* **17**, 6903-6911.

94. Galweiler, L., Guan, C., Muller, A., Wisman, E., Mendgen, K., Yephremov, A. & Palme, K. (1998) *Science* **282**, 2226-2230.
95. Wisniewska, J., Xu, J., Seifertova, D., Brewer, P. B., Ruzicka, K., Blilou, I., Roquie, D., Benkova, E., Scheres, B. & Friml, J. (2006) *Science*.
96. Benkova, E., Michniewicz, M., Sauer, M., Teichmann, T., Seifertova, D., Jurgens, G. & Friml, J. (2003) *Cell* **115**, 591-602.
97. Blakeslee, J. J., Peer, W. A. & Murphy, A. S. (2005) *Curr. Opin. Plant Biol.* **8**, 494-500.
98. Blilou, I., Xu, J., Wildwater, M., Willemsen, V., Paponov, I., Friml, J., Heidstra, R., Aida, M., Palme, K. & Scheres, B. (2005) *Nature* **433**, 39-44.
99. Geldner, N., Friml, J., Stierhof, Y. D., Jurgens, G. & Palme, K. (2001) *Nature* **413**, 425-428.
100. Okada, K., Ueda, J., Komaki, M. K., Bell, C. J. & Shimura, Y. (1991) *Plant Cell* **3**, 677-684.
101. Ottenschlager, I., Wolff, P., Wolverton, C., Bhalerao, R. P., Sandberg, G., Ishikawa, H., Evans, M. & Palme, K. (2003) *Pnas* vol. **100**, 2987-2991.
102. Shin, H., Shin, H. S., Guo, Z., Blancaflor, E. B., Masson, P. H. & Chen, R. (2005) *Plant J.* **42**, 188-200.
103. Friml, J., Benkova, E., Blilou, I., Wisniewska, J., Hamann, T., Ljung, K., Woody, S., Sandberg, G., Scheres, B., Jurgens, G. *et al.* (2002) *Cell* **108**, 661-673.
104. Friml, J., Vieten, A., Sauer, M., Weijers, D., Schwarz, H., Hamann, T., Offringa, R. & Jurgens, G. (2003) *Nature* **426**, 147-153.
105. Vieten, A., Vanneste, S., Wisniewska, J., Benkova, E., Benjamins, R., Beeckman, T., Luschnig, C. & Friml, J. (2005) *Development* **132**, 4521-4531.
106. Paponov, I. A., Teale, W. D., Trebar, M., Blilou, I. & Palme, K. (2005) *Trends Plant Sci.* **10**, 170-177.
107. Chen, R., Hilson, P., Sedbrook, J., Rosen, E., Caspar, T. & Masson, P. H. (1998) *Proc Natl. Acad. Sci. U S A* **95**, 15112-15117.
108. Petrasek, J., Mravec, J., Bouchard, R., Blakeslee, J. J., Abas, M., Seifertova, D., Wisniewska, J., Tadele, Z., Kubes, M., Covanova, M. *et al.* (2006) *Science*.
109. Noh, B., Murphy, A. S. & Spalding, E. P. (2001) *Plant Cell* **13**, 2441-2454.
110. Murphy, A. S., Hoogner, K. R., Peer, W. A. & Taiz, L. (2002) *Plant Physiol* **128**, 935-950.
111. Geisler, M., Blakeslee, J. J., Bouchard, R., Lee, O. R., Vincenzetti, V., Bandyopadhyay, A., Titapiwatanakun, B., Peer, W. A., Bailly, A., Richards, E. L. *et al.* (2005) *Plant J* **44**, 179-194.
112. Terasaka, K., Blakeslee, J. J., Titapiwatanakun, B., Peer, W. A., Bandyopadhyay, A., Makam, S. N., Lee, O. R., Richards, E. L., Murphy, A. S., Sato, F. *et al.* (2005) *Plant Cell* **17**, 2922-2939.
113. Butler, J. H., Hu, S., Brady, S. R., Dixon, M. W. & Muday, G. K. (1998) *Plant J* **13**, 291-301.

114. Steinmann, T., Geldner, N., Grebe, M., Mangold, S., Jackson, C. L., Paris, S., Galweiler, L., Palme, K. & Jurgens, G. (1999) *Science* **286**, 316-318.
115. Geldner, N., Anders, N., Wolters, H., Keicher, J., Kornberger, W., Muller, P., Delbarre, A., Ueda, T., Nakano, A. & Jurgens, G. (2003) *Cell* **112**, 219-230.
116. Paciorek, T., Zazimalova, E., Ruthardt, N., Petrasek, J., Stierhof, Y. D., Kleine-Vehn, J., Morris, D. A., Emans, N., Jurgens, G., Geldner, N. *et al.* (2005) *Nature* **435**, 1251-1256.
117. Bennett, S., Alvarez, J., Bossinger, G. & Smyth, D. (1995) *Plant J.* **8**, 505.
118. Christensen, S. K., Dagenais, N., Chory, J. & Weigel, D. (2000) *Cell* **100**, 469-478.
119. Benjamins, R., Quint, A., Weijers, D., Hooykaas, P. & Offringa, R. (2001) *Development* **128**, 4057-4067.
120. Friml, J., Yang, X., Michniewicz, M., Weijers, D., Quint, A., Tietz, O., Benjamins, R., Ouwerkerk, P. B., Ljung, K., Sandberg, G. *et al.* (2004) *Science* **306**, 862-865.
121. Garbers, C., DeLong, A., Deruere, J., Bernasconi, P. & Soll, D. (1996) *EMBO J* **15**, 2115-2124.
122. Dai, Y., Wang, H., Li, B., Huang, J., Liu, X., Zhou, Y., Mou, Z. & Li, J. (2006) *Plant Cell* **18**, 308-320.
123. Benjamins, R., Ampudia, C. S., Hooykaas, P. J. & Offringa, R. (2003) *Plant Physiol* **132**, 1623-1630.
124. Du, L. & Poovaiah, B. W. (2004) *Plant Mol. Biol.* **54**, 549-569.
125. Dieterle, M., Thomann, A., Renou, J. P., Parmentier, Y., Cognat, V., Lemonnier, G., Muller, R., Shen, W. H., Kretsch, T. & Genschik, P. (2005) *Plant J.* **41**, 386-399.
126. Figueroa, P., Gusmaroli, G., Serino, G., Habashi, J., Ma, L., Shen, Y., Feng, S., Bostick, M., Callis, J., Hellmann, H. *et al.* (2005) *Plant Cell*.
127. Benjamins, R. Functional analysis of the PINOID protein kinase in *Arabidopsis thaliana*. 2004. Leiden University.
128. Abas, L., Benjamins, R., Malenica, N., Paciorek, T., Wirniewska, J., Moulinier-Anzola, J. C., Sieberer, T., Friml, J. & Luschnig, C. (2006) *Nat. Cell Biol.* **8**, 249-256.

Chapter 2

The multi-functional scaffold PINOID Binding Protein 2 interacts with both cytoskeletal proteins and transcriptional regulators

Marcelo Kemel Zago, Douwe Doevendans, Remko Offringa

SUMMARY

The Arabidopsis PINOID (PID) protein serine/threonine kinase is a key regulator of plant growth that modulates the polar transport of the phytohormone auxin by controlling the polar subcellular localization of PIN auxin efflux facilitators. This chapter focuses on PID Binding Protein 2 (PBP2), a likely scaffold protein that - based on its possible localization at the cytoskeleton in onion cells - was considered as a promising link between PID and PIN vesicle trafficking. The presumed scaffold function of PBP2 was apparent, since the protein consists of two domains that are known to mediate protein-protein interactions: an amino-terminal Bric-a-brac, Tramtrack and Broad Complex/Pox virus and Zinc finger (BTB/POZ) domain, and a carboxy-terminal Transcriptional Adaptor putative Zinc Finger (TAZ) domain. In contrast to previous results, *in vitro* phosphorylation assays showed that PBP2 is not a phosphorylation target of PID, but that instead PID activity is repressed by PBP2. *In vitro* pull down assays suggested that PID interacts with the BTB/POZ domain, and transient expression of both proteins fused to GFP in Arabidopsis protoplasts suggested that this interaction occurs in the cytoplasm. The likely scaffold function of PBP2 indicated that other PBP2 interacting proteins (PBP2IPs) play a role in the PID signaling pathway. In an yeast two-hybrid screen sixteen putative PBP2IPs were identified that classified as cytoskeletal proteins, transcription factor-like proteins or proteins with an enzymatic function in primary metabolism. Three PBP2IPs, the putative microtubule-associated PBP2 BINDING MYOSIN-LIKE PROTEIN (PBMP), the transcription factor-like PBP2 BINDING MYB PROTEIN (PBMYP), and an uncharacterized AUXIN-INDUCIBLE PBP2 BINDING PROTEIN (APBP), were analyzed in more detail. *In vitro* pull down assays showed that PBMP and PBMYP interact with the C-terminal TAZ domain containing portion of PBP2, whereas APBP interacts with the N-terminal part of PBP2. *In vitro* phosphorylation assays did not show any evidence that these PBP2 partners are phosphorylated by PID, implying that PBP2 is not a scaffold for PID substrates. Further analysis did not provide evidence that PBMYP and PBMP are part of the PID signaling complex. In contrast, for APBP we concluded that it may be involved in modulating flowering time, and that it possibly competes with PID for the interaction with PBP2, and as a consequence activates the kinase by relieving it from PBP2-mediated repression. Overall, our data indicate that PBP2 is a scaffold protein with multiple functions, one of which is to be recruited to the PID signaling complex to regulate PIN polar targeting.

Abbreviations: APBP, auxin-inducible PBP2 binding protein; BTB/POZ, bric-a-brac, tramtrack and broad complex/Pox virus and zinc finger domain; CC, coiled-coil domain; F-actin, actin filament; GFP, green-fluorescent protein; GST, glutathione-S-transferase; IAA, indole-3-acetic acid; MBP, myelin basic protein; MPSS, massively parallel signature sequencing; NPA, 1-N-naphthylphthalamic acid; PAT, polar auxin transport; PBK, PBP2 binding kinesin; PBMP, PBP2 binding myosin-like protein; PBMYB, PBP2 binding MYB domain protein; PBP, pinoid binding protein; PBP2IP, PBP2 interacting protein; PID, pinoid; PM, plasma membrane; RRM, RNA recognition motif; SCF, SKP1/Cullin/F-box; TAZ, transcriptional adaptor putative zinc finger domain

INTRODUCTION

The plant hormone auxin plays a central role in plant growth and development. A distinctive feature of this compound concerns its transport in a polar fashion from sites of biosynthesis to sites of action. The unraveling of the molecular mechanism behind this polar transport started with the molecular characterization of the *Arabidopsis pin-formed 1 (pin1)* mutant, that is defective in polar auxin transport (PAT), and was named after its pin-shaped inflorescences that lack flowers and bracts (1, 2). The *PIN1* gene appeared to encode a transmembrane protein that – due to its polar subcellular localization and its apparent role in PAT – was considered to be a likely candidate for the auxin efflux carrier in the chemiosmotic model for PAT proposed in the 1970s. The *Arabidopsis* genome encodes eight PIN proteins, for several of which the polar subcellular localization was correlated with the direction of auxin efflux (3-5). The polar localization of PIN proteins was shown to be maintained by recycling of PIN-containing vesicles from endosomal compartments to the plasma membrane (PM) along the actin cytoskeleton (6).

Another *Arabidopsis* mutant that develops pin-shaped inflorescences is *pinoid (pid)* (7). Cloning of *PINOID* identified a gene encoding a plant-specific protein kinase (8), whose ectopic expression causes phenotypic changes that can be partly rescued by application of PAT inhibitors. This and other observations led to the hypothesis that PID is a positive regulator of PAT (9).

Despite their shared involvement in PAT and the phenotypic similarities between the corresponding loss-of-function mutants, the true relationship between PID and PIN1 remained elusive until recently, when it was shown that the polar subcellular targeting of PIN proteins is determined by threshold levels of PID (10). The strong phenotypes observed in either loss- or gain-of-function PID lines imply that PID-mediated phosphorylation is an important step in the control of PIN polar targeting and, as a consequence, in the directionality of the auxin flow in patterning processes.

Although there is clear regulation of PIN protein localization by PID activity, the molecular mechanism behind it is far from being understood. In order to uncover the link between these two proteins, a yeast two-hybrid screen was performed using

PID as bait, and one of the interactors identified was PINOID BINDING PROTEIN 2 (PBP2) (11). The function of this protein is still unknown, but its primary amino acid sequence shows the presence of two conserved protein-protein interaction domains. One is a Transcriptional Adaptor putative Zinc Finger (TAZ) domain (12), and the other is a 'Bric-a-brac, Tramtrack and Broad Complex/Pox virus and Zinc finger (BTB/POZ) domain that is known to mediate both homo- and heterodimerization (13, 14). The Arabidopsis genome encodes at least seventy-six BTB domain proteins that can be classified in eleven major families according to their domain architecture (15). BTB proteins seem to be involved in a broad range of processes, such as phototropic growth (16, 17), systemic acquired resistance (18) and targeted proteolysis (19, 20).

Proteins containing both a BTB/POZ domain and a TAZ domain are only found in plants and the Arabidopsis genome encodes four homologs of PBP2 corresponding to gene models At3g48360, At1g05690, At4g37610 and At5g67480. PBP2 and its homologous proteins share 60% or more of similarity at the amino acid level (Robert, unpublished data) (11).

Preliminary experimental data suggested that PBP2 had a role as regulator of PID activity when complexed with this protein kinase. Weak phosphorylation of PBP2 was observed in *in vitro* phosphorylation assays with PID, and the presence of PBP2 strongly inhibited PID auto-phosphorylation (11). Moreover, bombardment of onion cells with a 35S::GFP-PBP2 construct suggested that the corresponding fusion protein is associated with the cortical cytoskeleton (11). Similar experiments with tobacco cell suspension cultures showed, however, that PBP2-GFP is localized in the nucleus (21). Assuming that both observations are correct, PBP2 could have a dual role acting both in the nucleus and at the cortical cytoskeleton in the cytoplasm. Histochemical staining of Arabidopsis seedlings transgenic for a *PID-GUS* fusion construct indicate that PINOID localizes in the cytoplasm of vascular cells (9), suggesting that this is the sub-cellular region where the interaction between PBP2 and PID takes place.

In order to further elucidate the role of PBP2 in the PID signaling, we first repeated the *in vitro* phosphorylation assays. These experiments confirmed that PBP2 downregulates PID kinase activity. However, in contrast to previous assays, the results indicated that PBP2 is not a phosphorylation target of PID. Since PBP2 has two protein interaction domains, its function could be to bring PID in proximity of its phosphorylation targets. To test this hypothesis, we performed a yeast two-hybrid screen using PBP2 as bait. This identified several interacting proteins that classified as cytoskeletal proteins, transcription factor-like proteins or proteins with an enzymatic function in primary metabolism. *In vitro* protein pull-down experiments showed that the N-terminal BTB domain containing portion of PBP2 interacts with PID and one of its interactors, APBP, whereas the C-terminal TAZ domain

comprising part interacts with transcription factors or cytoskeletal proteins. None of the newly identified PBP2 binding proteins were phosphorylation targets of PID, implying that PBP2 does not function as scaffold for PID-mediated protein modification. The interaction of PBP2 with both cytoskeleton-associated and nuclear proteins suggests a functional multiplicity, which will be discussed in light of the known role of PID in directing PIN polar targeting.

MATERIALS AND METHODS

Molecular cloning and constructs

Molecular cloning was performed following standard procedures (22). The yeast two-hybrid bait plasmid pAS2-PBP2 was obtained by cloning a *PBP2* *Pst*I/*Sal*I-blunted fragment derived from pSDM6014 into pAS2 digested with *Pst*I/*Xma*I-blunted. The histidine tagged PID construct was created by excising the *PID* cDNA with *Xmn*I-*Sal*I from pSDM6005 (11) and cloning it into pET16H (pET16B derivative, J. Memelink, unpublished results) digested with *Bam*HI, blunted and subsequently digested with *Xho*I. The 35S::PID-GFP construct was generated by amplifying the *PID* cDNA using the primers 5'-TTAATATGACTCACTATAGG-3' and 5'-GCTCACCATAAAGTAATCGAACGC-3' and the *eGFP* coding region using the primers 5'-GATTACTTTATGGTGAGCAAGGGC-3' and 5'-TCAATCTGAGTACTTGTA CAG-3'. Both PCR products were used together with outer primers in a new PCR reaction to generate the *PID-GFP* fragment, which was cloned into pUC28 digested with *Nco*I/*Hinc*II. The resulting pUC28-PID-GFP was digested with *Eco*RI/*Stu*I-blunted and the *PID-GFP* fragment was ligated into *Eco*RI/*Sma*I digested pART7. Construction of histidine- and GFP-tagged PBP2 vectors are described by Benjamins (11). The GST-tagged PBP2 fusion (plasmid pGEX-PBP2) was generated by digesting pSDM6014 (11) with *Xho*I/*Sma*I and cloning the *PBP2* cDNA into pGEX-KG (23). The plasmid for production of a GST-tagged PBP2 BTB/POZ domain was created by digesting pGEX-PBP2 with *Nde*I, filling in with Klenow and re-ligating. This created a stop codon at position 220 aa of the protein. The plasmid encoding the GST-tagged PBP2 TAZ domain was created by deleting the *Nco*I fragment encoding the BTB/POZ domain from pGEX-PBP2. The *PBMP* cDNA was amplified by PCR using the primers 5'-ACGCTTGTCGACTATATGTATGAGCAGCAGCAACAT-3' and 5'-CGGGATCCAAACAACCCAAGGA GAGAAATATC-3', and the resulting PCR fragment was digested with *Bam*HI/*Sal*I and cloned into the corresponding sites in pBluescriptSK+. His-PBMP and GFP-PBMP were obtained by cloning *PBMP* *Bam*HI/*Sal*I and *PBMP* *Sal*I/*Not*I fragments into the plasmids pET16B (Novagen) and pTH2^{BN} (derived from pTH2 plasmid described by Chiu and co-workers (24)) digested with *Xho*I/*Bam*HI and *Xho*I/*Not*I, respectively. The *PBMYB* cDNA was amplified by PCR using the primers 5'-CCGCTCGAGTTGTGTCCGCCGTATATGA-3' and 5'-CGGGATCCTTGTTCCAAACTTAATCTTCA GG-3', and subsequently ligated into the pGEM-T cloning vector (Promega). The *PBMYB* fragment was excised from the resulting plasmid with *Xho*I and *Not*I and cloned into pTH2^{BN} using the corresponding enzymes, giving rise to *GFP-PBMYB*. His-PBMYB-CT was generated by ligating the *PBMYB-CT* *Nde*I/*Xho*I fragment derived from the original pACT2-*PBMYBCT* yeast two-hybrid clone into pET16B digested with the corresponding restriction enzymes. Finally, the His-APBP and GFP-APBP fusion proteins were obtained by cloning the *APBP* *Nde*I/*Xho*I and *APBP* *Bgl*II fragments (derived from the pACT2-APBP yeast two-hybrid clone) into the corresponding restriction sites of the vectors pET16B and pTH2^{BN}, respectively.

Yeast two hybrid screen

Using the Matchmaker II yeast two-hybrid system and *Saccharomyces cerevisiae* strain PJ69-4A (Clontech), an *Arabidopsis thaliana* cDNA library fused to the GAL4 activation domain (pACT2) was screened at 20°C with PBP2 fused to the GAL4 DNA binding domain (pAS2) as bait. The cDNA library

was constructed from RNA samples isolated from Arabidopsis root cultures in a one to one mix of untreated roots and roots treated for 24 hours with the auxin analog 1-naphthaleneacetic acid (1-NAA) (25). The positive clones were analyzed by colony hybridization as described in the Hybond-N+ Membrane Manual (Amersham Biosciences) and in the work of Memelink and co-workers (26).

***In vitro* pull down experiments**

GST tagged full-length PBP2, its deletion versions (GST-BTB/POZ and GST-TAZ) or GST protein alone were used in pull down assays with histidine (his)-tagged PBP2 interactors (H-interactors). Cultures of *E. coli* strain BL21 containing one of the constructs were grown at 37°C to OD₆₀₀ 0,8 in 50 ml LC supplemented with antibiotics. The cultures were then induced for 4 hours with 1 mM IPTG at 30°C, after which cells were harvested by centrifugation (10 min. at 4.000 RPM in tabletop centrifuge) and frozen overnight at -20°C. Precipitated cells were re-suspended in 2 ml Extraction Buffer (EB: 1x PBS, 2 mM EDTA, 2 mM DTT, supplemented with 0,1 mM of the protease inhibitors PMSF - Phenylmethanesulfonyl Fluoride, Leupeptin and Aprotinin, all obtained from Sigma) for the GST-tagged proteins or in 2 ml Binding Buffer (BB: 50 mM Tris-HCl pH 6,8, 100 mM NaCl, 10 mM CaCl₂, supplemented with PMSF 0,1 mM, Leupeptin 0,1 mM and Aprotinin 0,1 mM) for the his-tagged PBP2 interactors and sonicated for 2 min. on ice. From this point on, all steps were performed at 4°C. Eppendorf tubes containing the sonicated cells were centrifugated at full speed (14.000 RPM) for 20 min., and the supernatants were transferred to fresh 2 ml tubes. H-interactors supernatants were left on ice, while 100 µl pre-equilibrated Glutathione Sepharose resin (pre-equilibration performed with three washes of 10 resin volumes of 1x PBS followed by three washes of 10 resin volumes of 1x BB at 500 RCF for 5 min.) was added to the GST- fusion protein containing supernatants. Resin-containing mixtures were incubated with gentle agitation for 1 hour, subsequently centrifugated at 500 RCF for 3 min. and the precipitated resin was washed 3 times with 20 resin volumes of EB. Next, all H-interactors supernatants (approximately 2 ml per interactor) were added to GST-fusions-containing resins, and the mixtures were incubated with gentle agitation for 1 hour. After incubation, supernatants containing GST resins were centrifugated at 500 RCF for 3 min., the new supernatants were discarded and the resins subsequently washed 3 times with 20 resin volumes of EB. Protein loading buffer was added to the resin samples, followed by denaturation by 5 min. incubation at 95°C. Proteins were subsequently separated on a 12% polyacrylamide gel prior to transfer to an Immobilon™-P PVDF (Sigma) membrane. Western blots were hybridized using a horse radish peroxidase (HRP)-conjugated anti-pentahistidine antibody (Quiagen) and detection followed the protocol described for the Phototope-HRP Western Blot Detection Kit (New England Biolabs).

***In vitro* phosphorylation assays**

All proteins used in *in vitro* phosphorylation assays were his-tagged for purification from several (usually five) aliquots of 50 ml cultures of *E. coli* strain BL21 which were grown, induced, pelleted and frozen as described above for the *in vitro* pull down experiments. Each aliquot of frozen cells pellet was resuspended in 2 ml Lysis Buffer (25 mM Tris-HCl pH 8,0; 500 mM NaCl; 20 mM Imidazol; 0,1% Tween-20; supplemented with 0,1 mM of the protease inhibitors PMSF, Leupeptin and Aprotinin) and subsequently sonicated for 2 min. on ice. From this point on, all steps were performed at 4°C. Sonicated cells were centrifugated at full speed (14.000 RPM) for 20 min, the new pellets were discarded, and supernatants from all aliquots of the same construct were transferred to a 15 ml tube containing 100 µl of pre-equilibrated Ni-NTA resin (pre-equilibration performed with three washes of 10 resin volumes of Lysis Buffer at 500 RCF for 5 min.). Supernatant and resin were incubated with gentle agitation for 1 hour. After incubation, supernatant containing Ni-NTA resin was centrifuged at 500 RCF for 3 min., the new supernatant was discarded and the resin subsequently washed: 3 times with 20 resin volumes of Lysis Buffer, once with 20 resin volumes of Wash Buffer 1 (25 mM Tris.Cl pH 8,0; 500 mM NaCl; 40 mM Imidazol; 0,05% Tween-20) and once with 20 resin volumes of Wash Buffer 2 (25 mM Tris-HCl pH 8,0; 600 mM NaCl; 80 mM Imidazol). In between the washes, the resin was centrifugated for 5 min. at 500 RCF. After the washing steps, 20 resin volumes of Elution Buffer (25 mM Tris.HCl pH 8,0; 500 mM NaCl; 500 mM Imidazol) was added to the resin and incubated for 15 min. with gentle agitation. The resin was

centrifugated for 3 min. at 500 RCF, and the supernatant containing the desired protein was diluted a 1000-fold in Tris Buffer (25 mM Tris.HCl pH7,5; 1 mM DTT) and concentrated to a workable volume (usually 50 µl) using Vivaspin microconcentrators (10 kDa cut off, maximum capacity 600 µl, manufacturer: Vivascience). Glycerol was added as preservative to a final concentration of 10% and samples were stored at -80°C.

Approximately 1 µg of each purified his-tag protein (PID and substrates) in maximal volumes of 10 µl were added to 20 µl kinase reaction mix, containing 1x kinase buffer (25 mM Tris-HCl pH 7,5; 1 mM DTT; 5 mM MgCl₂) and 1 x ATP solution (100 µM MgCl₂/ATP; 1 µCi ³²P-γ-ATP). Reactions were incubated at 30°C for 30 min. and stopped by the addition of 5 µl of 5 x protein loading buffer (310 mM Tris-HCl pH 6,8; 10 % SDS; 50% Glycerol; 750 mM β-Mercaptoethanol; 0,125% Bromophenol Blue) and 5 min. boiling. Reactions were subsequently separated over 12,5% acrylamide gels, which were washed 3 times for 30 min. with kinase gel wash buffer (5% TCA – Trichloroacetic Acid; 1% Na₂H₂P₂O₇), coomassie stained, destained, dried and exposed to X-ray films for 24 to 48 hours at -80°C using intensifier screens.

Protoplast transformations

Protoplasts were obtained from *Arabidopsis thaliana* Col-0 cell suspension cultures that were propagated as described by Schirawski and co-workers (27). Protoplast isolation and PEG-mediated transformation followed the protocol described originally by Axelos and co-workers (28) and adapted by Schirawski and co-workers (27). The transformations were performed with 20 µg of plasmid DNA, after which the protoplasts were incubated for at least 16h. Images were obtained by laser scanning confocal microscopy.

Plant growth and lines

Seeds were germinated and seedlings grown *in vitro* on MA medium (29) supplemented with antibiotics or other compounds when required, at 21°C, 50% relative humidity and a 16 hours photoperiod of 2500 lux. Flowering Arabidopsis plants were grown on substrate soil, in growth rooms at 20°C, 40% relative humidity and a 16 hours photoperiod of 2500 lux.

The Arabidopsis mutant lines N620810 and FLAG_371C08 with T-DNA insertions in the *PBMP* and *APBP* genes, respectively, were obtained from the Salk Institute (N620810) and INRA (FLAG_371C08). For the PCR identification of the mutant alleles, we used the primers 5'-GAAATGATGCA AACATTTGGCG-3', 5'-TCTGGGTTTGGGGACGATAGC-3' and 5'-TGGTTCACGTAGTGGGCCATCG-3' for the *pbmp* allele N620810, and 5'-CATGCCCTTACACATTTCCACA-3', 5'-TGATGAGGCTCG TAGCTTCCG-3' and 5'-CGTGTGCCAGGTGCCACGGAATAGT-3' or 5'-CTACAAATTGCCTTTTCTT ATCGAC-3' for the *apbp* FLAG_371C08 allele.

RESULTS

PBP2 could be a regulator of PINOID activity

Previous *in vitro* phosphorylation experiments suggested that PBP2 is a phosphorylation target of PID and that PBP2 significantly inhibits PID auto-phosphorylation (11). New experiments using Myelin Basic Protein (MBP) as phospho-substrate confirmed the negative effect of PBP2 on both auto- and trans-phosphorylation activity of PID (Figures 1A and 1B). The previously observed weak labeling of PBP2 in the presence of PID (11) was only found occasionally (Figure 1B). Control reactions, in which PBP2 was incubated with radio-labeled ATP alone showed the same weak labeling of PBP2 (Figure 1B), indicating that PBP2 binds ATP at low-affinity. The results imply that PBP2 is not a target of PID phosphorylation, but instead functions as a regulator of PID activity.

PINOID binds the BTB/POZ domain containing part of PBP2 *in vitro*

BTB domain proteins are known as scaffold- or linker-proteins that organize protein complexes (30). PBP2 has two typical protein-protein interaction domains, and to test which of them binds to PID, GST-tagged full length PBP2, or the GST-tagged BTB/POZ or TAZ domain alone (Figure 1C) were incubated *in vitro* with histidine-tagged PID, and protein complexes were pulled down with glutathione beads. Western blot analysis using anti-His antibodies showed that PID efficiently binds the BTB/POZ domain containing part, whereas the TAZ domain containing part only pulls down background levels of the kinase (Figure 1D). In view of the established role of the BTB and TAZ domains in protein-protein interaction, this result suggests that PID interacts with the BTB/POZ domain, and that PBP2 indeed acts as a scaffold that – through its TAZ domain - recruits proteins that are phosphorylation targets of PID or that regulate PID activity.

PINOID and PBP2 co-localize in the cytoplasm of Arabidopsis protoplasts

In order to identify the subcellular compartments in which PID and PBP2 are localized, we transformed the plasmids *35S::PID-GFP* and *35S::GFP-PBP2* into Arabidopsis protoplasts. PID-GFP primarily localized at the plasma membrane, but in 50% of the protoplasts also cytoplasmic localization was observed (Figure 1E). GFP-PBP2 was nuclear localized in 80% of the protoplasts, whereas 20% of the protoplasts showed cytoplasmic localization (Figure 1E). The nuclear localization of PBP2 was reported previously (21), and corroborates the presence of a functional nuclear localization signal in the protein (Figure 1C). Based on these and previous results (10) it can be hypothesized that PID-mediated regulation of PIN polar targeting occurs through direct interaction between PINs and the PID protein kinase at the plasma membrane. PID, however, is also found in the cytoplasm, where PBP2 possibly down-regulates its activity through its interaction with the protein kinase. The predominant nuclear localization of PBP2 may relate to another function of PBP2 that is unrelated to PID. An interesting possibility is that PBP2 and PID alter each others subcellular localization when co-expressed in plant cells.

Identification of PBP2 interacting proteins suggests multiplicity in PBP2 function

In order to obtain more insight into the protein complexes that involve PBP2, a yeast two-hybrid screen was performed using PBP2 as bait. Yeast cells were co-transformed with the full-length cDNA of PBP2 fused to the GAL4 DNA binding domain (bait) and a cDNA library prepared from a 1:1 mixture of uninduced and NAA-induced root cultures fused to the GAL4 activation domain (prey library). Selection for three different markers resulted in 78 positive clones from an

estimated total of 1.4×10^6 transformants (Table 1), which corresponds to a near-complete screening of the original mRNA population (31). Following the subsequent selection steps, twenty-eight apparently distinct positive clones were obtained, which after sequence analysis appeared to represent sixteen

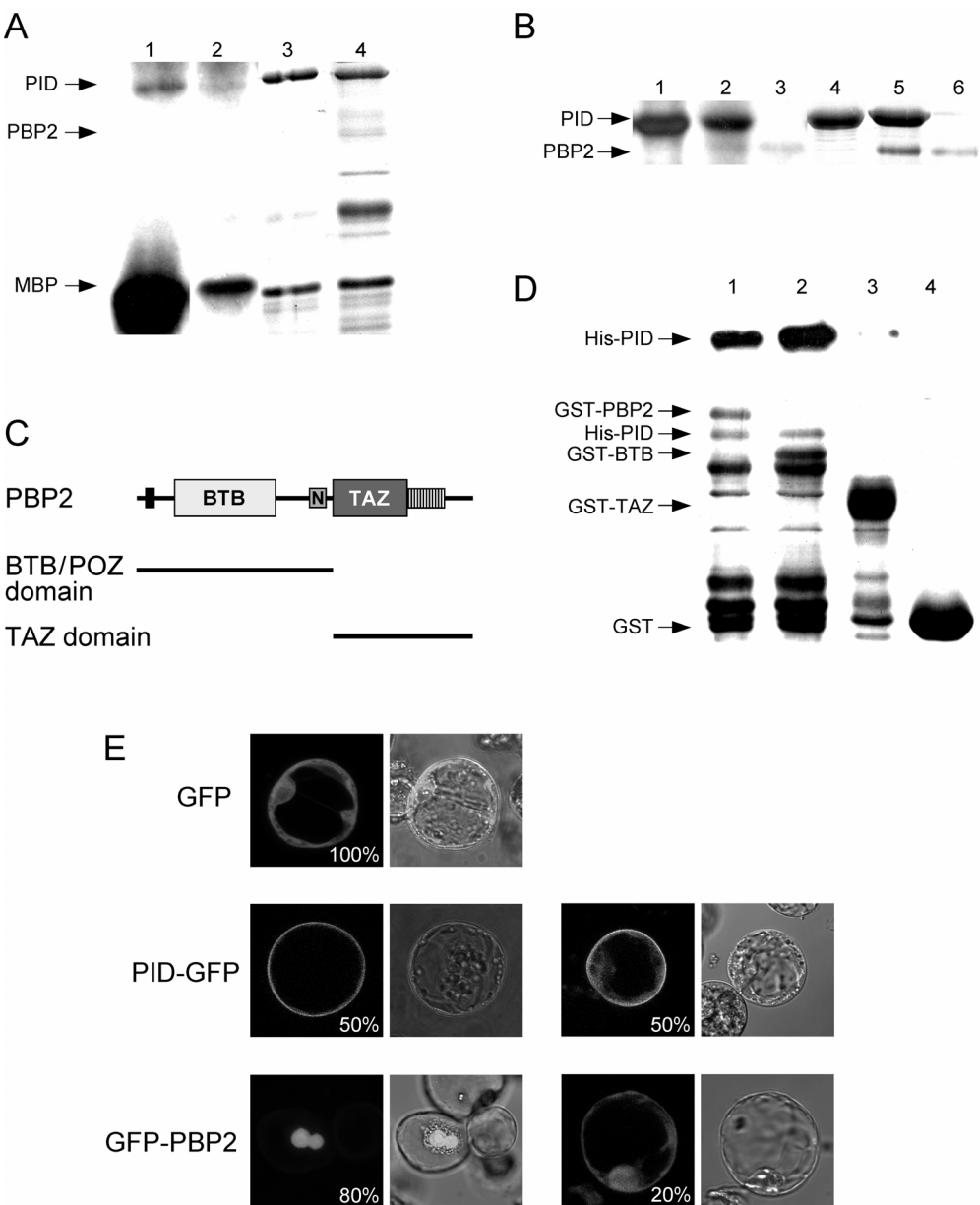


Figure 1. PID binding to the BTB domain portion of PBP2 negatively regulates PID kinase activity.

(A) Autoradiograph (1 and 2) and coomassie stained gel (3 and 4) of a phosphorylation assay containing PID and MBP (lanes 1 and 3); or PID, PBP2 and MBP (lanes 2 and 4). (B) Autoradiograph (1 to 3) and coomassie stained gel (4 to 6) of a phosphorylation assay containing PID (lanes 1 and 4), PID and PBP2 (lanes 2 and 5) or PBP2 alone (lanes 3 and 6). (C) Schematic representation of PBP2 (365 aa) and the two deletion derivatives containing either the BTB/POZ- or the TAZ domain. The N-box and the striped box indicate the positions of respectively an NLS and a putative calmodulin binding site (Du and Poovaiah, 2004). (D) *In vitro* pull-down of his-tagged PID with GST-tagged PBP2 (lane 1), GST-tagged BTB domain (lane 2) or -TAZ domain (lane 3) containing portions of PBP2 or GST alone (lane 4). Top: immunodetection of his-tagged PID. Bottom: coomassie stained gel with the positions of the different input proteins indicated. (E) Arabidopsis protoplasts transformed with 35S::GFP (top), 35S::PID-GFP (middle) or 35S::GFP-PBP2 (bottom). Per construct one or two couples of a fluorescence image (left) and a merged transmission light and fluorescence images (right) of a representative protoplast are shown.

unique cDNAs (Table 1). A BLAST sequence comparison with the NCBI database showed that, although the function of several of the PBP2 interactors is still unknown, most of the encoded proteins contain reasonably well-characterized domains, thereby allowing the assignment of hypothetical functions. Based on this analysis, PBP2 interactors can be roughly classified in three groups: i) proteins involved in gene expression regulation, ii) cytoskeletal proteins and iii) proteins with a specific enzymatic function in primary metabolism (Table 2). Curiously, the most frequent interactor of PBP2 that was represented by almost 50% of the His, Ade and α -Gal positive yeast colonies, as determined by the subsequent analysis steps, does not fall in any of these groups (Table 2) due to insufficient functional information.

Table 1. Yeast two-hybrid screen for PBP2 interactors.

Transformants	+His	+Ade	+His +Ade + α -GAL	Molecular analysis **	Colony hybridization	Sequencing - Final unique clones
1,4x10 ⁶	510*	196*	78*	48	28	16

* Colonies with positive phenotype concerning the respective selection marker

** Selection steps consisting of PCR followed by restriction analysis to eliminate redundant clones

Despite the finding of a considerable number of proteins that interact with PBP2, only few of them were chosen for further research. The choice was mainly based on the reliability of interaction with PBP2 and the likelihood that the protein participates in the PID signaling pathway. In particular, the PBP2 interactors of the class of enzymatic proteins were excluded for further analysis, since a direct link with the

elusive PID signaling pathway was unclear or unlikely. Concerning the remaining proteins, a functional relationship between PID, PBP2 and the PBP2-interactors can be explained by three hypotheses: i) PBP2 acts as a scaffold to recruit phosphorylation targets of PID; ii) the three proteins are part of a functional complex in which PID does not phosphorylate the PBP2-interactor; iii) PBP2 interacts with PID and the PBP2-interactor independently but as part of the same regulatory pathway. Below, these possibilities will be discussed for the selected PBP2-interactors in context of their possible functions.

PBP2 Interacts with Putative Cytoskeletal Proteins

Of the sixteen PBP2 interactors identified, five are likely components of the cellular cytoskeleton (Table 2). Since it has recently been demonstrated that PID activity directs the subcellular localization of PIN proteins (10) and the localization of PIN proteins is regulated and maintained by vesicle trafficking along the cytoskeleton, the cytoskeletal PBP2 interactors may be part of the PID signaling complex.

Two of the putative cytoskeletal proteins are homologous proteins that have a typical N-terminal microtubule motor domain and thus belong to the super-family of kinesins. The proteins were named PBP2 BINDING KINESIN 1 and 2 (PBK1 and 2, respectively) and their detailed functional analysis will be presented in Chapter 3.

The third putative cytoskeletal PBP2 interactor contains three Armadillo repeats (At3g22990). Comparison of these repeats with the Pfam database showed that they are found in proteins involved in vacuolar targeting of macromolecules via microtubuli.

The possible cytoskeletal function of the fourth PBP2 interactor is indicated by its internal CXC box (At5g25790). In *Drosophila*, the CXC box is present in kinesins associated with the spindle apparatus during meiosis and fertilization (32, 33). In *Arabidopsis*, CXC boxes are found in proteins such as TSO1 and CURLY LEAF, whose functions are related to cytokinesis and cell elongation, respectively (34-36). Although At3g22990 and At5g25790 seem to be clearly linked with the cytoskeleton, there are virtually no data concerning their true function, making an association with the actual molecular function of the PID kinase a difficult task. As a consequence, they were not studied in further detail.

PBP2 Binding Myosin-like Protein suggests association of PBP2 to the microtubule cytoskeleton

The fifth cytoskeleton-related PBP2 interactor, PBMP (for PBP2 Binding Myosin-like Protein), is a protein of unknown function that contains a long coiled-coil domain (Figure 2A). Long coiled-coil (CC) domains are present in proteins involved in a variety of functions, for example attachment of protein complexes to cellular structures such as the Golgi, the nuclear envelope or centrosomes. This domain is

Table 2. Proteins interacting with PBP2 in the Yeast Two-Hybrid System.

CLASS	GENE MODEL	ASSIGNED NAME	FEATURES	# CLONES*	PROTEIN (aa)	MIN. SIZE (aa)**	PBP2 PORTION ****
Cytoskeleton Related	At2g21300	PBP2 Binding Kinesin 2 (PBK2)	Kinesin motor domain	4	862	257	TAZ
	At4g38850	PBP2 Binding Kinesin 1 (PBK1)	Kinesin motor domain	2	836	286	n.d.
	At3g22990	-	Armadiillo-repeat	1	460	379	n.d.
	At5g25790	-	CXC box	1	408	161	n.d.
	At5g08120	PBP2 Binding Myosin-like Protein (PBMP)	Long coiled-coil domain	2	326	247	TAZ
Regulator of Gene Expression	At5g41020	PBP2 Binding MYB domains protein (PBMYB)	MYB DNA binding domains	2	588	164	TAZ
	At3g56510	-	Transcription co-factor like; RRM domain	2	266	266	n.d.
	At4g08150	KNAT1	KNAT1 transcription factor	1	398	386	n.d.
	At3g53920	-	SIGC transcription factor	1	571	179	n.d.
	At3g09850	-	G-patch, RRM and ATP-binding site	1	781	771	n.d.
	At2g43190	-	ribonuclease P family protein	1	296	226	n.d.
Enzymatic Proteins	At3g53120	-	glutamyl-tRNA reductase	3	217	217	n.d.
	At2g46200	Putative Chromatin-Remodeling PBP2 Binding Protein (CROP)	Zinc Metalloenzyme	2	382	338	BTB/POZ
	At3g03420	-	Zinc Metalloprotease domain	1	194	98	n.d.
	At3g23940	-	Dehydratase protein	1	608	254	n.d.
Auxin-Inducible	At2g39870	Auxin-Inducible PBP2 Binding Protein (APBP)	Auxin Inducible gene	30	330	330	BTB/POZ
Not further characterized***	-	-	-	23	-	-	-

*Number of times a gene was found among the 78 His, Ade and α -GAL positive clones (Table 1).

**Minimal number of carboxy-terminal amino acids encoded by the shortest positive cDNA clones.

***These 23 clones were not further characterized because they either autoactivated in yeast, encoded truncated or out-of-frame proteins or failed to promote yeast growth when back-transformed.

**** Portion of PBP2 with which the interactor binds, as determined by *in vitro* pull-down assays.

also found in proteins of the intermediate filaments, which together with actin and microtubules are involved in enhancing structural integrity, cell shape, and cell and organelle motility. Finally, CC domains are present in proteins related to nuclear and chromosomal organization, microtubule structure and organization and in proteins related to targeting to membrane systems (37). PBMP has previously been identified in a screen for Arabidopsis proteins related to cytoskeleton in *Schizosaccharomyces pombe* (38). In this screen, an Arabidopsis cDNA library was expressed in *S. pombe* cells, and transformed cells displaying cytoskeletal defects, such as the ones expressing PBMP, were isolated and characterized. This observation, combined with the fact that PBMP contains a long coiled-coil domain, led to its initial naming as myosin-related protein. That this initial naming may not be entirely correct was suggested by the fact that the tobacco ortholog MPB2C is associated with microtubules, and seems to function in the inter- or intra-cellular transport of macromolecules (39). The experimental data suggesting that PBMP has a function in cytoskeleton-related processes and the finding that it interacts with PBP2, a putative cytoskeletal protein that binds PID, leads us to speculate that PBMP could play a role in the PID signaling pathway that determines the polar targeting of PIN proteins.

To confirm the data from the yeast two-hybrid screen, *in vitro* protein pull-down experiments were performed using GST-tagged full length PBP2, or the GST-tagged BTB/POZ or TAZ domain containing portion alone, together with his-tagged PBMP. The results showed that PBMP preferentially binds the C-terminal TAZ domain containing part of PBP2 (Figure 2B). Interestingly, this observation and the fact that PID likely interacts with the BTB domain (Figure 1D) fit to the model that PBP2 acts as a scaffold protein.

Subsequently we tested the possibility that PBMP is a phosphorylation target of PID. *In vitro* phosphorylation experiments showed that PBMP is not phosphorylated by PID either in the presence or absence of PBP2 (Figure 2C). As observed before, PID kinase activity is inhibited in the presence of PBP2.

Even though PBMP is not a phosphorylation target of PID, it may still have a function in the PID signaling pathway. PBMP could affect the subcellular localization of PID, or be involved in altering cytoskeletal properties as part of the PID-PBP2-PBMP complex. Since a requirement for such function involves that PBMP is localized in the same subcellular compartments as PID and PBP2, we transformed a *35S::GFP-PBMP* construct to Arabidopsis protoplasts. GFP-PBMP was found to localize in the cytoplasm (Figure 2D). Considering that PID and PBP2 were also present in this compartment (Figure 1E), it is possible that the three proteins form a complex. Although PBMP is predicted to be microtubule-associated, its overexpression in Arabidopsis protoplasts may have prevented us to observe the

microtubule-specific pattern that has previously been reported for its tobacco ortholog (39).

If PBMP is crucial for proper functioning of PID, *pbmp* loss-of-function may lead to phenotypes related to those of the *pid* mutant. A mutant Arabidopsis line was obtained from the Salk Institute with a T-DNA insertion in the second intron of the gene (Figure 2A). Unfortunately, no striking mutant phenotypes were observed in *pbmp* seedlings, even when they were grown on 0,1 μ M IAA or 0,3 μ M NPA. After bolting, the young primary inflorescence of mutant plants was significantly shorter compared to wild type (Figure 2E). In fully matured plants, however, the inflorescence length did not significantly differ from wild type (figure 2E), suggesting that the shorter primary inflorescence is caused by a delay in bolting rather than by a defect in elongation growth. Experimental data from publicly available microarray and MPSS (Massively Parallel Signature Sequencing) datasets (40, 41) (Figures 2F and 2G, respectively) show that PBMP is constitutively expressed at moderate levels in most Arabidopsis tissues, including the inflorescence, therefore partly corroborating phenotypes observed in the *pbmp* insertion mutant plants. These same data indicate that PBP2 is also expressed in inflorescences, although at reduced levels, suggesting that both PBMP and PBP2 proteins are present in the same cells as PID.

The data presently shown suggest that PID, PBMP and PBP2 could form a complex, since the first two interact with different domains of PBP2, and the three proteins are expressed in the same tissues and co-occur in the same subcellular compartment. However, the lack of clear mutant phenotypes of *pbmp* mutant line prevents us to speculate on a function for such a complex. The fact that there is no significant PBMP homolog and thus no clear redundancy in gene function in Arabidopsis indicates that PBMP can not play an important role in PID action. The *in vivo* occurrence and the exact function of a complex involving PID, PBP2 and PBMP therefore remain to be investigated.

PBP2 Interacts with Regulators of Gene Expression

Six of the PBP2 interactors are putative or known transcriptional regulators or have domains related to RNA recognition and binding (Table 2). This finding, together with the observed nuclear localization of PBP2 (Figure 1E), implies a role for PBP2 in transcription regulation.

Two of the PBP2 interactors contain an RRM motif (At3g56510 and At3g09850; Table 2), which has been found in different types of RNA-related proteins, such as heterogeneous nuclear ribonucleoproteins, small nuclear ribonucleoproteins and pre-RNA and mRNA associated proteins (42). The protein corresponding to gene model At3g56510 is relatively similar to the mouse TATA-BINDING-BINDING PROTEIN (ABT1), which was found to be associated with mouse TATA-BINDING

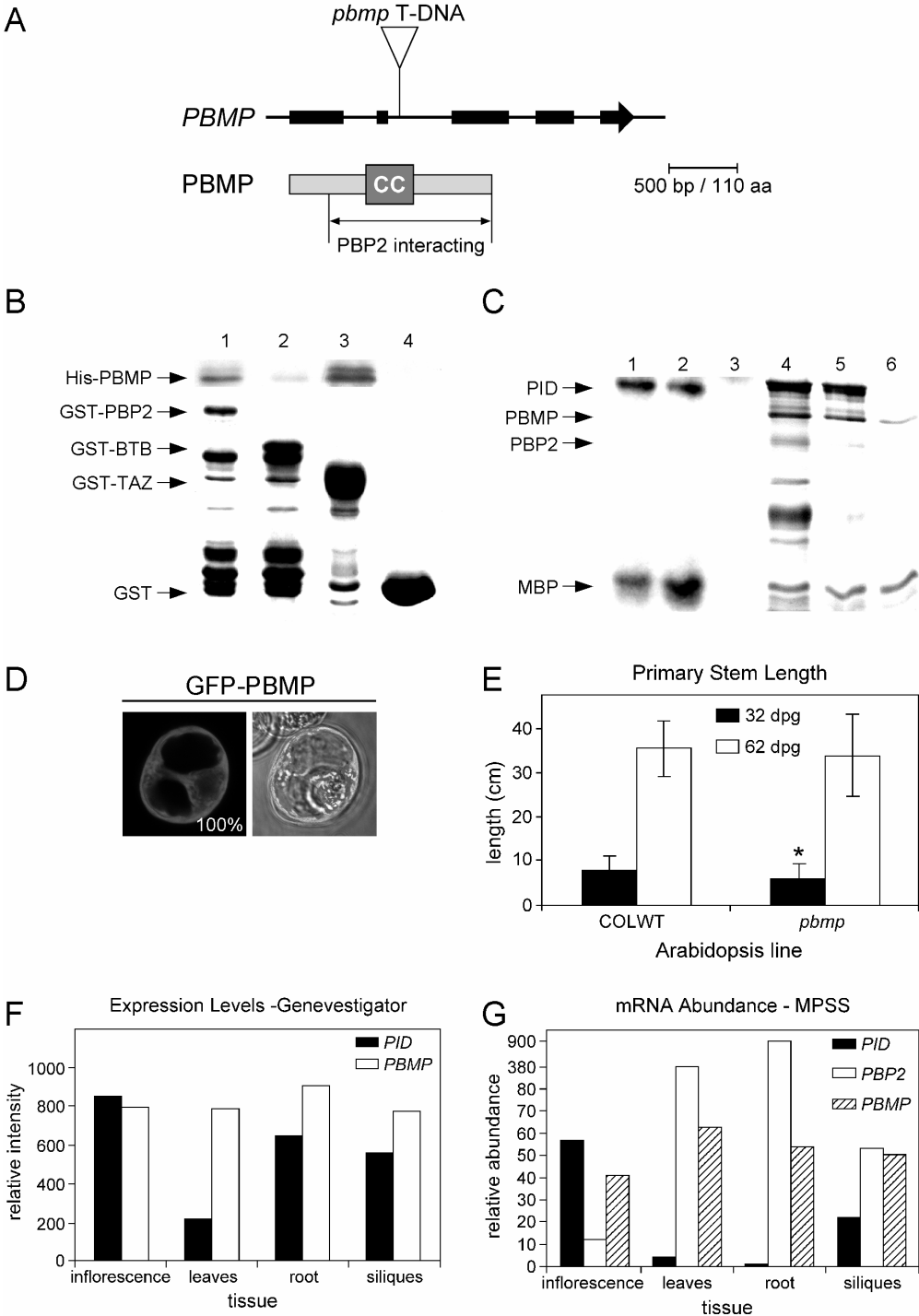


Figure 2. PBMP is a constitutively expressed protein that interacts with the TAZ domain portion of PBP2. (A) Schematic representation of the Arabidopsis *PBMP* gene (top) and the PBMP protein (bottom). Exons of *PBMP* are represented by thick black lines and the position of the T-DNA insertion in the Arabidopsis mutant line N620810 from the Salk Institute is indicated. For PBMP the coiled-coil domain (CC) as well as the PBP2 interacting portion are indicated. (B) *In vitro* pull-down of his-tagged PBMP with GST-tagged PBP2 (lane 1), GST-tagged BTB domain (lane 2) or -TAZ domain (lane 3) containing portions of PBP2 or GST alone (lane 4). Top: immunodetection of his-tagged PBMP; Bottom: coomassie stained gel with the positions of the different input proteins indicated. (C) Autoradiograph (1 to 3) and coomassie stained gel (4 to 6) of phosphorylation assays showing that PBMP is not a phospho-substrate of PID. The relative positions of PID, PBP2, PBMP and MBP are indicated. Lanes 1 and 4: PID, PBP2, PBMP and MBP; Lanes 2 and 5: PID, PBMP and MBP; Lanes 3 and 6: PBMP and MBP. (D) Arabidopsis protoplasts transformed with *35S::GFP-PBMP*. A fluorescence image (left) and a merged fluorescence and transmission light images (right) of a representative protoplast are shown. (E) The primary inflorescence stem of young *pbmp* loss-of-function mutants is significantly shorter (star) than wild type plants, but in adult plants there is no significant difference. (F and G) Gene expression data available through Genevestigator (F) and Arabidopsis MPSS (G) databases show that PBMP is constitutively expressed in Arabidopsis.

PROTEIN *in vitro* and shown to act as transcriptional activator (43). The PBP2 interactor corresponding to gene model At3g09850 contains an RRM motif coupled to a G-Patch domain. A G-Patch domain is characterized by the presence of seven highly conserved glycines, and is found in a number of RNA binding proteins, and in proteins that contain RNA binding domains (44). The combination of G-Patch and RRM domains has been described for DNA repair and RNA recognition proteins (45).

A PBP2 interactor that represents a well-characterized transcription factor is KNAT1. This protein belongs to the KNOTTED-class of homeodomain proteins, and phenotypes of the *knat1/brevipedicellus* loss-of-function mutants (46) imply that it is an important regulator of the growth and cell differentiation of the inflorescence stem, pedicel, and style in *Arabidopsis*. KNAT1 was shown to traffic between cells and it was suggested to play a role in the intercellular trafficking of macromolecules (47). Interestingly, plants overexpressing KNAT1 were shown to ectopically produce meristems, implying a role for this protein in meristem maintenance and organogenesis (48). Since both PID and KNAT1 are regulators of organogenesis at the inflorescence meristem, it is possible that PBP2 plays a role in this process as well. The interaction of KNAT1 with PBP2 in the yeast two-hybrid system, however, was very weak, and expression of this transcription factor fused to the GAL4 activation domain in the yeast strain PJ69-4A promoted background growth on selective medium. Based on these results and the fact that KNAT1 was identified only once, we decided to exclude this protein from further studies.

The observation in protoplasts that PID-GFP seems to be cytoplasmic or plasma membrane-localized implies that this kinase and transcription factors cannot be part of the same protein complex. At this stage we cannot exclude, however, that the

subcellular localization of PID is tissue dependent. Therefore, it could be possible that PID is nuclear localized in cells of different organs, in which case the interaction with KNAT1 or other PBP2 partners related to transcriptional regulation becomes more likely.

PBP2 Binding MYB-domain protein possibly represents a cell-cycle-related transcription factor

One of the transcription factor-like PBP2 interactors that was identified twice contains four MYB DNA binding domains at the carboxy-terminal portion and a lysine-rich region at the amino-terminal portion, which also comprises a putative NLS (Figure 3A). The protein was named PBP2 Binding MYB-domain protein (PBMYP). PBMYP shows reasonable similarity (43%) with a mouse homolog of CYCLIN-D BINDING MYB LIKE TRANSCRIPTION FACTOR 1 (DMP1). DMP1 is a three MYB domain protein that seems to be involved in the regulation of cell cycle arrest, probably through inhibition of S-phase entry (49).

The interaction between PBP2 and PBMYP was confirmed by *in vitro* protein pull-down assays. The his-tagged C-terminal portion of PBMYP (PBMYP-CT) was efficiently pulled down with GST-tagged PBP2 and -TAZ domain, and less efficiently with the GST-tagged BTB domain, suggesting that PBMYP-CT preferably binds the TAZ domain containing portion of PBP2 (Figure 3B).

Transformation of Arabidopsis protoplast with the *35S::GFP-PBMYP* construct showed that PBMYP is a nuclear protein, as expected for a transcription factor (Figure 3C).

Additional phosphorylation assays using PID, PBP2 and PBMYP did not provide any evidence that the kinase is able to phosphorylate the C-terminal portion of PBMYP (Figure 3D). As we have not yet been able to test the full length cDNA in this assay, we can not exclude that the N-terminus may interfere with the interaction or that this part of the protein is phosphorylated by PID.

Massive Parallel Signature Sequencing (MPSS) data (40) reveal that *PBMYP* is expressed at moderate to high levels in different Arabidopsis tissues (Figure 3E) but, like *PID*, its expression is highest in the inflorescence. These data indicate that PBMYP, PBP2 and PID may be part of the same signaling pathway involved in cell division in the inflorescence. On the other hand, PBMYP localization is restricted to the nucleus, and the fact that PID-GFP is cytoplasmic or plasma membrane localized implies that the proteins can hardly be part of the same protein complex. Considering that, as mentioned above, the subcellular localization of PID could be tissue dependent, it could be possible that PID is nuclear localized in cells of different organs, in which case the interaction with PBMYP would be allowed. The *in vivo* existence and functionality of the PID-PBP2-PBMYP complex remains to be investigated.

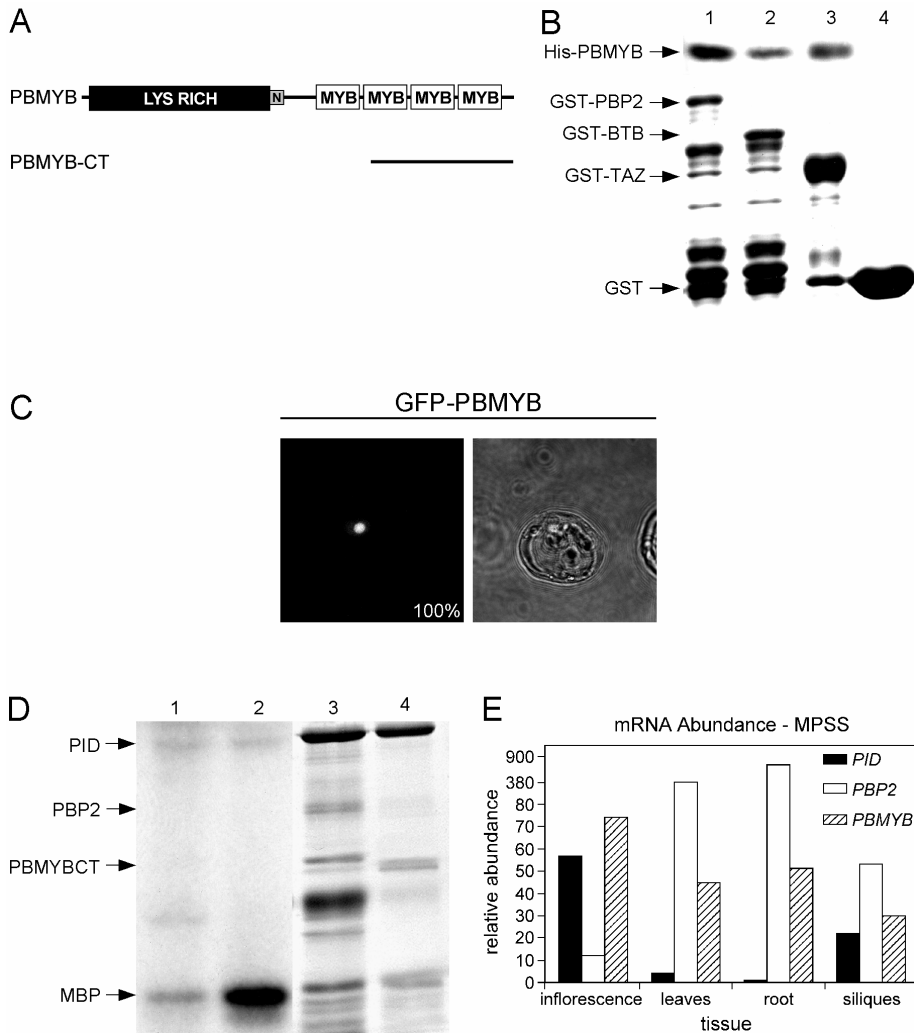


Figure 3. PBMYB interacts with the TAZ domain portion of PBP2 and shows highest expression in inflorescences. (A) Schematic representation of PBMYB (588 amino acids) and the 217 amino acids C-terminal part (PBMYB-CT) that interacts with PBP2 in the yeast two-hybrid system and was used in *in vitro* pull down assays. The lysine rich region, the NLS (N) and the MYB domains are represented by boxes. (B) *In vitro* protein pull-down of his-tagged PBMYBCT with GST-tagged PBP2 (lane 1), GST-tagged BTB domain (lane 2) or -TAZ domain (lane 3) containing part of PBP2 or GST alone (lane 4). Top: immunodetection of his-tagged PBMYB-CT. Bottom: coomassie stained gel with the positions of the different input proteins indicated. (C) Arabidopsis protoplasts transformed with 35S::GFP-PBMYB. A fluorescence image (left) and a merged fluorescence and transmission light images (right) of a representative protoplast are shown. (D) Autoradiograph (1 and 2) and coomassie gel (3 and 4) showing the relative positions of PID, PBP2, PBMYBCT and MBP, and autophosphorylation and transphosphorylation activities of PID. Lanes 1 and 3: PID, PBP2, PBMYBCT and MBP; Lanes 2 and 4: PID, PBMYBCT and MBP. (E) In the expression data retrieved from the Arabidopsis MPSS Database, higher expression of PBMYB and PID, but not of PBP2, occurs in Arabidopsis inflorescences.

The Auxin-inducible PBP2 Binding Protein may compete with PID for PBP2 interaction

The most abundant interactor of PBP2, representing almost 50% of the positive clones identified in the screen was named Auxin-inducible PBP2 Binding Protein (APBP; Figure 4A). This protein seems to be unique to plants, as the only clear ortholog of APBP has been identified in rice (*Oryza sativa*). In Arabidopsis, the protein shows significant homology with the protein predicted by gene model At3g55690 (APBPH; Figure 4B), but this homology is confined to a stretch of 138 amino acid residues (aa 28 to 165 in APBP; Figure 4B), suggesting that this conserved region represents a functional domain. Apparently, the conserved domain is somehow important for the interaction with PBP2, since all the six sequenced yeast two-hybrid clones comprise the coding region for this part (Figure 4A). APBP and APBPH have no other conserved domain that could provide insight into their function.

Analysis of publicly available micro array data (TAIR Database) indicates that *APBP* gene expression is induced upon auxin stimulation (data not shown), and that it is strongly expressed in the shoot apex of Arabidopsis (Figure 4C) (41). Interestingly, a very similar expression pattern is observed for PID (Figure 4C) (9, 41), suggesting that the proteins are present in the same cells and that they possibly participate in the same pathway.

In vitro phosphorylation assays did not provide evidence that PID phosphorylates APBP, either in presence or absence of PBP2 (Figure 4D). *In vitro* protein pull-down assays showed that APBP interacts strongly with both full length PBP2 and its BTB domain containing part (Figure 4E). The fact that PID also interacts with the BTB domain (Figure 1D) makes it less likely that APBP and PID co-exist in the same protein complex with PBP2.

A function of APBP could be to repress the PID-PBP2 interaction, but for that, all three proteins must be present in the same subcellular compartments. Transformation of the *35S::GFP-APBP* construct into Arabidopsis protoplasts showed that GFP-APBP, like PID-GFP and GFP-PBP2, localizes to the cytoplasm (Figure 4F).

To further look into the function of APBP, we identified an Arabidopsis mutant line with a T-DNA insertion in the first exon of the corresponding gene (Figure 4A). Plants of the *apbp* mutant line develop significantly bigger leaves (both petiole and leaf blade; Figure 4G). In addition, the *apbp* mutant plants show a delay in bolting, which explains the shorter primary inflorescences at 28 days post germination (Figure 4G). The fact that the *apbp* inflorescences are longer at 46 days post germination excludes that mutant plants are defective in elongation growth. The combination of such phenotypes suggests that APBP could negatively regulate vegetative development thereby enhancing bolting, allowing the plant to enter the

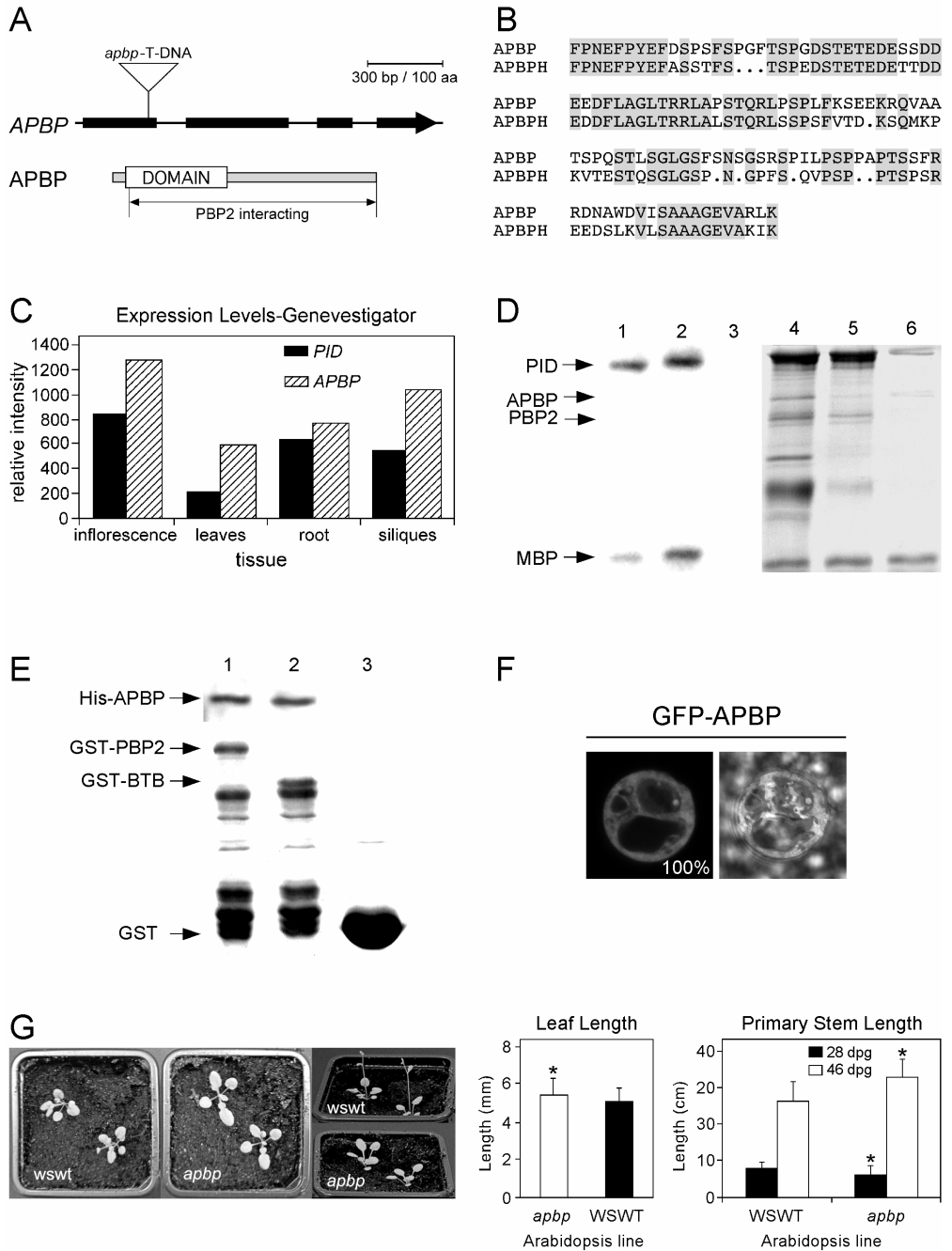


Figure 4. APBP interacts with the BTB/POZ domain of PBP2 and it is highest expressed in inflorescences. (A) Top: *APBP* gene. Exons are shown as thick lines and the T-DNA insertion is indicated by the arrowhead. Bottom: APBP protein. APBP conserved domain as well as PBP2 interacting portion are indicated. (B) Alignment of the conserved domain shared by APBP and APBP homolog (APBPH encoded by *At3g55690*). Identical residues are shaded. (C) According to Genevestigator Database, APBP generally follows the same expression pattern as PID and is highest expressed in inflorescences. (D) Autoradiograph (1 to 3) and coomassie gel (4 to 6) showing the relative positions of PID, PBP2, APBP and MBP, and autophosphorylation and transphosphorylation activities of PID. Lanes 1 and 4: PID, PBP2, APBP and MBP; Lanes 2 and 5: PID, APBP and MBP; Lanes 3 and 6: APBP and MBP. (E) *In vitro* protein pull-down of his-tagged APBP with GST-tagged PBP2 (lane 1), GST-tagged BTB domain (lane 2) containing part of PBP2 or GST- protein (lane 3); Top: immunodetection of his-tagged APBP; Bottom: coomassie stained gel showing the different input of proteins. (F) Arabidopsis protoplasts transformed with *35S::GFP-APBP*. A fluorescence image (left) and a merged fluorescence and transmission light images (right) of a representative protoplast are shown. (G) *apbp* grow more their rosette leaves (figures left and center and graph) and initially grows shorter primary inflorescence (28 dp; figure right and graph) which at latter stages become more elongated than WT (46 dp; graph). Stars indicate statistically significant variations.

reproductive phase by shortening the generation time. Such a regulatory process could be triggered, for example, under conditions where nutrients or light are rate limiting.

In summary, a few interesting facts were observed for the APBP protein: APBP and PID show very similar expression patterns; APBP and PID bind the PBP2 BTB/POZ domain; APBP, PBP2 and PID localize in the cytoplasm of Arabidopsis protoplasts; APBP knock-out mutants show longer vegetative stage, indicating that APBP could be involved in promoting shorter generation time. These observations, combined with the fact that mild PID overexpressing plants show shorter generation time, lead to the speculation that APBP may possibly compete with PID for the interaction with PBP2, and as a consequence activates the kinase by relieving it from PBP2-mediated repression. This hypothesis, however, remains to be further assessed.

DISCUSSION

The function of PID has been tightly correlated with the regulation of PAT, since activity of the kinase determines the subcellular polar localization of proteins belonging to the PIN family of auxin efflux facilitators. To further elucidate the molecular mechanism behind PID-dependent basal-to-apical switch in PIN polar targeting, we studied the functional relationship between PID and PID Binding Protein 2. Our research specifically focused on this PID interactor since preliminary experiments suggested that it may be a cytoskeleton-associated protein, and cytoskeletal elements such as F-actin have been shown to be essential for the proper localization of PINs (6). Here we further characterized the interaction

between PID and PBP2, and performed a yeast two-hybrid screen using PBP2 as bait in an attempt to identify proteins that are partners of PBP2 and putative PID regulators or phosphorylation targets.

PID binding to the BTB/POZ domain portion of PBP2 represses its kinase activity

In our efforts to unravel the function of PBP2 in the PID signaling pathway, several *in vitro* assays were performed employing both proteins. *In vitro* phosphorylation experiments showed that PBP2 inhibits both the auto- and transphosphorylation activity of PID. Moreover, with *in vitro* protein pull-down experiments we could demonstrate that PID likely binds to the BTB/POZ domain portion of PBP2. To date, an inhibitory role of BTB/POZ domain proteins has been shown only for transcriptional regulators (50-52), and our observation that PBP2 represses PID kinase activity therefore probably reveals a new functional aspect of BTB/POZ domain proteins.

Besides acting as repressors, BTB domain proteins have been shown to act as scaffolds that organize protein complexes (20, 30, 53). In this chapter we describe the identification of sixteen putative PBP2 interacting proteins, and the more detailed analysis of the nature of the interaction between PBP2 and a selection of these proteins is in line with a role of PBP2 as scaffold protein. For example, we showed that several PBP2 binding proteins interact with the C-terminal TAZ domain portion, while PID interacts with the N-terminal BTB/POZ domain portion of PBP2 (Figure 5). These results raise the possibility that the PBP2 scaffold recruits PID phosphorylation targets or connects PID with other functional structures. Such scaffold- and phosphorylation-enabling function has been described for 14-3-3 proteins, that through dimerization create two protein-protein interaction domains which facilitate phosphorylation activity of certain kinases on their specific substrates (54). However, the fact that none of the tested PBP2 interactors is a phosphorylation substrate of PID, and the observation that PBP2 represses PID kinase activity, rather suggest that the scaffold function of PBP2 is employed to regulate the activity or the subcellular localization of PID (Figure 5).

Our protoplast transformation experiments suggest that PID is predominantly localized at the PM, which is in line with its function as regulator of the polar subcellular targeting of the transmembrane PIN auxin efflux facilitators (10). In fact, this co-localization opens the possibility that PID mediates its effect through direct phosphorylation of PIN proteins. In 50% of the protoplasts, PID-GFP also shows a cytoplasmic localization, and since GFP-PBP2 is also present in the cytoplasm, it is likely that both proteins interact in this subcellular compartment. In this view, it will be interesting to test in co-transformation experiments if PBP2 - through its interaction with PID - alters the subcellular localization of this kinase.

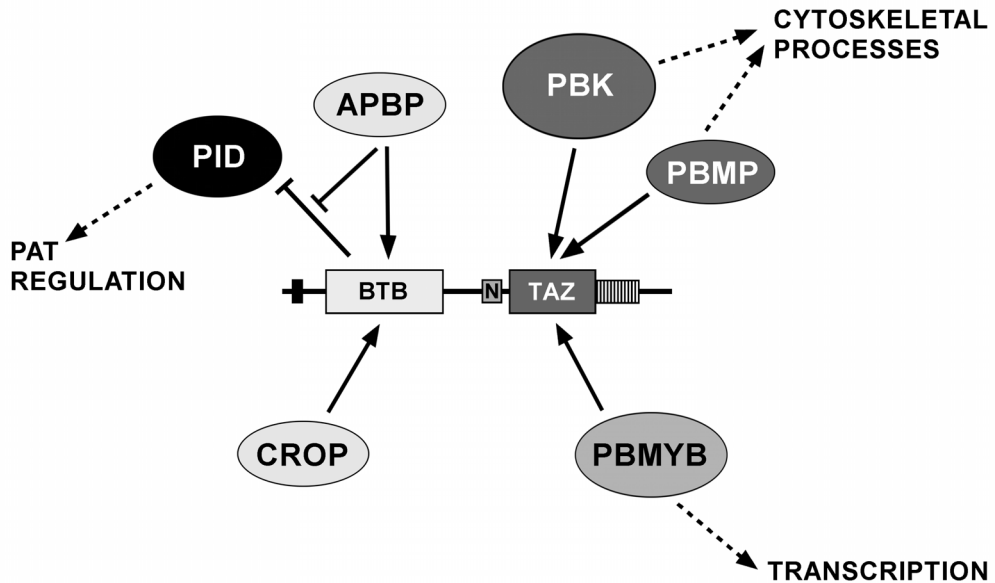


Figure 5. PBP2 is a multifunctional scaffold protein that connects PID-related and -unrelated pathways. PBP2 interacting proteins are shown for which the interaction domain in PBP2 has been mapped by *in vitro* pull down experiments (see Figures 1 to 4 and Table 2 for further details). PID kinase activity is repressed by PBP2. APBP possibly competes with PID for its interaction with the BTB domain of PBP2, thereby activating the PID kinase.

In this chapter, the inhibitory effect of PBP2 on PID activity was only demonstrated *in vitro*. Presently, crosses between mutant Arabidopsis lines with altered expression levels of *PID* or *PBP2* are being analyzed and preliminary observations confirm the inhibitory role of PBP2 on PID activity *in vivo* (Robert, unpublished data). These data combined with *in vivo* protein pull downs will more conclusively address the functional relationship between PID, PBP2 and the PBP2 interacting proteins.

PBP2 as a multi-functional scaffold protein

BTB/POZ domain proteins are known to interact with a wide diversity of proteins (55). In line with these earlier observations, our yeast two-hybrid screen has identified a wide range of PBP2 interacting proteins that can be roughly classified into three classes: cytoskeletal proteins, transcriptional regulators and proteins with enzymatic activity.

Several reports describe the interaction of BTB proteins with the cytoskeleton in various organisms and correlate this interaction with a change in stability and dynamics of F-actins (55). Accordingly, it has been speculated that the PBP2-

related *Caenorhabditis elegans* MEL26 protein promotes cytokinesis by reducing the activity of the cytoskeletal protein POD-1, possibly by blocking the F-actin cross-linking capability of POD-1 (56). In spite of that, from the apparent functions of most of the cytoskeletal partners of PBP2, it is only possible to hypothesize that in *Arabidopsis* cells PBP2 is involved in microtubular trafficking. Whether PBP2 reduces the activity of its cytoskeletal interactors in a similar way as MEL26 does towards POD-1 remains to be investigated.

The interaction between BTB proteins and transcription factors has also been well documented. It has been consistently shown, for example, that BTB/POZ and C2H2 zinc finger domains containing proteins mediate transcriptional repression (50-52). Therefore, it is inevitable to speculate that the function of PBP2 towards its transcription factor partners is to repress them. The role of PBP2 in transcription regulation is not contradictory with its previously observed cytoskeletal localization. In fact, such dual cytoplasmic-nuclear localization of PBP2 is supported by its potential partner KNAT1, whose rice ortholog KNOX1 has been found to be present in both cellular compartments (47, 57). Considering the well established fact that regulation of transcription factor activity can be performed by their nuclear uptake, it is plausible that PBP2 acts as transcription factor transporter. Alternatively, PBP2 could perform different functions in the cytoplasm and in the nucleus. The actual role of PBP2 in transcription regulation has to be studied in further detail.

Not much is known about the relationship between BTB proteins and catalytic enzymes. The most informative example consists in the demonstration that isoforms of the mouse BTB/POZ protein NAC1 recruit histone deacetylases for transcriptional repression (58). The role of PBP2 towards its enzymatic interactors is yet to be determined.

As discussed above, our recent findings on the function of PID (10) could explain a hypothetical relationship between PID and cytoskeletal activity. Our observations that PBP2 interacts with putative cytoskeletal proteins may indicate that PBP2 represents the actual link between the PID and the cytoskeleton. However, none of the PBP2 binding proteins described in this chapter could unequivocally be related to PID activity, making this connection unclear. The observation that several proteins that are likely to play a role in unrelated processes interact with PBP2, leads us to conclude that PBP2 is a multi-functional scaffold protein that connects different networks and participates in both PID-related and -unrelated signaling pathways. This view is again supported by the extremely well described case of the 14-3-3 scaffold proteins, which are known to play a role in a large variety of processes such as the regulation of ATP production, DNA conformation and cell cycle (59, 60). Which PBP2 interactors are truly part of the PID signaling complex remains to be addressed.

APBP could possibly be an activator of the PID protein kinase

The most frequent interactor of PBP2, the APBP protein, does not classify to any of the pre-defined groups of PBP2 partners. APBP does not contain any acknowledged domain or signal-peptide, and it is therefore impossible to assign a clear cellular function to this protein. Publicly available microarray data, combined with *in vitro* and *in vivo* data provided in this chapter tend to favor the hypothesis that APBP competes with PID for binding the BTB domain of PBP2. By competing with PID, APBP could release PBP2-induced PID inhibition, thereby activating the kinase. The fact that both APBP and PID have the same expression profile may indicate tight feed-back of PID activity control. Crosses between mutants and overexpression lines and *in vitro* phosphorylation assays using titrated quantities of PBP2, APBP and PID could help to clarify this model.

PBP2 does not seem to interact with calmodulins or CUL3

Previously, a calmodulin, two fsh/Ring class transcription factors and CULLIN3 have been reported as interactors of PBP2 (20, 21). Curiously, none of these proteins were identified in our screen, nor did we identify PID itself as an interactor of PBP2. The fact that these putative PBP2 interactors were not identified may be explained by the fact that the root-specific cDNA library that was used for our screen insufficiently represented the indicated proteins. For some of the putative PBP2 interactors there are however alternative explanations why they were not represented by the positive clones.

The absence of PID among the PBP2IPs may be explained by two previous observations: i) yeast two-hybrid interaction tests using the GAL4AD-PID fusion always resulted in poor growth on selective medium (data not shown), indicating that PID is relatively toxic to yeast when fused to the GAL4 activation domain; ii) when PID (bait) and PBP2 (target) were transformed to yeast, optimal growth was never reached upon selective pressure for the interaction, suggesting that PID and PBP2 bind weakly in this system, or that PID as bait is also mildly toxic. As shown in this chapter, the *in vitro* interaction between PID and PBP2 is strong and stable, corroborating our previous findings that these two proteins do interact (11).

The binding of PBP2 to a calmodulin was identified in a screen that used an Arabidopsis library as target and potato Calmodulin 6 (Cam6) as bait. The interaction between PBP2 and the Arabidopsis ortholog of Cam6 was never tested, indicating that the significance of this interaction in Arabidopsis remains to be addressed.

In several organisms BTB domain proteins have been demonstrated to interact with CULLIN3 (CUL3). The BTB/CUL3 complex forms a new class of E3 ligases, in which the BTB domain protein acts as the SCF E3 ligase SKP1/F-BOX protein sub-complex, by interacting with CUL3 through its BTB domain, while recruiting

ubiquitination and proteolysis targets through its second domain (19, 20, 53, 61, 62). Not many BTB protein ubiquitination targets have been identified, but in *Caenorhabditis elegans* it has been shown that during the meiosis-to-mitosis transition the microtubule-severing protein MEL-1/katanin is recruited for degradation by the BTB protein MEL26 (19, 62). Recently, a report suggested that also PBP2 interacts with CUL3 in *in vitro* pull down assays (20). However, neither CUL3 nor its homologs were found in the yeast two-hybrid screen described in this chapter. Our observations are corroborated by the work of Gingerich and co-workers (63) and Dieterle and co-workers (15), who showed that the PBP2 class of BTB domain proteins does not interact with CUL3 to participate in proteolysis. Such finding, combined with our own results, assign a debatable character to the conclusion that PBP2 is part of the CUL3-containing E3 ubiquitin ligase complex.

ACKNOWLEDGEMENTS

This work was financially supported by CAPES (Brazilian Federal Agency for Post-Graduate Education, M. K.-Z.). We thank Bert van der Zaal for providing the root-specific cDNA library, Rene Benjamins for providing constructs pSDM6006 (H-PBP2), pSDM6014 (pBSSK-PBP2) and pSDM6025 (pTH2GFP-PBP2), Johan Memelink for providing pET16H, Carlos Galvan for the plasmid pART7-PID-GFP encoding PID-GFP, Gerda Lamers for help with the laser scanning confocal microscopy, Helene Robert for helpful comments on the manuscript, Peter Hock for art work, and the Salk Institute Genomic Analysis Laboratory for providing the sequence indexed Arabidopsis T-DNA insertion mutant *pbmp*.

REFERENCE LIST

1. Galweiler, L., Guan, C., Muller, A., Wisman, E., Mendgen, K., Yephremov, A. & Palme, K. (1998) *Science* **282**, 2226-2230.
2. Okada, K., Ueda, J., Komaki, M. K., Bell, C. J. & Shimura, Y. (1991) *Plant Cell* **3**, 677-684.
3. Friml, J. & Palme, K. (2002) *Plant Mol. Biol.* **49**, 273-284.
4. Benkova, E., Michniewicz, M., Sauer, M., Teichmann, T., Seifertova, D., Jurgens, G. & Friml, J. (2003) *Cell* **115**, 591-602.
5. Friml, J. (2003) *Curr. Opin. Plant Biol.* **6**, 7-12.
6. Geldner, N., Friml, J., Stierhof, Y. D., Jurgens, G. & Palme, K. (2001) *Nature* **413**, 425-428.
7. Bennett, S., Alvarez, J., Bossinger, G. & Smyth, D. (1995) *Plant J.* **8**, 505.
8. Christensen, S. K., Dagenais, N., Chory, J. & Weigel, D. (2000) *Cell* **100**, 469-478.

9. Benjamins, R., Quint, A., Weijers, D., Hooykaas, P. & Offringa, R. (2001) *Development* **128**, 4057-4067.
10. Friml, J., Yang, X., Michniewicz, M., Weijers, D., Quint, A., Tietz, O., Benjamins, R., Ouwerkerk, P. B., Ljung, K., Sandberg, G. *et al.* (2004) *Science* **306**, 862-865.
11. Benjamins, R. Functional analysis of the PINOID protein kinase in *Arabidopsis thaliana*. 2004. Leiden University.
12. Goto, N. K., Zor, T., Martinez-Yamout, M., Dyson, H. J. & Wright, P. E. (2002) *J. Biol. Chem.* **277**, 43168-43174.
13. Zollman, S., Godt, D., Prive, G. G., Couderc, J. L. & Laski, F. A. (1994) *Proc. Natl. Acad. Sci. U S A* **91**, 10717-10721.
14. Bardwell, V. J. & Treisman, R. (1994) *Genes Dev.* **8**, 1664-1677.
15. Dieterle, M., Thomann, A., Renou, J. P., Parmentier, Y., Cognat, V., Lemonnier, G., Muller, R., Shen, W. H., Kretsch, T. & Genschik, P. (2005) *Plant J.* **41**, 386-399.
16. Motchoulski, A. & Liscum, E. (1999) *Science* **286**, 961-964.
17. Sakai, T., Wada, T., Ishiguro, S. & Okada, K. (2000) *Plant Cell* **12**, 225-236.
18. Cao, H., Glazebrook, J., Clarke, J. D., Volko, S. & Dong, X. (1997) *Cell* **88**, 57-63.
19. Pintard, L., Willis, J. H., Willems, A., Johnson, J. L., Srayko, M., Kurz, T., Glaser, S., Mains, P. E., Tyers, M., Bowerman, B. *et al.* (2003) *Nature* **425**, 311-316.
20. Figueroa, P., Gusmaroli, G., Serino, G., Habashi, J., Ma, L., Shen, Y., Feng, S., Bostick, M., Callis, J., Hellmann, H. *et al.* (2005) *Plant Cell* **17**, 1180-1195.
21. Du, L. & Poovaiah, B. W. (2004) *Plant Mol. Biol.* **54**, 549-569.
22. Sambrook, J., Fritsch, F. & Maniatis, T. (1989) *Molecular Cloning - A Laboratory Manual* (Cold Spring Harbour Laboratory Press, New York).
23. Guan, K. L. & Dixon, J. E. (1991) *Anal. Biochem* **192**, 262-267.
24. Chiu, W., Niwa, Y., Zeng, W., Hirano, T., Kobayashi, H. & Sheen, J. (1996) *Curr. Biol.* **6**, 325-330.
25. Neuteboom, L. W., Ng, J. M., Kuyper, M., Clijdesdale, O. R., Hooykaas, P. J. & van der Zaal, B. J. (1999) *Plant Mol. Biol.* **39**, 273-287.
26. Memelink, J., Swords, K., Staehelin, L. & Hoge, J. (1994) in *Plant Molecular Biology Manual*, eds. Gelvin, S., Schilperoort, R., & Verma, D. (Kluwer Academic Publishers, Dordrecht), pp. 1-26.
27. Schirawski, J., Planchais, S. & Haenni, A. L. (2000) *J Virol. Methods* **86**, 85-94.
28. Axelos, M., Curie, C., Mazzolini, L., Bardet, C. & Lescure, B. (1992) *Plant Physiol Biochem* **30**, 123-128.
29. Masson, J. & Paszkowski, J. (1992) *Plant J* **2**, 208-218.

30. Albagli, O., Dhordain, P., Deweindt, C., Lecocq, G. & Leprince, D. (1995) *Cell Growth Differ.* **6**, 1193-1198.
31. Klickstein, L. B. (1987) in *Current Protocols in Molecular Biology*, eds. Ausubel, F. M., Brent, R., Kingston, R. E., Moore, D. D., Seidman, J. G., Smith, J. A., & Struhl, K. (Greene Publishing Associates, New York), p. 5.8.1-5.8.8.
32. Williams, B. C., Dernburg, A. F., Puro, J., Nokkala, S. & Goldberg, M. L. (1997) *Development* **124**, 2365-2376.
33. Williams, B. C., Riedy, M. F., Williams, E. V., Gatti, M. & Goldberg, M. L. (1995) *J. Cell Biol.* **129**, 709-723.
34. Chanvivattana, Y., Bishopp, A., Schubert, D., Stock, C., Moon, Y. H., Sung, Z. R. & Goodrich, J. (2004) *Development* **131**, 5263-5276.
35. Kim, G. T., Tsukaya, H. & Uchimiya, H. (1998) *Planta* **206**, 175-183.
36. Hauser, B. A., He, J. Q., Park, S. O. & Gasser, C. S. (2000) *Development* **127**, 2219-2226.
37. Rose, A., Manikantan, S., Schraegle, S. J., Maloy, M. A., Stahlberg, E. A. & Meier, I. (2004) *Plant Physiol* **134**, 927-939.
38. Xia, G., Ramachandran, S., Hong, Y., Chan, Y. S., Simanis, V. & Chua, N. H. (1996) *Plant J.* **10**, 761-769.
39. Kragler, F., Curin, M., Trutnyeva, K., Gansch, A. & Waigmann, E. (2003) *Plant Physiol* **132**, 1870-1883.
40. Meyers, B. C., Lee, D. K., Vu, T. H., Tej, S. S., Edberg, S. B., Matvienko, M. & Tindell, L. D. (2004) *Plant Physiol* **135**, 801-813.
41. Zimmermann, P., Hirsch-Hoffmann, M., Hennig, L. & Gruissem, W. (2004) *Plant Physiol* **136**, 2621-2632.
42. Birney, E., Kumar, S. & Krainer, A. R. (1993) *Nucleic Acids Res.* **21**, 5803-5816.
43. Oda, T., Kayukawa, K., Hagiwara, H., Yudate, H. T., Masuho, Y., Murakami, Y., Tamura, T. A. & Muramatsu, M. A. (2000) *Mol. Cell Biol.* **20**, 1407-1418.
44. Aravind, L. & Koonin, E. V. (1999) *Trends Biochem Sci.* **24**, 342-344.
45. Dendouga, N., Callebaut, I. & Tomavo, S. (2002) *Eur. J. Biochem.* **269**, 3393-3401.
46. Venglat, S. P., Dumonceaux, T., Rozwadowski, K., Parnell, L., Babic, V., Keller, W., Martienssen, R., Selvaraj, G. & Datla, R. (2002) *Proc. Natl. Acad. Sci. U S A* **99**, 4730-4735.
47. Kim, J. Y., Yuan, Z. & Jackson, D. (2003) *Development* **130**, 4351-4362.
48. Chuck, G., Lincoln, C. & Hake, S. (1996) *The Plant Cell* **8**, 1277-1289.
49. Inoue, K. & Sherr, C. J. (1998) *Mol. Cell Biol.* **18**, 1590-1600.
50. Deweindt, C., Albagli, O., Bernardin, F., Dhordain, P., Quief, S., Lantoine, D., Kerckaert, J. P. & Leprince, D. (1995) *Cell Growth Differ.* **6**, 1495-1503.

51. Sasai, N., Matsuda, E., Sarashina, E., Ishida, Y. & Kawaichi, M. (2005) *Genes Cells* **10**, 871-885.
52. Dhordain, P., Albagli, O., Lin, R. J., Ansieau, S., Quief, S., Leutz, A., Kerckaert, J. P., Evans, R. M. & Leprince, D. (1997) *Proc. Natl. Acad. Sci. U S A* **94**, 10762-10767.
53. Weber, H., Bernhardt, A., Dieterle, M., Hano, P., Mutlu, A., Estelle, M., Genschik, P. & Hellmann, H. (2004) *Plant Physiol.*
54. Yuan, Z., Agarwal-Mawal, A. & Paudel, H. K. (2004) *J. Biol. Chem.* **279**, 26105-26114.
55. Stogios, P., Downs, G., Jauhal, J., Nanadra, S. & Prive, G. (2005) *Genome Biology* **6**, R82-1-R82-18.
56. Luke-Glaser, S., Pintard, L., Lu, C., Mains, P. E. & Peter, M. (2005) *Curr. Biol.* **15**, 1605-1615.
57. Kuijt, S. J., Lamers, G. E., Rueb, S., Scarpella, E., Ouwerkerk, P. B., Spaink, H. P. & Meijer, A. H. (2004) *Plant Mol. Biol.* **55**, 781-796.
58. Korutla, L., Wang, P. J. & Mackler, S. A. (2005) *J. Neurochem.* **94**, 786-793.
59. Bridges, D. & Moorhead, G. B. (2005) *Sci. STKE*. **2005**, re10.
60. van Heusden, G. P. & Steensma, H. Y. (2006) *Yeast* **23**, 159-171.
61. Geyer, R., Wee, S., Anderson, S., Yates, J. & Wolf, D. A. (2003) *Mol. Cell* **12**, 783-790.
62. Furukawa, M., He, Y. J., Borchers, C. & Xiong, Y. (2003) *Nat. Cell Biol.* **5**, 1001-1007.
63. Gingerich, D. J., Gagne, J. M., Salter, D. W., Hellmann, H., Estelle, M., Ma, L. & Vierstra, R. D. (2005) *J. Biol. Chem.* **280**, 18810-18821.

A BTB/POZ domain protein-kinesin complex is likely to provide polarity to PINOID kinase signaling

SUMMARY

The Arabidopsis PINOID (PID) protein serine/threonine kinase regulates plant development by modulating the polar transport of the phytohormone auxin (polar auxin transport or PAT). We have demonstrated that PID directs PAT by regulating the baso-apical subcellular localization of the PIN auxin efflux facilitators. To further investigate the PID signaling pathway we performed a series of yeast two-hybrid screens and found that PID interacts with the BTB/POZ domain protein PINOID BINDING PROTEIN 2 (PBP2), and that PBP2 interacts with several proteins, amongst which two paralogous plant-specific microtubule motor proteins. Here we describe a more detailed study of the interaction of PBP2 with the motor proteins PBP2 BINDING KINESIN 1 (PBK1) and 2 (PBK2). *In vitro* pull down and phosphorylation assays suggested that PBP2 functions as a scaffold protein, since the PBKs bind the C-terminal TAZ domain portion and the PID kinase binds the N-terminal BTB/POZ domain portion of PBP2. The possible existence of such a protein complex at the cytoplasm-plasma membrane boundary was corroborated by the overlapping spatio-temporal expression of *PID*, *PBP2* and the *PBKs*, and by the fact that the proteins - when fused to GFP - co-localize in the cytoplasm of Arabidopsis protoplasts. Analysis of *pbk1/pbk2* mutant plants and *35S::PBK1* overexpression lines showed phenotypes that were also observed in mutants defective in PAT and in *pid* loss-of-function seedlings, respectively. These observations suggest that the PBKs are involved in the suppression of PID or PID-like kinase activity. As PBP2 was shown to inhibit PID activity *in vitro*, we propose that PBK1 and PBK2 act as the transporters of PBP2 that result in asymmetric subcellular suppression of PID and PID-like activity at the cytoplasm-plasma membrane boundary, thereby providing polarity to the signaling of these kinases.

Abbreviations: ARF-GEF, ADP-ribosylation factor-GTP exchange factor; BTB/POZ, bric-a-brac, tramtrack and broad complex/Pox virus and zinc finger domain; CC, coiled-coil domain; C-kinesin, C-terminal motor kinesin; F-actin, actin filament; GFP, green-fluorescent protein; GST, glutathione-S-transferase; IAA, indole-3-acetic acid; MBP, myelin basic protein; M-kinesin, middle motor kinesin; MT, microtubules; N-kinesin, N-terminal motor kinesin; PAT, polar auxin transport; PBK, PBP2 binding kinesin; PBP, pinoid binding protein; PID, pinoid; PM, plasma membrane; TAZ, transcriptional adaptor putative zinc finger domain

INTRODUCTION

The plant cellular cytoskeleton is a versatile structure. It is required for a variety of functions, such as organelle positioning, cytokinesis, intra- and intercellular trafficking and signaling. The two main components of the plant cytoskeleton are actin filaments (F-actin) and microtubules (MT) (1). A great variety of proteins

associate with the cytoskeleton, but it is believed that molecular motors such as myosins and kinesins are most essential for F-actin and MT function, respectively. Myosins share a head domain with ATPase activity that binds to F-actin and moves along the filament upon ATP hydrolysis. Plant myosins have not been well studied, but it is generally assumed that these motor proteins have similar functions as their orthologs in other organisms, such as reorientation of MT through F-actin, the control of intercellular transfer of macromolecules through plasmodesmata, transport of secretory vesicles to the plasma membrane, phragmoplast organization and deposition of cell wall material (2-7).

Kinesins also share a motor domain with ATPase activity, but differently than myosins, these proteins bind to and move over MT. Plant kinesins have been studied in more detail and the function of some of them is quite well understood. It has been shown, for example, that plant kinesins with the motor domain positioned at their carboxy-terminus (C-kinesins) move from the plus to the minus end of MT. C-kinesins participate in MT organization at spindle poles and midzone during meiosis and mitosis (*Arabidopsis* KATA and ATK5) (8, 9), in MT stabilization of cortical arrays in interphase cells (*Arabidopsis* and cotton KCBP) (10), and act as putative MT and F-actin cross-linkers (cotton KHC) (11). Interestingly, the protein KIN13A is the only partly characterized *Arabidopsis* internal motor domain containing kinesin (M-kinesin), and its motility has been characterized as plus end directed. KIN13A was demonstrated to associate with Golgi stacks, but it did not have MT de-polymerizing activity, as shown for M-kinesins of animal cells (12). Most of the characterized plant kinesins belong to the group of the N-kinesins, which have an amino-terminal motor domain and move from the minus to the plus end of MT. N-kinesins were shown to be involved in the orientation of cellulose microfibril deposition (*Arabidopsis* FRA1) (13), organization of MT at the phragmoplast (*Arabidopsis* PAKRP1 and PAKRP1L) (14), delivery of Golgi vesicles to the phragmoplast (*Arabidopsis* PAKRP2) (15), and cell plate formation during mitotic (*Arabidopsis* NACK1) (16, 17) and meiotic cytokinesis (*Arabidopsis* NACK2) (18). One of the best characterized N-kinesins is the tobacco NACK1. NACK1 was found to interact with and thereby activate the MAPKK kinase NPK1 at the phragmoplast during cell division (16).

From the few specific examples described above, and many other observations in different organisms, it can be deduced that one particular F-actin- and MT-dependent mechanism must be governed by the action of molecular motors: the intracellular trafficking of macromolecules and vesicles (19, 20). Interestingly, polar transport of the plant hormone auxin (polar auxin transport, or PAT) has also been shown to be dependent on cytoskeleton-mediated intracellular trafficking. PAT is facilitated by a family of transporter-like PIN proteins that show a polar subcellular localization that correlates with the direction of transport (21, 22). Geldner and co-

workers showed that in interphase cells PIN1 loaded vesicles travel to and from the plasma membrane (PM), and that this cyclic trafficking depends on F-actins (23). Recently it was found that the Arabidopsis myosin XI is possibly involved in this process (24). MTs have also been shown to be essential for PIN targeting. For example, Boutté and co-workers (25) showed that MT, and probably its associated proteins, are indirectly required for the polar localization of PINs. During cytokinesis, PIN1 accumulation at the cell plate also seems to be MT-dependent (23).

Our knowledge on the signaling mechanisms governing PIN targeting and cyclic trafficking of PIN vesicles is still limited. On one hand, proper polar deposition of PIN1 at the PM was found to depend on the BFA sensitive ADP Ribosylation Factor GDP/GTP Exchange Factor (ARF-GEF) GNOM (26, 27). On the other hand, we have demonstrated that PIN1 polar targeting is directed to the apical (top) side of the cell by the activity of the protein serine/threonine kinase PINOID (PID) (28).

To further elucidate the mechanism underlying PIN polar targeting, we performed a yeast two-hybrid screen for proteins interacting with PID. Interestingly, one of the PID binding proteins, the PINOID Binding Protein 2 (PBP2), was found to localize at the cortical cytoskeleton in onion cells (29). PBP2 has two protein-protein interaction domains, an amino-terminal Bric-a-brac, Tramtrack and Broad Complex/Pox virus and Zinc finger (BTB/POZ) domain, and a carboxy-terminal Transcriptional Adaptor putative Zinc Finger (TAZ) domain. This feature suggests that PBP2 possibly acts as scaffold protein that organizes protein complexes. *In vitro* pull down assays indicated that PID binds to the BTB/POZ domain containing part, and a yeast two hybrid screen for PBP2 interacting proteins revealed several proteins that interact with the TAZ domain-containing part (see Chapter 2).

Here we describe the functional analysis of two of these proteins, which are the paralogous N-kinesins PBP2 Binding Kinesin 1 and 2 (PBK1 and PBK2), in the context of their putative role in PID signaling. Our data suggest that PID, PBP2 and the PBKs are expressed in the same tissues in Arabidopsis and that they co-localize in the cytoplasm. Moreover, *in vitro* phosphorylation assays indicated that PID does not phosphorylate the PBKs or PBP2, suggesting that these proteins may be involved in regulating PID activity. The analysis of *pbk1/pbk2* loss-of-function mutants revealed that these plants are slightly defective in root growth and gravitropic response. Interestingly, PBK1 gain-of-function seedlings display an enhanced frequency of cotyledon abnormalities, a phenotype also observed in *pid* loss-of-function seedlings. Our observations indicate that the *in vivo* formation of a PID-PBP2-PBK protein complex is plausible and that PBKs are possibly involved in repressing PID or PID-like activity.

MATERIALS AND METHODS

Molecular cloning and constructs

Molecular cloning was performed following standard procedures (30). The yeast two-hybrid bait plasmid pAS2-PBP2 was obtained by cloning a *PBP2* *Pst*I/*Sal*I-blunted fragment derived from pSDM6014 into pAS2 digested with *Pst*I/*Xma*I-blunted. The histidine tagged PID construct was created by excising the *PID* cDNA with *Xmn*I-*Sal*I from pSDM6005 (29) and cloning it into pET16H (pET16B derivative, J. Memelink, unpublished results) digested with *Bam*HI, blunted and subsequently digested with *Xho*I. The 35S::PID-GFP construct was generated by amplifying the *PID* cDNA using the primers 5'-TTAATATGACTCACTATAGG-3' and 5'-GCTCACCATAAAGTAATCGAACGC-3' and the *eGFP* coding region using the primers 5'-GATTACTTTATGGTGAGCAAGGGC-3' and 5'-TCAATCTGAGTACTTGTACAG-3'. Both PCR products were used together with outer primers in a new PCR reaction to generate the *PID*-GFP fragment, which was cloned into pUC28 digested with *Nco*I/*Hinc*II. The resulting pUC28-PID-GFP was digested with *Eco*RI/*Stu*I-blunted and the *PID*-GFP fragment was ligated into *Eco*RI/*Sma*I digested pART7. Construction of histidine- and GFP-tagged PBP2 vectors are described by Benjamins (29). The GST-tagged PBP2 fusion (plasmid pGEX-PBP2) was generated by digesting pSDM6014 (29) with *Xho*I/*Sma*I and cloning the *PBP2* cDNA into pGEX-KG (31). The plasmid for production of a GST-tagged PBP2 BTB/POZ domain was created by digesting pGEX-PBP2 with *Nde*I, filling in with Klenow and re-ligating. This created a stop codon at position 220 aa of the protein. The plasmid encoding the GST-tagged PBP2 TAZ domain was created by deleting the *Nco*I fragment encoding the BTB/POZ domain from pGEX-PBP2. The *PBK1* and *PBK2* cDNAs were amplified using respectively the primer pairs PBK1F (5'-ACGCAAGTCGACAATATGGAGAAGACACAGATGCC-3') and PBK1R (5'-CGGGATCCAATCAGAGGAAATGAAATGACACC-3'), and PBK2F (5'-GGGAATCCATATGATGGGAGCGATTGCTGGAGAAG-3') and PBK2R (5'-GTCCTTTCCATATGCCATTATATGAACGTGTTG-3'). The amplified *PBK1* cDNA was digested with *Sal*I/*Bam*HI and cloned into the corresponding restriction sites in pUC28. The *PBK2* cDNA PCR product was digested with *Nde*I and cloned into the corresponding restriction site in pUC28. The *GFP-PBK1* fusion was constructed by excising *PBK1* from pUC28 with *Sal*I/*Not*I and cloning this fragment into the *Xho*I/*Not*I sites of pTH2^{BN} (derived from the pTH2 plasmid described by Chiu and co-workers) (32). Histidine tagged PBK1CT and PBK2CT expression vectors were created by excising *PBK1CT* and *PBK2CT* from the pACT2-PBK1CT and pACT2-PBK2CT yeast two-hybrid clones with *Nde*I/*Xho*I and cloning these fragments into the corresponding restriction sites in pET16B (Novagen). 35S::PBK1 was constructed by cloning a *PBK1* *Sal*I/*Bam*HI fragment into the *Xho*I/*Bam*HI site of pART7. 35S::PBK1CT and 35S::PBK2CT were created by cloning *Bgl*II fragments comprising *PBK1CT* and *PBK2CT* from the pACT2 yeast two-hybrid clones into the *Bam*HI site of pART7. All 35S::PBK constructs were transferred as *Not*I fragments from pART7 into pART27 (33).

Yeast two hybrid screen

Using the Matchmaker II yeast two-hybrid system and *Saccharomyces cerevisiae* strain PJ69-4A (Clontech), an *Arabidopsis thaliana* cDNA library fused to the GAL4 activation domain (pACT2) was screened at 20°C with PBP2 fused to the GAL4 DNA binding domain (pAS2) as bait. The cDNA library was constructed from RNA samples isolated from Arabidopsis root cultures in a one to one mix of untreated roots and roots treated for 24 hours with the auxin analog 1-naphthaleneacetic acid (1-NAA) (34). The positive clones were analyzed by colony hybridization as described in the Hybond-N+ Membrane Manual (Amersham Biosciences) and in the work of Memelink and co-workers (35).

In vitro pull down experiments

GST tagged full-length PBP2, its deletion versions (GST-BTB/POZ and GST-TAZ) or GST protein alone were used in pull down assays with histidine (his)-tagged PBK2CT (H-PBK2CT). Cultures of *E. coli* strain BL21 containing one of the constructs were grown at 37°C to OD₆₀₀ 0,8 in 50 ml LC supplemented with antibiotics. The cultures were then induced for 4 hours with 1 mM IPTG at 30°C, after which cells were

harvested by centrifugation (10 min. at 4.000 RPM in tabletop centrifuge) and frozen overnight at -20°C. Precipitated cells were re-suspended in 2 ml Extraction Buffer (EB: 1x PBS, 2 mM EDTA, 2 mM DTT, supplemented with 0,1 mM of the protease inhibitors PMSF - Phenylmethanesulfonyl Fluoride, Leupeptin and Aprotinin, all obtained from Sigma) for the GST-tagged proteins or in 2 ml Binding Buffer (BB: 50 mM Tris-HCl pH 6,8, 100 mM NaCl, 10 mM CaCl₂, supplemented with PMSF 0,1 mM, Leupeptin 0,1 mM and Aprotinin 0,1 mM) for the his-tagged PBK2CT and sonicated for 2 min. on ice. From this point on, all steps were performed at 4°C. Eppendorf tubes containing the sonicated cells were centrifuged at full speed (14.000 RPM) for 20 min, and the supernatants were transferred to fresh 2 ml tubes. H-PBK2CT supernatant was left on ice, while 100 µl pre-equilibrated Glutathione Sepharose resin (pre-equilibration performed with three washes of 10 resin volumes of 1x PBS followed by three washes of 10 resin volumes of 1x BB at 500 RCF for 5 min.) was added to the GST- fusion protein containing supernatants. Resin-containing mixtures were incubated with gentle agitation for 1 hour, subsequently centrifugated at 500 RCF for 3 min. and the precipitated resin was washed 3 times with 20 resin volumes of EB. Next, all H-PBK2CT supernatant (approximately 2 ml) was added to GST-fusions-containing resins, and the mixtures were incubated with gentle agitation for 1 hour. After incubation, supernatants containing GST resins were centrifugated at 500 RCF for 3 min., the new supernatants were discarded and the resins subsequently washed 3 times with 20 resin volumes of EB. Protein loading buffer was added to the resin samples, followed by denaturation by 5 min. incubation at 95°C. Proteins were subsequently separated on a 12% polyacrylamide gel prior to transfer to an Immobilon™-P PVDF (Sigma) membrane. Western blots were hybridized using a horse radish peroxidase (HRP)-conjugated anti-pentahistidine antibody (Quiagen) and detection followed the protocol described for the Phototope-HRP Western Blot Detection Kit (New England Biolabs).

***In vitro* phosphorylation assays**

All proteins used in *in vitro* phosphorylation assays were his-tagged for purification from several (usually five) aliquots of 50 ml cultures of *E. coli*. strain BL21 which were grown, induced, pelleted and frozen as described above for the *in vitro* pull down experiments. Each aliquot of frozen cells pellet was resuspended in 2 ml Lysis Buffer (25 mM Tris-HCl pH 8,0; 500 mM NaCl; 20 mM Imidazol; 0,1% Tween-20; supplemented with 0,1 mM of the protease inhibitors PMSF, Leupeptin and Aprotinin) and subsequently sonicated for 2 min. on ice. From this point on, all steps were performed at 4°C. Sonicated cells were centrifugated at full speed (14.000 RPM) for 20 min, the new pellets were discarded, and supernatants from all aliquots of the same construct were transferred to a 15 ml tube containing 100 µl of pre-equilibrated Ni-NTA resin (pre-equilibration performed with three washes of 10 resin volumes of Lysis Buffer at 500 RCF for 5 min.). Supernatant and resin were incubated with gentle agitation for 1 hour. After incubation, supernatant containing Ni-NTA resin was centrifuged at 500 RCF for 3 min., the new supernatant was discarded and the resin subsequently washed: 3 times with 20 resin volumes of Lysis Buffer, once with 20 resin volumes of Wash Buffer 1 (25 mM Tris.Cl pH 8,0; 500 mM NaCl; 40 mM Imidazol; 0,05% Tween-20) and once with 20 resin volumes of Wash Buffer 2 (25 mM Tris-HCl pH 8,0; 600 mM NaCl; 80 mM Imidazol). In between the washes, the resin was centrifugated for 5 min. at 500 RCF. After the washing steps, 20 resin volumes of Elution Buffer (25 mM Tris.HCl pH 8,0; 500 mM NaCl; 500 mM Imidazol) was added to the resin and incubated for 15 min. with gentle agitation. The resin was centrifugated for 3 min. at 500 RCF, and the supernatant containing the desired protein was diluted a 1000-fold in Tris Buffer (25 mM Tris.HCl pH 7,5; 1 mM DTT) and concentrated to a workable volume (usually 50 µl) using Vivaspin micro-concentrators (10 kDa cut off, maximum capacity 600 µl, manufacturer: Vivascience). Glycerol was added as preservative to a final concentration of 10% and samples were stored at -80°C.

Approximately 1 µg of each purified his-tag protein (PID and substrates) in maximal volumes of 10 µl were added to 20 µl kinase reaction mix, containing 1x kinase buffer (25 mM Tris-HCl pH 7,5; 1 mM DTT; 5 mM MgCl₂) and 1 x ATP solution (100 µM MgCl₂/ATP; 1 µCi ³²P-γ-ATP). Reactions were incubated at 30°C for 30 min. and stopped by the addition of 5 µl of 5 x protein loading buffer (310 mM Tris-HCl pH 6,8; 10 % SDS; 50% Glycerol; 750 mM β-Mercaptoethanol; 0,125% Bromophenol Blue) and 5 min.

boiling. Reactions were subsequently separated over 12,5% acrylamide gels, which were washed 3 times for 30 min. with kinase gel wash buffer (5% TCA – Trichloroacetic Acid; 1% $\text{Na}_2\text{H}_2\text{P}_2\text{O}_7$), coomassie stained, de-stained, dried and exposed to X-ray films for 24 to 48 hours at -80°C using intensifier screens.

Protoplast transformations

Protoplasts were obtained from *Arabidopsis thaliana* Col-0 cell suspension cultures that were propagated as described by Schirawski and co-workers (36). Protoplast isolation and PEG-mediated transformation followed the protocol described originally by Axelos and co-workers (37) and adapted by Schirawski and co-workers (36). The transformations were performed with 20 µg of plasmid DNA, after which the protoplasts were incubated for at least 16h. Images were obtained by laser scanning confocal microscopy.

Plant growth, -lines and -transformation

Seeds were germinated and seedlings grown on MA medium (38) supplemented with kanamycin 25 µg/ml or other compounds (for example, IAA 0,1 µM, NPA 0,3 µM) when required, at 21°C in 50% relative humidity and a 16 hours photoperiod of 2500 lux. Adult or flowering *Arabidopsis* plants were grown on substrate soil, in growth rooms at 20°C, 40% relative humidity and a 16 hours photoperiod of 2500 lux. The gravitropism assay was performed according to Luschign and co-workers (39).

Arabidopsis mutant lines N506264 and N508956 with T-DNA insertions in *PBK1* and *PBK2*, respectively, were obtained from the Salk Institute. For the PCR identification of the mutant alleles we used primers 5'-TTCTCACCCTGACGTTCTGGC-3', 5'-GATTGCTGTCTTTGGCATGCTT-3' and 5'-TGGTTCACGTAGTGGGCCATCG-3' for *pbk1* allele N506264 and primers 5'-GCAAATCCTGAGCAAGCTCCAT-3', 5'-GCGATTGCTGGAGAAGAGCTG-3' and 5'-TGGTTCACGTAGTGGGCCATCG-3' for the *pbk2* allele N508956.

Binary vectors were transferred to *Agrobacterium tumefaciens* strain GV2260, and transgenic lines were obtained by the floral dip procedure (40).

Northern blot analysis

Total RNA extraction was performed using the RNeasy Plant Mini Kit (Quiagen). Northern blotting and hybridization were performed as described by Memelink and co-workers (35) with the following modifications: pre-hybridizations as well as hybridizations were conducted at 65°C using a new Pre-hybridization mix (10% Dextran Sulfate; 1% SDS; 1M NaCl; 50 µg/ml of Single Stranded Herring Sperm DNA). The final washing steps were performed at 42°C. *PBK1* and *PBK2* probes were synthesized using the *PBK1CT* *XmaI/SacI* and *PBK2CT* *NcoI/XhoI* cDNA fragments derived from the pACT2 yeast two-hybrid clones as templates. The probes were radio-labeled using the Prime-a-gene Labeling System Kit (Promega) and $\alpha\text{-P}^{32}\text{-dCTP}$ (Amersham).

RESULTS

PBP2 interacts with two paralogous kinesins

Two of the PBP2 interactors identified in the yeast two-hybrid screen described in Chapter 2 are paralogs belonging to the large family of sixty-one kinesins in *Arabidopsis*. The proteins were named PBK1 and PBK2 for PBP2 Binding Kinesin 1 and 2, respectively. The six cDNA clones that were picked up in the yeast two-hybrid screen, two for *PBK1* (At4g38950) and four for *PBK2* (At2g21300), all were partials encoding only the C-terminal portions PBK1CT and PBK2CT, respectively.

These results indicate that the C-terminal portion of the kinesins interacts with PBP2 (Figure 1A and 2).

To independently confirm the data from the yeast two-hybrid screen, *in vitro* protein pull down experiments were performed using affinity-purified histidine-tagged PBK2CT and GST-tagged PBP2 or GST-tagged versions of the BTB domain- or the TAZ domain containing portion of PBP2, respectively. These experiments showed that PBK2CT specifically interacts with the part of PBP2 that contains the TAZ domain (Figure 1B). Previously, we showed that PID interacts with the BTB domain containing portion of PBP2 (Figure 1, Chapter 2), and our current finding suggests that PBP2 may act as a scaffold protein, possibly forming a protein complex that comprises PBK1/2 and PID via its two interaction domains.

PBK1 and PBK2 belong to a plant specific clade of kinesins

Alignment of the PBK1 and 2 amino acid sequences showed that these proteins are very similar, sharing an overall amino acid identity of 81,6% (Figure 2). Protein domain analysis using ScanProsite software identified their motor domains to be located at the amino-terminus, suggesting a minus to plus-end motility on MT strands. Separate analysis of the different parts of the PBK proteins indicated that they share respectively 91% and 75,4% amino acid identity in their motor- and carboxy-terminal PBP2 interacting domains (Figure 1A and 2). A previous large scale comparison of kinesins from Arabidopsis and other organisms indicated that PBK1 and PBK2 belong to a plant specific clade that includes the proteins encoded by the genes At3g51150, At4g24170, At5g42490 and At5g66310, and the well-characterized kinesins AtNACK1 and 2 that were shown to be involved in cytokinesis (18, 41). Our own alignments using either the full length sequences or the motor domains of the Arabidopsis kinesins confirmed these results (Figure 1C). The eight clade members share four highly conserved domains: an amino-terminal motor domain, a single coiled-coil domain and two domains of unknown function in the carboxy-terminal region (Figure 1A). The hypothetical binding site for the Arabidopsis NPK1-ortholog (AtNPK1) (16) that is present in the carboxy-terminus of AtNACK1 and 2, could not be identified in other members of the clade (Figure 1A). This implies that AtNPK1 acts specifically on the AtNAKCs and not on the other kinesins of this clade.

The carboxy-terminal portions of PBK1 and 2 are not phosphorylated by PID

PBP2-dependent recruitment of PBK1 and PBK2 could function to alter their activity through phosphorylation by PID. To test this possibility, we performed *in vitro* phosphorylation assays using PID and PBK2CT or PBK1CT with or without PBP2 in separate reactions. The general phosphorylation substrate Myelin Basic Protein

(MBP) was used as a positive control. While strong phosphorylation of MBP could be detected, no significant PID-dependent phosphorylation of PBK1CT or PBK2CT was observed in these experiments, even in the presence of PBP2 (Figure 1D), indicating that CT domains of the kinesins are not targets for phosphorylation by PINOID. This observation, however, does not exclude the possibility that PID phosphorylates residues in the N-terminal part of PBK1/2. Interestingly, the presence of PBP2 reproducibly reduced the auto-phosphorylation activity of PID, which is in line with the proposed function of PBP2 as negative regulator of PID activity (Chapter 2).

The PBKs, PBP2 and PID are expressed in the same tissues and co-localize in the cytoplasm

Even though there is no data indicating that PBKs are phosphor-substrates of PID, they may still function in the PID signaling pathway. The kinesins could affect the subcellular localization or -activity of PID, or be involved in altering cytoskeletal properties as part of the PID-PBP2-PBK complex. Such functions require that the PBKs are co-expressed in the same cells and co-localize to the same subcellular compartments as PID and PBP2.

To assess the spatio-temporal expression of the corresponding genes, we compiled publicly available data from the Genevestigator and Arabidopsis MPSS databases (42, 43). Data extracted from the Genevestigator database indicated that both *PBKs* and *PID* reach highest expression levels at the bolting stage (Figure 3A, right), although these genes are also significantly expressed at rosette stage 1 (Figure 3A, right). In Arabidopsis tissues, high expression of the *PBKs* and *PID* coincides in flowers, more specifically in petals (Figure 3A, left). Interestingly, the expression pattern of *PBK2* is most similar to that of *PID*, with highest expression in the shoot apex (Figure 3A, left). In contrast to *PID*, the *PBKs* show a mild but significant expression in lateral roots and in the root elongation zone.

The expression data for the *PBKs* and *PID* in the Arabidopsis MPSS database partly corroborate those from Genevestigator, with highest mRNA abundance detected in the inflorescence (Figure 3B). Notably, *PBP2* expression appears to be minor in these organs, whereas it is very high in tissues where the other three mRNAs are not very abundant, such as leaves and roots (Figure 3B). Our and other studies have shown that *PBP2* expression reaches intermediate levels in inflorescences and floral organs (Robert *et al.*, unpublished data) (44, 45). These results indicate that *PID*, *PBK1*, *PBK2* and *PBP2* expression patterns overlap, in particular in the inflorescence where PID is known to play an important role.

To compare the sub-cellular localization of the PBKs with that of PID and PBP2, we transformed *35S::GFP*, *35S::GFP-PBK1*, *35S::PID-GFP* and *35S::GFP-PBP2* constructs to Arabidopsis protoplasts. Both GFP-PBK1 and PID-GFP predominantly

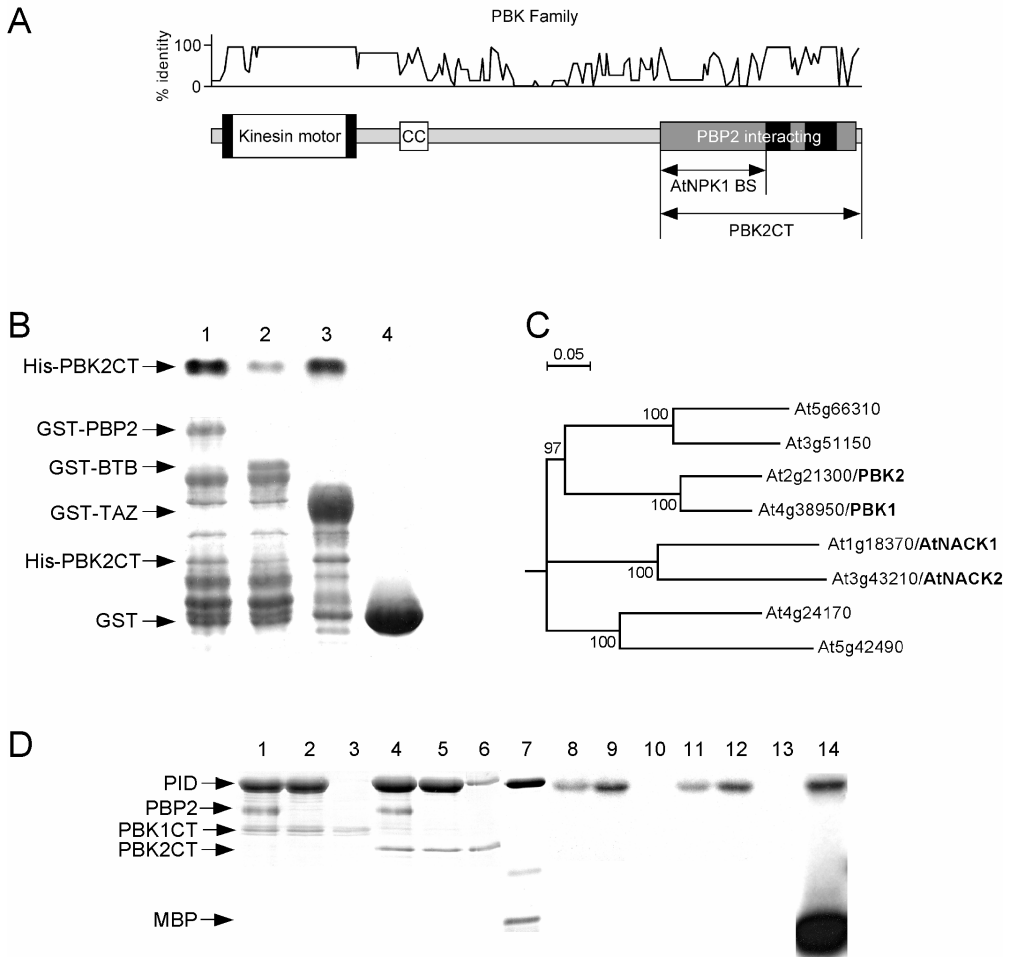


Figure 1. The plant specific kinesins PBK1 and PBK2 interact with PBP2 but are not phosphorylated by PID *in vitro*. (A) Graph showing the percentage of identity between the eight PBK clade members (upper part) in relation to their different conserved domains (lower part). Indicated are the kinesin motor domain, the coiled-coil domain (CC), the Arabidopsis NPK1-ortholog binding site (AtNPK1 BS) in AtNACK1/2, and the two PBK clade-specific PFam signatures (black boxes). Those PBK clade-specific domains are present in the region corresponding to the 258 amino acid PBP2-interacting C-terminal portion of PBK2 (PBK2CT) that was picked up in the yeast two-hybrid screen and subsequently used in the *in vitro* pull down. (B) Immuno-detection (top) and coomassie stained gel (bottom) of an *in vitro* protein pull down assay using his-tagged PBK2CT together with GST-tagged PBP2 (lane 1), GST-tagged BTB (lane 2) or TAZ domain containing portion (lane 3) of PBP2 or the GST protein alone (lane 4). (C) Phylogenetic tree showing the PBKs and their plant-specific relatives. Bootstrap values are indicated. (D) Coomassie stained gel (lanes 1 to 7) and autoradiograph (lanes 8 to 14) of an *in vitro* phosphorylation assay using PID (lanes 1, 2, 4, 5, 7, 8, 9, 11, 12 and 14), PBP2 (lanes 1, 4, 8 and 11), PBK1CT (lanes 1 to 3 and 8 to 10), PBK2CT (lanes 4 to 6 and 11 to 13) and MBP (lanes 7 and 14).

PBK1MEKTQMPVA	REEKILVLVR	<i>α</i> LRPLNQKEIA	ANEAADWECI
PBK2	MGAIAEELK	KMEKTQVHVA	REEKILVLVR	LRPLNEKEIL	ANEAADWECI
PBK1	<u>NDTTILYRNT</u>	<u>LREGSNFP</u> SA	<u>YSFDKVYRGE</u>	<u>CPTRQVYEDG</u>	<u>TKEIALSVVK</u>
PBK2	<u>NDTTVLYRNT</u>	<u>LREGSTFP</u> SA	<u>YSFDRVYRGE</u>	<u>CPTRQVYEDG</u>	<u>PKEVALSVVK</u>
PBK1	<u>GINCSI</u> FAYC	<u>QTSSGKTY</u> TM	TGITEFAVAD	IFDYIFQHEE	RAFSVKFSAI
PBK2	<u>GINSSI</u> FAYC	<u>QTSSGKTY</u> TM	SGITEFAVAD	IFDYIFKHED	RAFVVKFSAI
PBK1	<u>EIYNEAIRDL</u>	<u>LSSDGTSLRL</u>	<u>RDDPEKGT</u> TV	<u>EKATEETLRD</u>	<u>WNHLKELLSI</u>
PBK2	<u>EIYNEAIRDL</u>	<u>LSPDSTPLRL</u>	<u>RDDPEKGA</u> AV	<u>EKATEETLRD</u>	<u>WNHLKELISV</u>
PBK1	<u>CEAQRKIGET</u>	<u>SLNERSSRSH</u>	<u>QMIRLTVESS</u>	<u>AREFLGKENS</u>	<u>TTLMASVNFI</u>
PBK2	<u>CEAQRKIGET</u>	<u>SLNERSSRSH</u>	<u>QIIKLTVESS</u>	<u>AREFLGKENS</u>	<u>TTLMASVNFI</u>
PBK1	<u>DLAGSERASQ</u>	<u>AMSAGTRLKE</u>	<u>GCHINRSLLT</u>	<u>LGTVIRKL</u> SK	<u>GRQGHINFRD</u>
PBK2	<u>DLAGSERASQ</u>	<u>ALSAGARLKE</u>	<u>GCHINRSLLT</u>	<u>LGTVIRKL</u> SN	<u>GRQGHINVRD</u>
PBK1	<u>SKLTRIQLPC</u>	<u>LGGNARTAI</u> I	<u>CTLSPARSHV</u>	<u>ELTKNTLLFA</u>	<u>CCAKEVTTKA</u>
PBK2	<u>SKLTRIQLPC</u>	<u>LGGNARTAI</u> V	<u>CTLSPARSHV</u>	<u>EQTRNTLLFA</u>	<u>CCAKEVTTKA</u>
PBK1	RINVMSDKA	LLKQLQRELA	RLETELRNPA	SSPASNCDC	MTVRKKDLQI
PBK2	QINVMSDKA	LVKQLQRELA	RLESELNPA	PATSS.CDCG	VTLRKKDLQI
PBK1	<u>QKMEKEIAEL</u>	<u>RKQORDLAQSR</u>	<u>LEDFMRMIEH</u>	<u>NVASKPGTPH</u>	<u>FGNHTDKWED</u>
PBK2	<u>QKMEKQLAEM</u>	<u>TKQORDIAQSR</u>	<u>LEDFMKMVEH</u>	<u>DASSKAGTPH</u>	<u>FRNRTNWKED</u>
PBK1	GSVSETSGVV	DSDRRSFISD	GMSTPLSISR	AYVHSHSDDD	DLDEDLPRRS
PBK2	GSVSEISGVV	DPDRTSFISD	GTSTPLSTAR	AHVRSHSDDD	LEEEMSPRHS
PBK1	EDLSEYYCRE	VQCIETEESV	TVYNNKKDKR	AEPENVLGCG	EDANGET...
PBK2	GDQSEYYCKE	VQCIEMEEEST	RDINNNDSEER	TDAETLLGHN	AEANGETGSA
PBK1SVSQ	NVRVRSWNR	ETVSGPSTPP	ENIGTGFLGR	PESHKIAFPD
PBK2	QHRIPSSVRS	VRRRKSWSRG	DTMTGTSTPP	DALETDYRGR	PEGHGFAFPD
PBK1	LEFGS..TVS	RNDMSMSSCGS	DSTGTQSIRT	PLG.EEGGIT	SIRTFVEGLK
PBK2	LEFGSGGKLL	RNDSMTSRGS	DSTEAHSIGT	PLVGEEGGIT	SIRSFVEGLK
PBK1	EMAKRQGEVS	NAEDSGKMRR	DIGLDSMDR.	EFERQRQEIL
PBK2	EMVSDP....	..ENSGKMRK	DIGVDAMEEE	VSGTMTNWSE	EFERQREQIL
PBK1	ELWQTCNISL	VHRTYFYLLF	KGDEADSIYI	GVELRRLLFM	KDSFSQGNQA
PBK2	GLWQTCHVSL	VHRTYFFLLF	TGDAQDSIYI	GVELRRLSFM	KESFSQGNHA
PBK1	LEGGETLTLA	SSRKELHRER	KMLSKLVGKR	FSGEERKRIY	HKFGIAINSK
PBK2	FERGQTLTIA	SSLKALHRER	RMLSKLVGKR	FTGEERKRLY	QKFGIAVNSK
PBK1	RRRLQLVNEL	WSNPKDMTQV	MESADVAKL	VRFAEQGRAM	KEMFGLTFTP
PBK2	RRRLQLANQL	WSKPNIDITHA	VESAADVAKL	VRFVEQGRAM	KEMFGLSFTP
PBK1	PSFLTTRRSH	SWRKSPALF			
PBK2	P.LPTTRRSL	NWRKSMATLF			

Figure 2. PBK1 and PBK2 are paralogous N-kinesins. PBK1 and PBK2 show 81,6% overall amino acid identity and 91% and 75,4% identity in the motor domain (underlined) and the carboxy-terminal PBP2-interacting region (bold), respectively. Identical amino acid residues are shown in gray shading. The coiled-coil domain is indicated in italics. Putative neck sequences (α , in which absence of the GN motif suggests MT plus-end motility, and γ), the ATP binding site (β) and other nucleotide phosphates binding sites (ξ) or the microtubule interacting site (ζ) are shown in black shading.

localized to the PM, but some fluorescent signal was observed in the cytoplasm (Figure 3C). Notably, GFP-PBP2 localization varied between protoplasts: in 80% of the GFP positive protoplasts nuclear localization was observed, whereas 20% of those protoplasts showed a cytoplasmic fluorescent signal (Figure 3C and Chapter 2). Due to the even signal intensity through the cellular regions in the latter case, we can not exclude that part of GFP-PBP2 also localizes to the PM (Figure 3C). In conclusion, the combined data allow us to speculate that the hypothesized PID-PBP2-PBK complex functions at the cytoplasm-PM boundary of cells in the inflorescence meristem to regulate organ development. The *in vivo* occurrence of such a complex remains however to be determined.

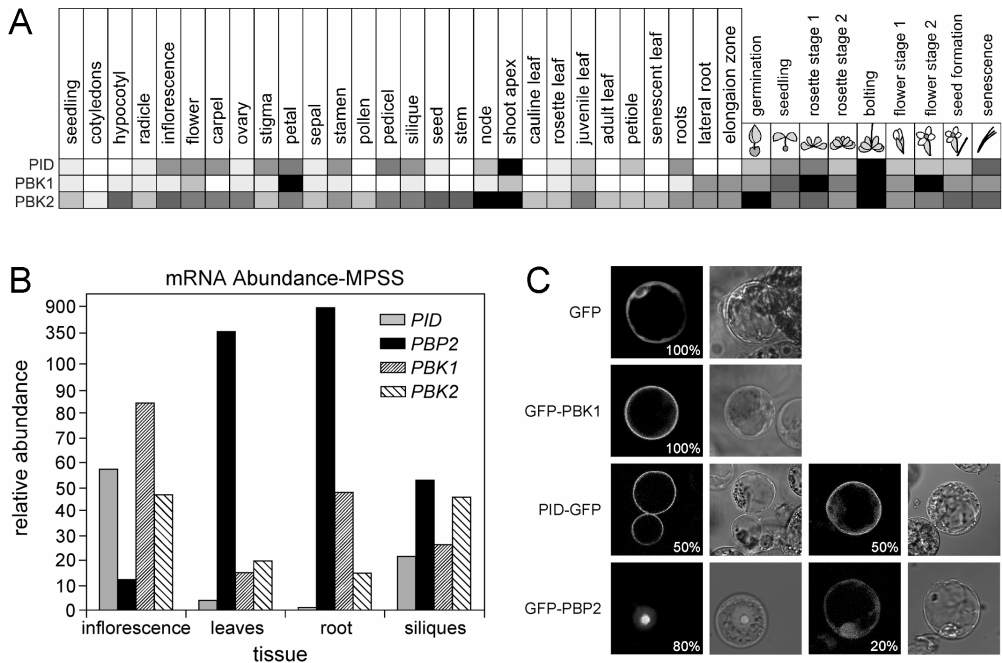


Figure 3. PBKs, PID and PBP2 are expressed in the same tissues and co-localize in the cytoplasm. (A) Expression profiles of *PID*, *PBK1* and *PBK2* in different Arabidopsis tissues (left) and developmental stages (right) according to Genevestigator Database. Black: tissue or developmental stage in which a certain gene reaches maximal expression; white: tissue or developmental stage in which a certain gene is not expressed; grayscale: intermediate expression levels. (B) Expression profiles of *PID*, *PBK1*, *PBK2* and *PBP2* in Arabidopsis tissues according to the Arabidopsis MPSS Database. (C) Confocal laser scanning and transmission light microscopy images (merged with fluorescent images) of representative Arabidopsis protoplasts transformed with *35S::GFP*, *35S::GFP-PBK1*, *35S::PID-GFP* and *35S::GFP-PBP2*. The frequencies observed for the different localizations are indicated.

PBK1 and PBK2 act redundantly in the control of root growth

Assuming that one of the functions of PBK1 and 2 could be to regulate PID and that this action could be essential for proper PAT, it is possible that loss-of-function mutants for both kinesins show phenotypes related to defects in PAT, similar to plants with altered *PID* expression levels. Lines N506264 (*pbk1*) and N508956 (*pbk2*) were obtained from the Salk Institute and PCR analysis confirmed that the T-DNA insertions in these lines are in exons 9 and 4 of the *PBK1* and *PBK2* genes, respectively (Figure 4A). The complete knock-out of *PBK1* and *PBK2* transcription in such plants, however, could not be conclusively determined due to the very low expression levels of both genes in wild type seedlings (data not shown). Nevertheless, *pbk1* and *pbk2* were crossed in order to generate the *pbk1/pbk2* double mutant. Subsequently, the single and double *pbk* loss-of-function lines were subjected to detailed phenotypic analysis.

The single *pbk* mutants did not show significant phenotypic differences compared to wild type under standard growth conditions, both at the seedling and flowering stage. The *pbk1/pbk2* double mutant seedlings, however, showed a slight but statistically significant reduction in root elongation (Figure 4B) and a slower gravitropic root response compared to wild type (Figure 4C). At the flowering stage *pbk1/pbk2* plants were indistinguishable from wild type.

The observed reduced gravitropic response of *pbk1/pbk2* seedlings could indicate a possible role for both kinesins in the regulation of PAT in the roots. Interestingly, *PID* overexpression also results in agravitropic root growth, and although *PID* itself does not seem to have an apparent function in this organ, its overexpression may trigger the signaling pathway of some of its family members. In the view of the indirect link between the PBKs and *PID*, we interpret our results as an indication that the kinesins act redundantly in the control of root growth, possibly by repressing the activity of the *PID* kinase family members.

Overexpression of PBK1 leads to defects in cotyledon positioning

To further investigate the function of the PBKs, we tested overexpression of the full length *PBK1* cDNA and the 3' end of the *PBK* cDNAs encoding the PBP2 interacting C-terminal portions (*PBK1CT* and *PBK2CT*) under the control of the *CaMV 35S* promoter. With the latter constructs we expected to observe dominant negative effects, since it produces a non-functional protein that possibly titrates out PBP2 protein complexes.

Approximately twenty T2 lines carrying a single locus insertion of the constructs *35S::PBK1CT* and *35S::PBK2CT* were analyzed, but none of them showed obvious phenotypes, in spite of the fact that several of these lines showed strong overexpression levels (Figure 4D).

In seven of the nineteen *35S::PBK1* single locus lines, T2 seedlings with three or sometimes fused cotyledons were observed at frequencies ranging from 1:1000 in line *35S::PBK1-5* to 1:30 in line *35S::PBK1-3* (Table 1 and Figure 4E). Most of the *35S::PBK1* lines did not show any further defects at the rosette or flowering stage.

Table 1. PBK1 overexpression results in cotyledon defects

<i>Arabidopsis thaliana</i> line	Generation	Seedlings with abnormal cotyledons/total seedlings	Frequency of cotyledon abnormalities
Columbia wild type	-	0/1740	< 0,05%
<i>35S::PBK1-3</i>	T2/T3	13/500	2,60 %
<i>35S::PBK1-5</i>	T2	1/1061	0,10 %
<i>35S::PBK1-18-1</i>	T2	2/557	0,35 %
<i>35S::PBK1-19-2</i>	T2	4/1346	0,30 %
<i>35S::PBK1-19-3</i>	T2	2/852	0,23 %
<i>35S::PBK1-19-4</i>	T2	2/656	0,30 %
<i>35S::PBK1-21-2</i>	T2	3/400	0,75 %
<i>35S::PBK1-7</i>	T3	0/500	< 0,20 %
<i>35S::PBK1CT-13</i>	T3	0/500	< 0,20 %
<i>35S::PBK2CT-4</i>	T3	0/500	< 0,20 %

For line *35S::PBK1-3*, however, one in four T2 plants developed short roots, had a dwarf stature and bolted with great delay, although not producing flowers (Figure 4F). The Mendelian segregation ratio and the fact that we were not able to generate homozygous T3 lines indicated that the plants with strong phenotypes were homozygous for the overexpression construct. Northern analysis showed that *35S::PBK1-3* seedlings contain very high *PBK1* expression levels compared to those of other *35S::PBK1* lines (Figure 4D). This strongly suggested that the frequent cotyledon phenotypes, and possibly also the dwarf phenotypes of homozygous *35S::PBK1-3* plants, are induced by high levels of *PBK1* overexpression. For these latter phenotypes we can not exclude, however, that they are the result of a loss-of-function mutation caused by the insertion of the overexpression construct. The cotyledon defects are however observed in multiple overexpression lines, and their frequency seems to correlate with the level of overexpression. Interestingly, *pid* mutant plants show similar cotyledon abnormalities, and the penetrance of the mutant phenotype has been correlated with the strength of the mutant *pid* allele (46). Our observations on the *PBK1* overexpression lines corroborate our previous hypothesis that the PBKs repress the activity of the PID protein kinase and its closely related family members. The low frequency of the *35S::PBK1* cotyledon defects could be due to the fact that the *CaMV 35S* promoter usually becomes active during embryonic stages where the cotyledons boundaries have already been defined. The use of promoters that are

active during early embryogenesis to drive ectopic *PBK1* expression should confirm our hypothesis.

DISCUSSION

The plant cellular cytoskeleton has been shown to play a crucial role in several important processes, including polar transport of the plant hormone auxin (PAT). PAT is mediated by the PIN auxin efflux facilitators, whose asymmetric distribution over the cell membrane correlates with the directionality of transport (47, 48). In interphase cells, the polar subcellular localization of PIN proteins requires indirect MT action and is maintained by cyclic trafficking of PIN loaded vesicles along the actin cytoskeleton, whereas localization of PIN1 to the cell plate during cytokinesis was found to be MT-dependent (23, 25, 27, 47, 48). Previously, we demonstrated that the protein serine/threonine kinase PINOID (PID) is a key regulator of the apico-basal polarity of PIN proteins (28). PID was found to interact with the BTB/POZ domain protein PBP2 that - when fused to GFP - showed a possible cytoskeletal localization in onion cells (29). The data presented in this chapter suggest that PBP2 interacts with two homologous Arabidopsis kinesins PBK1 and PBK2, and that the PBP2-PBK complex is involved in the regulation of PID activity. Our findings provide the first clues for a third MT-dependent pathway in the regulation of the subcellular localization of PIN proteins.

The plant-specific N-kinesins PBK1 and PBK2 may be part of the PID signaling complex

Alignment of PBK1 and 2 with the other fifty-nine kinesins encoded by the Arabidopsis genome showed that they cluster in a plant specific clade of eight kinesins that are characterized by the presence of two unique conserved carboxy-terminal domains. Except for AtNACK1 and 2, which have been characterized as essential for the completion of cytokinesis during mitosis and meiosis (16-18), not much is known about the function of the other clade members.

The yeast two-hybrid data and *in vitro* pull down experiments indicate that PBP2 interacts with the C-terminal region of PBK1 and PBK2. The fact that this region contains domains that are conserved among PBK-like proteins allows the possibility that PBP2 interacts with other kinesins of the PBK/NACK clade. This is likely to be the case, as the lack of strong mutant phenotypes in the *pbk1pbk2* double mutant indicates functional redundancy among the members of the PBK/NACK clade. On the other hand, the C-terminal AtNPK1 binding domain is only present in AtNACK1 and 2 and not in other members of the PBK/NACK clade, which illustrates that some PBK relatives also have their specific, unrelated function. Since it is believed that C-

terminal domains of kinesins are involved in cargo binding, it is logical to assume that PBP2 is the cargo of PBK1/2 and possibly also the cargo of PBK relatives. Our findings that PID and the PBKs interact with different protein interaction domains of PBP2, and that PID and PBK1 predominantly localize at the PM but that the three proteins co-localize in the cytoplasm, led us to speculate that these proteins form a regulatory complex at the cytoplasm-PM boundary. The overlapping expression patterns of *PID*, *PBP2* and the *PBKs* seem to corroborate this hypothesis. However, the existence of a functional PID-PBP2-PBK protein complex requires further *in vivo* confirmation.

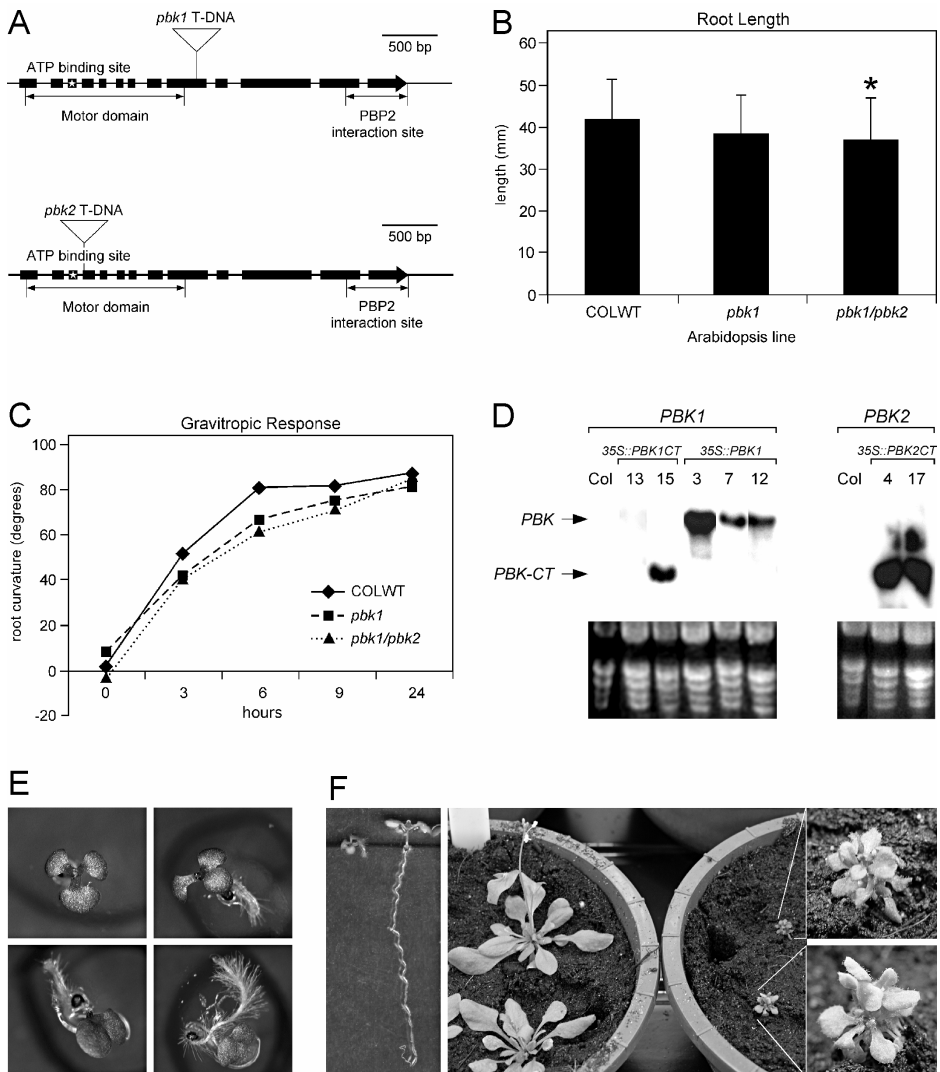


Figure 4. PBK1 and 2 act redundantly in the control of root growth and their overexpression affects cotyledon positioning. (A) Schematic diagram of the *PBK1* and *PBK2* genes indicating the T-DNA insertion sites in *pbk1* and *pbk2*. Boxes represent exons. The regions encoding the putative motor domain, the ATP binding site (star), and the BBP2 interaction site are indicated. (B) Ten-day-old seedlings of the *pbk1/pbk2* double mutant, but not of the *pbk1* single mutant, develop statistically significant shorter roots (star) compared to Columbia wild type (COLWT; Student's t-test $t=2.5$; $p>0.05$; $n=40$ for COLWT and $n=78$ for *pbk1/pbk2*). (C) Gravitropic response of COLWT, *pbk1* and *pbk1/pbk2* seedlings. Seedlings were grown for 5 days on vertically oriented plates, after which the plates were rotated 90°. The curvature of the root tips with the horizontal axis was monitored in time. At 6 and 9 hours post-reorientation, the roots of *pbk1/pbk2* showed statistically significant reduced curvature compared to COLWT (Student's t-test: for 6h $t=2.93$, $p>0.05$, $n=39$ for COLWT and $n=63$ for *pbk1/pbk2*; for 9h: $t=2.61$, $p>0.05$, $n=37$ for COLWT and $n=60$ for *pbk1/pbk2*). (D) Top panel: autoradiograph of a Northern blot of total RNA from 7-day-old seedlings of Columbia wild-type (Col), and of different *35S::PBK1*, *35S::PBK1-CT* and *35S::PBK2-CT* lines after hybridization with the *PBK1* and *PBK2* cDNA probes. Bottom panel: ethidium bromide stained gel. (E) *35S::PBK1* lines produce a significantly enhanced number of seedlings with cotyledon malformations. (F) Homozygous *35S::PBK1-3* seedlings (left picture; left seedling) show cotyledon defects combined with dwarf stature. These dwarf plants bolt with great delay but do not flower (middle picture; plants on the left are wild type looking heterozygous *35S::PBK1-3* plants; bushy plants on the right and inset are homozygous *35S::PBK1-3* plants).

PBK1 and PBK2 are possible regulators of PID activity

In this chapter we show that altered levels of PBK expression lead to discrete phenotypes that are also observed in Arabidopsis mutants that are defective in auxin transport. Roots of the *pbk1/pbk2* double mutant are slightly shorter and agravitropic compared to those of wild type plants. The mild phenotypic effects are probably due to the functional redundancy within the PBK clade. Triple and quadruple mutants in *PBK1*, *PBK2*, and their closest homologs are currently being generated to test this hypothesis. Furthermore, overexpression of *PBK1* under control of the *CaMV 35S* promoter resulted in defects in cotyledon positioning. Several independent *35S::PBK1* lines produced seedlings with three or fused cotyledons, a phenotype that is typically observed in *pid* loss-of-function mutants.

One of the *35S::PBK1* lines displayed severe phenotypes: seedlings had a dwarf stature and very short roots, and adult plants developed into bushy dwarfs that did not flower. The phenotypes of these plants resemble those of gibberellic acid (GA) or brassinosteroid biosynthesis or insensitive mutants (*ga1-3*, *det2*, *bri1*, *bin1* or *bin2*) (49-51). Interestingly, this particular line showed a very high level of *PBK1* overexpression, and segregation analysis suggested that the phenotypes were only observed in plants that are homozygous for the T-DNA insert. It is tempting to speculate that the observed phenotypes are dose dependent, and therefore only observed with above-threshold levels of *PBK1* overexpression. At this stage, however, we can not exclude that the phenotypes are the result of a recessive loss-of-function mutation caused by insertion of the overexpression T-DNA construct, possibly in a gene involved in brassinosteroid or GA signaling or biosynthesis.

In spite of the inconclusive phenotypes of the homozygous *35S::PBK1-3* plants, the tricotyledon phenotype is observed in several independent overexpression lines, with a highest frequency in the strong *35S::PBK1-3* line. In this respect, *PBK1* gain-of-function plants mimic *pid* loss-of-function mutants. The relatively low frequency of tricotyledon seedlings (2,6% in line *35S::PBK1-3* versus 10-50% in *pid* mutants alleles) may relate to the use of the *35S* promoter, which comes on relatively late during embryogenesis, mostly at stages where cotyledon primordia have already been established. In order to obtain more conclusive data on the effect of *PBK1* overexpression on embryo development, we are currently analyzing plants that express the *PBK1* cDNA under control of the *RPS5A* promoter that is highly active during early embryogenesis (52). As this promoter also provides high expression in meristems, we may find more lines that mimic the strong post-embryonic phenotypes of line *35S::PBK1-3*.

These results suggest that PBK1 and PID act antagonistically, but how is still unclear. From the *in vitro* phosphorylation experiments we can deduce that the PBP2-interacting C-terminus of PBK2 is not a phosphor-substrate of PID. Although new assays using the full length PBK proteins should determine whether other parts can be phosphorylated by PID, we hypothesize that PBKs – through their interaction with PBP2 – are rather involved in negatively regulating PID activity. Can we - based on this model - explain the mildly agravitropic and shorter roots observed for *pbk1/pbk2* double mutant seedlings? Both root growth and the gravitropic response of roots are depending on proper redistribution of auxin from the columella to the epidermal cells in the elongation zone of the root. This redistribution is mediated by the concerted action of PIN3 and PIN2, which redirect the auxin flow by their specific subcellular localization (53, 54). The observed phenotypic defects of the *pbk1/pbk2* seedlings could be the result of mis-localization of PIN2 and PIN3 due to a defect in repression of protein kinase activity by PBP2. As PID is not expressed in the root tip (55), it is most likely that PID-related protein kinases affect the PIN polarity in this organ. In line with this it was recently reported that loss-of-function mutants in *AtPK3/WAG1* and its closest homolog *AtPK3-like/WAG2* have a defective root waving response (56).

Concluding remarks

Although the results described in this chapter are far from being conclusive, they provide possible initial clues linking cytoskeletal-dependent intracellular trafficking to PID-mediated signaling in the control of PAT. We have identified two N-kinesins that could possibly play a role in this process by regulating the activity of PID and its family members. In the view of the possible interaction between PBP2 and the PBKs and the inhibitory effect of PBP2 on PID, it is plausible that the PBKs function

to transport PBP2 to repress the activity of PID or its related kinases in an asymmetric manner, thereby providing polarity to the signaling of these kinases.

ACKNOWLEDGEMENTS

This work was financially supported by CAPES (Brazilian Federal Agency for Post-Graduate Education, M. K.-Z.). We thank Bert van der Zaal for providing the root-specific cDNA library, Rene Benjamins for providing constructs pSDM6006 (H-PBP2), pSDM6014 (pBSSK-PBP2) and pSDM6025 (pTH2GFP-PBP2), Carlos Galvan for the plasmids encoding H-PID and PID-GFP, Johan Memelink for providing pET16H, Gerda Lamers for help with confocal laser scanning microscopy, Helene Robert for helpful comments on the manuscript, Peter Hock for art work, and the Salk Institute Genomic Analysis Laboratory for providing the sequence indexed Arabidopsis T-DNA insertion mutants *pbk1* and *pbk2*.

REFERENCE LIST

1. Kost, B., Bao, Y. Q. & Chua, N. H. (2002) *Philos. Trans. R. Soc. Lond B Biol. Sci.* **357**, 777-789.
2. Dong, C. H., Xia, G. X., Hong, Y., Ramachandran, S., Kost, B. & Chua, N. H. (2001) *Plant Cell* **13**, 1333-1346.
3. Schwab, B., Mathur, J., Saedler, R., Schwarz, H., Frey, B., Scheidegger, C. & Hulskamp, M. (2003) *Mol. Genet. Genomics* **269**, 350-360.
4. Hasezawa, S., Sano, T. & Nagata, T. (1998) *Protoplasma* **202**, 105-114.
5. Blackman, M. & Overall, L. (1998) *Plant Journal* **14**, 733-741.
6. Heinlein, M. (2002) *Curr. Opin. Plant Biol.* **5**, 543-552.
7. Jurgens, G. (2005) *Trends Cell Biol.* **15**, 277-283.
8. Chen, C., Marcus, A., Li, W., Hu, Y., Calzada, J. P., Grossniklaus, U., Cyr, R. J. & Ma, H. (2002) *Development* **129**, 2401-2409.
9. Ambrose, J. C., Li, W., Marcus, A., Ma, H. & Cyr, R. (2005) *Mol. Biol. Cell* **16**, 1584-1592.
10. Mathur, J. & Chua, N. H. (2000) *Plant Cell* **12**, 465-477.
11. Preuss, M. L., Kovar, D. R., Lee, Y. R., Staiger, C. J., Delmer, D. P. & Liu, B. (2004) *Plant Physiol* **136**, 3945-3955.
12. Lee, Y. R. & Liu, B. (2004) *Plant Physiol* **136**, 3877-3883.
13. Zhong, R., Burk, D. H., Morrison, W. H., III & Ye, Z. H. (2002) *Plant Cell* **14**, 3101-3117.
14. Pan, R., Lee, Y. R. & Liu, B. (2004) *Planta* **220**, 156-164.
15. Lee, Y. R., Giang, H. M. & Liu, B. (2001) *Plant Cell* **13**, 2427-2439.

16. Nishihama, R., Soyano, T., Ishikawa, M., Araki, S., Tanaka, H., Asada, T., Irie, K., Ito, M., Terada, M., Banno, H. *et al.* (2002) *Cell* **109**, 87-99.
17. Strompen, G., El Kasmi, F., Richter, S., Lukowitz, W., Assaad, F. F., Jurgens, G. & Mayer, U. (2002) *Curr. Biol.* **12**, 153-158.
18. Tanaka, H., Ishikawa, M., Kitamura, S., Takahashi, Y., Soyano, T., Machida, C. & Machida, Y. (2004) *Genes Cells* **9**, 1199-1211.
19. Hirokawa, N. & Takemura, R. (2004) *Exp. Cell Res.* **301**, 50-59.
20. Krendel, M. & Mooseker, M. S. (2005) *Physiology (Bethesda.)* **20**, 239-251.
21. Friml, J. & Palme, K. (2002) *Plant Mol. Biol.* **49**, 273-284.
22. Paponov, I. A., Teale, W. D., Trebar, M., Blilou, I. & Palme, K. (2005) *Trends Plant Sci.* **10**, 170-177.
23. Geldner, N., Friml, J., Stierhof, Y. D., Jurgens, G. & Palme, K. (2001) *Nature* **413**, 425-428.
24. Holweg, C. & Nick, P. (2004) *Proc. Natl. Acad. Sci. U S A* **101**, 10488-10493.
25. Boutte, Y., Crosnier, M. T., Carraro, N., Traas, J. & Satiat-Jeunemaitre, B. (2006) *J Cell Sci.*
26. Steinmann, T., Geldner, N., Grebe, M., Mangold, S., Jackson, C. L., Paris, S., Galweiler, L., Palme, K. & Jurgens, G. (1999) *Science* **286**, 316-318.
27. Geldner, N., Anders, N., Wolters, H., Keicher, J., Kornberger, W., Muller, P., Delbarre, A., Ueda, T., Nakano, A. & Jurgens, G. (2003) *Cell* **112**, 219-230.
28. Friml, J., Yang, X., Michniewicz, M., Weijers, D., Quint, A., Tietz, O., Benjamins, R., Ouwerkerk, P. B., Ljung, K., Sandberg, G. *et al.* (2004) *Science* **306**, 862-865.
29. Benjamins, R. Functional analysis of the PINOID protein kinase in *Arabidopsis thaliana*. 2004. Leiden University.
30. Sambrook, J., Fritsch, F. & Maniatis, T. (1989) *Molecular Cloning - A Laboratory Manual* (Cold Spring Harbour Laboratory Press, New York).
31. Guan, K. L. & Dixon, J. E. (1991) *Anal. Biochem* **192**, 262-267.
32. Chiu, W., Niwa, Y., Zeng, W., Hirano, T., Kobayashi, H. & Sheen, J. (1996) *Curr. Biol.* **6**, 325-330.
33. Gleave, A. P. (1992) *Plant Mol Biol* **20**, 1203-1207.
34. Neuteboom, L. W., Ng, J. M., Kuyper, M., Clijdesdale, O. R., Hooykaas, P. J. & van der Zaal, B. J. (1999) *Plant Mol. Biol.* **39**, 273-287.
35. Memelink, J., Swords, K., Staehelin, L. & Hoge, J. (1994) in *Plant Molecular Biology Manual*, eds. Gelvin, S., Schilperoort, R., & Verma, D. (Kluwer Academic Publishers, Dordrecht), pp. 1-26.
36. Schirawski, J., Planchais, S. & Haenni, A. L. (2000) *J Virol. Methods* **86**, 85-94.
37. Axelos, M., Curie, C., Mazzolini, L., Bardet, C. & Lescure, B. (1992) *Plant Physiol Biochem* **30**, 123-128.

38. Masson, J. & Paszkowski, J. (1992) *Plant J* **2**, 208-218.
39. Luschnig, C., Gaxiola, R. A., Grisafi, P. & Fink, G. R. (1998) *Genes Dev.* **12**, 2175-2187.
40. Clough, S. J. & Bent, A. F. (1998) *Plant J.* **16**, 735-743.
41. Reddy, A. S. & Day, I. S. (2001) *BMC. Genomics* **2**, 2.
42. Meyers, B. C., Lee, D. K., Vu, T. H., Tej, S. S., Edberg, S. B., Matvienko, M. & Tindell, L. D. (2004) *Plant Physiol* **135**, 801-813.
43. Zimmermann, P., Hirsch-Hoffmann, M., Hennig, L. & Gruissem, W. (2004) *Plant Physiol* **136**, 2621-2632.
44. Gingerich, D. J., Gagne, J. M., Salter, D. W., Hellmann, H., Estelle, M., Ma, L. & Vierstra, R. D. (2005) *J. Biol. Chem.* **280**, 18810-18821.
45. Du, L. & Poovaiah, B. W. (2004) *Plant Mol. Biol.* **54**, 549-569.
46. Bennett, S., Alvarez, J., Bossinger, G. & Smyth, D. (1995) *Plant J.* **8**, 505.
47. Benkova, E., Michniewicz, M., Sauer, M., Teichmann, T., Seifertova, D., Jurgens, G. & Friml, J. (2003) *Cell* **115**, 591-602.
48. Friml, J., Vieten, A., Sauer, M., Weijers, D., Schwarz, H., Hamann, T., Offringa, R. & Jurgens, G. (2003) *Nature* **426**, 147-153.
49. Li, J. & Chory, J. (1997) *Cell* **90**, 929-938.
50. Li, J., Nam, K. H., Vafeados, D. & Chory, J. (2001) *Plant Physiol* **127**, 14-22.
51. Sun, T., Goodman, H. M. & Ausubel, F. M. (1992) *Plant Cell* **4**, 119-128.
52. Weijers, D., Franke-van Dijk, M., Vencken, R. J., Quint, A., Hooykaas, P. & Offringa, R. (2001) *Development* **128**, 4289-4299.
53. Friml, J. (2003) *Curr. Opin. Plant Biol.* **6**, 7-12.
54. Bliilou, I., Xu, J., Wildwater, M., Willemsen, V., Paponov, I., Friml, J., Heidstra, R., Aida, M., Palme, K. & Scheres, B. (2005) *Nature* **433**, 39-44.
55. Benjamins, R., Quint, A., Weijers, D., Hooykaas, P. & Offringa, R. (2001) *Development* **128**, 4057-4067.
56. Santner, A. A. & Watson, J. C. (2006) *Plant J* **45**, 752-764.

PINOID phosphorylates the PIN cytoplasmic loop at multiple conserved serine residues

SUMMARY

The Arabidopsis PINOID (PID) protein serine/threonine kinase is a key regulator of auxin-mediated plant development, as threshold PID levels direct polar transport of auxin by determining the apico-basal polar targeting of the PIN auxin efflux transporters to the plasma membrane. The subcellular localization of animal transporters is known to be regulated by direct phosphorylation, mostly in a large cytoplasmic domain of these membrane proteins. Here we investigated the possibility that PIN proteins are direct phosphorylation targets of PID. *In silico* analysis of PIN1 revealed twenty-three putative phosphorylation sites, twenty-one of which are localized at the large cytoplasmic loop (CL) of this protein, and five of which are 100% conserved among the CL-containing PINs in Arabidopsis. *In vitro* assays using PID and synthetic PIN1 peptides containing most of the predicted phosphorylation sites identified four highly phosphorylated peptides comprising three of the predicted phosphorylated residues that are 100% conserved in the CL containing PINs. Notably, two of the strongly phosphorylated peptides comprise the T-P-R-X-S-N motif. By testing CLs of different PIN proteins and through site directed mutagenesis we deduced that the serines 231 and 290, both positioned in the conserved T-P-R-X-S-N motifs, are the major substrates for PID-mediated phosphorylation, and that the serines 377 and 380, that were previously shown to be phospho-substrates in PIN7 *in vivo*, may also be modified by PID. Our results suggest that the PID kinase affects PIN polarity through direct modification of multiple conserved serine residues in the large cytoplasmic loop of these auxin efflux facilitators.

Abbreviations: ARF-GEF, ADP-ribosylation factor-GTP exchange factor; BFA, Brefeldin A; F-actin, actin filament; GFP, green-fluorescent protein; GST, glutathione-S-transferase; IAA, indole-3-acetic acid; PAT, polar auxin transport; PBP, pinoid binding protein; PID, pinoid; PIN-CL, PIN cytoplasmic loop; PKA, cAMP-dependent protein kinase; PKC, protein kinase C; PM, plasma membrane

INTRODUCTION

The plant hormone auxin is an important regulator of plant development, and its - polar transport-driven - differential distribution in young growing organs is instrumental for a wide variety of developmental processes such as embryogenesis (1), root development (2), shoot organogenesis (3), and tropisms (4-6). The chemiosmotic model proposed for polar auxin transport (PAT) in the 1970s (7, 8), predicted that efflux carriers with a polar subcellular localization are essential for the direction of PAT, and thus for the positioning and maintenance of instructive auxin gradients in plants.

Molecular genetic studies in *Arabidopsis thaliana* identified the PIN family of membrane proteins as likely candidates for the auxin efflux carriers. These proteins were named after the *pin-formed* or *pin1* mutant, a loss-of-function mutant in the *PIN1* gene that is defective in PAT and develops pin-shaped inflorescences. The *Arabidopsis* genome encodes seven PIN1 homologs that have been named PIN2 to PIN8. PIN proteins contain two sets of five transmembrane domains that are linked by short and moderately conserved hydrophilic loops. In six of the PIN proteins the two transmembrane regions flank a large central hydrophilic cytoplasmic loop which contains several conserved stretches (4, 9). This domain structure is typical for proteins involved in transmembrane transport processes, and to date there is reasonably convincing evidence for the actual transport function of PIN proteins (10, 11). It has also been shown that PIN polar subcellular localization at the plasma membrane (PM) correlates well with the direction of PAT, and that their proper positioning is crucial for the correct directionality of the transport of auxin (1, 12, 13). Studies on the expression and subcellular localization of the different PIN proteins have drawn a complex picture that highlights specific roles for most of the PINs in auxin circulation and redistribution. The borders of action of each PIN, however, are far from being defined, and their functions commonly overlap. For example, it has been demonstrated that some PINs have their expression either enhanced and/or broadened to different cell files in the root tip in other *pin* loss-of-function backgrounds (14). This explains in part the observed functional redundancy among the different *PIN* genes (15-17).

The polar localization of PIN1 appears to primarily depend on the actin cytoskeleton (F-actin). It has been shown that the asymmetric localization of PIN1 in the PM is reduced in response to treatment with actin depolymerizing drugs. Interestingly, this treatment impairs PAT, corroborating the importance of F-actin and polar localization of PIN1 for this process. Actin depolymerization also prevents the internalization of PIN1 to endosomal compartments upon treatment with the vesicle trafficking inhibitor Brefeldin A (BFA), and the restoration of PIN1 localization after BFA wash-out, indicating that F-actin provides tracks for vesicle movement between the endosomal compartments and the PM (39). The ADP-Ribosylation Factor-GTP Exchange Factor (ARF-GEF) membrane protein GNOM was shown to be the BFA sensitive component that is required for recycling of PIN1 to the PM (18, 19). It remains to be established, however, whether GNOM is the polarity determinant in the recycling of PIN vesicles.

A true regulator of PIN polar targeting was identified through the *Arabidopsis pinoid* loss-of-function mutant that phenocopies the *pin formed* mutant. The *PINOID* gene was found to encode a protein serine/threonine kinase (20, 21) that determines the direction of PAT by regulating the subcellular polar localization of PIN proteins (22). Overexpression of *PID* results in targeting of PINs to the upper (apical) side of cells

in the root meristem, whereas PIN1 accumulates at the lower (basal) side of cells in the shoot meristem of *pid* loss-of-function mutants.

The fact that ectopic PID expression induces apical targeting of several PIN proteins suggests that the PID-dependent pathway recognizes a common feature in the PIN proteins. One possibility is that PID regulates an intermediate factor that in turn alters the polar targeting of PINs. The most attractive hypothesis, however, is that PID regulates the polar localization of PINs, and thereby the direction of PAT, through phosphorylation of PIN proteins. An interesting analogy exists between PID-dependent PIN polar localization in plant cells and signaling involved in polar deployment of transporters in animal cells. For example, asymmetric dispatch of the glucose transporter GLUT4 through secretory vesicles (GLUT4 secretory vesicles, or GSVs) has been demonstrated to be dependent on Protein Kinase C (PKC) phosphorylation of one particular GSV component, the insulin-responsive aminopeptidase (IRAP), at its amino terminal cytoplasmic loop (23). PKC has also been observed to mediate biphasic phosphorylation of the serotonin transporter (SERT), probably leading to SERT's silencing and subsequent internalization (24). It has also been shown that internalization of the dopamine transporter (DAT) is accelerated upon PKC activation, ultimately resulting in DAT accumulation in recycling endosomes (25). Finally, cAMP-dependent protein kinase (PKA) phosphorylation of the carboxy-terminal cytoplasmic loop of Aquaporin 2 (AQP2) has been demonstrated to be essential for the vesicle transport-mediated exocytosis of this water transporter to the apical membrane of renal duct cells (26, 27). Considering that PID and family members represent the likely plant orthologs of animal PKAs and PKCs (Galvan-Ampudia & Offringa, unpublished data) (28), it is possible that PID targets polar localization of PINs through phosphorylation of the central cytoplasmic loop of these proteins.

In this chapter we show that PID phosphorylates PIN proteins in the large cytoplasmic loop *in vitro*. By using deletion versions and generating single amino acid substitutions in the PIN1 loop, we were able to demonstrate that multiple conserved serine residues are targets for PID phosphorylation *in vitro*.

MATERIALS AND METHODS

Molecular cloning and constructs

Molecular cloning was performed following standard procedures (29). The generation of the yeast two-hybrid constructs pAS2-PID and pACT2-PBP2, the GST-PID construct (30, 31) and the histidine tagged-PIN fusions pET-PIN1CLsv (9), pET-PIN3CL (5), pET-PIN4CL (32) and pET-PIN7CL (1) and pGEX-PIN2CL (33) have been described previously. The yeast two-hybrid plasmid pACT2-PIN1CL and the pET-PIN6CL construct were kindly provided by Dr. Klaus Palme (Freiburg University, Germany) and Dr. Jiri Friml (University of Tübingen, Germany), respectively. The histidine tagged PID construct was created by digesting the *PID* cDNA with *XmnI-SalI* enzymes from a pBluescriptSK+-PID plasmid (31) and

cloned into pET16H (pET16B derivative, J. Memelink, unpublished results) treated with *Bam*HI and blunted and subsequently treated with *Xho*I. The GST-PIN1CL fusion was generated by cloning the *PIN1CL* *Sma*I/*Sall* fragment from pACT2-PIN1CL into the corresponding restriction sites in plasmid pGEX-KG (34).

Yeast two-hybrid interaction

Using the Matchmaker II yeast two-hybrid system and *Saccharomyces cerevisiae* strain PJ69-4A (Clontech), PBP2 and PIN1CL fused to the GAL4 activation domain (pACT2) were directly tested at 20°C for interaction with PID fused to the GAL4 DNA binding domain (pAS2).

In vitro pull down experiments

GST tagged full-length PID or GST protein alone were used in pull down assays with histidine (his)-tagged PIN1CLsv (H-PIN1CLsv). Cultures of *E. coli* strain BL21 containing one of the constructs were grown at 37°C to OD₆₀₀ 0,8 in 50 ml LC supplemented with antibiotics. The cultures were then induced for 4 hours with 1 mM IPTG at 30°C, after which cells were harvested by centrifugation (10 min. at 4.000 RPM in tabletop centrifuge) and frozen overnight at -20°C. Precipitated cells were re-suspended in 2 ml Extraction Buffer (EB: 1x PBS, 2 mM EDTA, 2 mM DTT, supplemented with 0,1 mM of the protease inhibitors PMSF - Phenylmethanesulfonyl Fluoride, Leupeptin and Aprotinin, all obtained from Sigma) for the GST-tagged proteins or in 2 ml Binding Buffer (BB: 50 mM Tris-HCl pH 6,8, 100 mM NaCl, 10 mM CaCl₂, supplemented with PMSF 0,1 mM, Leupeptin 0,1 mM and Aprotinin 0,1 mM) for the his-tagged PIN1CLsv and sonicated for 2 min. on ice. From this point on, all steps were performed at 4°C. Eppendorf tubes containing the sonicated cells were centrifugated at full speed (14.000 RPM) for 20 min., and the supernatants were transferred to fresh 2 ml tubes. H-PIN1CLsv supernatant was left on ice, while 100 µl pre-equilibrated Glutathione Sepharose resin (pre-equilibration performed with three washes of 10 resin volumes of 1x PBS followed by three washes of 10 resin volumes of 1x BB at 500 RCF for 5 min.) was added to the GST- fusion protein containing supernatants. Resin-containing mixtures were incubated with gentle agitation for 1 hour, subsequently centrifugated at 500 RCF for 3 min. and the precipitated resin was washed 3 times with 20 resin volumes of EB. Next, H-PIN1CLsv supernatant (approximately 2 ml) was added to GST-fusion-containing resins, and the mixtures were incubated with gentle agitation for 1 hour. After incubation, supernatants containing GST resins were centrifugated at 500 RCF for 3 min., the new supernatants were discarded and the resins subsequently washed 3 times with 20 resin volumes of EB. Protein loading buffer was added to the resin samples, followed by denaturation by 5 min. incubation at 95°C. Proteins were subsequently separated on a 12% polyacrylamide gel prior to transfer to an Immobilon™-P PVDF (Sigma) membrane. Western blots were hybridized using a horse radish peroxidase (HRP)-conjugated anti-pentahistidine antibody (Quiagen) and detection followed the protocol described for the Phototope-HRP Western Blot Detection Kit (New England Biolabs).

In vitro phosphorylation assays

Proteins used in *in vitro* phosphorylation assays were his- or GST- tagged for purification from several (usually five) aliquots of 50 ml cultures of *E. coli* strain BL21 which were grown, induced, pelleted and frozen as described above for the *in vitro* pull down experiments. Each aliquot of frozen cells pellet was resuspended in 2 ml Lysis Buffer (25 mM Tris-HCl pH 8,0; 500 mM NaCl; 20 mM Imidazol; 0,1% Tween-20; supplemented with 0,1 mM of the protease inhibitors PMSF, Leupeptin and Aprotinin) for the his-tagged proteins, or in 2ml of EB (supplemented with 0,1 mM of the protease inhibitors PMSF, Leupeptin and Aprotinin) for the GST-tagged proteins, and subsequently sonicated for 2 min. on ice. From this point on, all steps were performed at 4°C. Sonicated cells were centrifugated at full speed (14.000 RPM) for 20 min, the new pellets were discarded, and supernatants from all aliquots of the same construct were transferred to a 15 ml tube containing 100 µl of pre-equilibrated Ni-NTA resin (pre-equilibration performed with three washes of 10 resin volumes of Lysis Buffer at 500 RCF for 5 min.) for the his-tagged proteins or 100 µl of pre-equilibrated (see above) Glutathione Sepharose for the GST-tagged proteins.

Supernatants and resins were incubated with gentle agitation for 1 hour. After incubation, supernatants containing resins were centrifuged at 500 RCF for 3 min., the new supernatants were discarded and the resins subsequently washed: 3 times with 20 resin volumes of Lysis Buffer, once with 20 resin volumes of Wash Buffer 1 (25 mM Tris.Cl pH 8,0; 500 mM NaCl; 40 mM Imidazol; 0,05% Tween-20) and once with 20 resin volumes of Wash Buffer 2 (25 mM Tris-HCl pH 8,0; 600 mM NaCl; 80 mM Imidazol) for the his-tagged proteins; 3 times with 20 resin volumes of EB for the GST-tagged proteins. In between the washes, the resins were centrifugated for 5 min. at 500 RCF. After the washing steps, 20 resin volumes of Elution Buffer (25 mM Tris.HCl pH 8,0; 500 mM NaCl; 500 mM Imidazol) was added to the Ni-NTA resin and incubated for 15 min; the resin was subsequently centrifugated for 3 min. at 500 RCF and the supernatant containing the desired protein transferred to a new tube. For the GST-tagged proteins, the elution was performed by adding to the Glutathione Sepharose resin 3 resin volumes of Glutathione Elution Buffer (Reduced Glutathione 10 mM, Tris-HCl pH 8,0 50 mM), the mixture was gently agitated for 10 min at R.T., the resin was subsequently centrifugated for 3 min. at 500 RCF and the supernatant containing the desired protein transferred to a new tube; this process was repeated twice more. The solutions containing the proteins were diluted a 1000-fold in Tris Buffer (25 mM Tris.HCl pH7,5; 1 mM DTT) and concentrated to a workable volume (usually 50 µl) using Vivaspin microconcentrators (10 kDa cut off, maximum capacity 600 µl, manufacturer: Vivascience). Glycerol was added as preservative to a final concentration of 10% and samples were stored at -80°C.

Approximately 1 µg of each purified protein (PID and substrates) in maximal volumes of 10 µl were added to 20 µl kinase reaction mix, containing 1x kinase buffer (25 mM Tris-HCl pH 7,5; 1 mM DTT; 5 mM MgCl₂) and 1 x ATP solution (100 µM MgCl₂/ATP; 1 µCi ³²P-γ-ATP). Reactions were incubated at 30°C for 30 min. and stopped by the addition of 5 µl of 5 x protein loading buffer (310 mM Tris-HCl pH 6,8; 10 % SDS; 50% Glycerol; 750 mM β-Mercaptoethanol; 0,125% Bromophenol Blue) and 5 min. boiling. Reactions were subsequently separated over 12,5% acrylamide gels, which were washed 3 times for 30 min. with kinase gel wash buffer (5% TCA – Trichloroacetic Acid; 1% Na₂H₂P₂O₇), coomassie stained, destained, dried and exposed to X-ray films for 24 to 48 hours at -80°C using intensifier screens. For the peptides assays, 1µg of purified PID was incubated with 4 nmol of 9^{mer} biotinilated peptides (Pepscan) in a phosphorylation reaction as described above. Reaction processing, spotting and washing of the SAM² Biotin Capture Membrane (Promega) were performed as described in the corresponding protocol. Following washing, the membranes were wrapped in plastic film and exposed to X-ray films for 24 to 48 hours at -80°C using intensifier screens. The phosphorylation intensities of each peptide were determined by densitometry analysis of the autoradiographs using the ImageQuant software (Molecular Dynamics).

Site directed mutagenesis

For the site directed mutagenesis we used the Quickchange XL site directed mutagenesis kit (Stratagene). The oligonucleotides used to introduce mutations in the *PIN1CL* cDNA were 5'-CGACACCTAGACCTGCGAATCTAACCAACG-3' and 5'-CGTTGGTTAGATTGCGAGGTCTAGGTGT CG-3' to change the serine 231 for alanine, 5'-CCTACTCCGAGACCTGCCAACTACGAAGAAG-3' and 5'-CTTCTTCGTAGTTGGCAGGTCTCGGAGTAGG-3' to change serine 290 for alanine, 5'-GGCTT ATCTGCGGCACCTAGACC-3' and 5'-GGTCTAGGTGCCGCAGATAAGCC-3' to change threonine 227 for alanine, 5'-GGCTTATCTGCGGCACCTAGACCTGCGAATCTAACCAACG-3' and 5'-CGTTGGTT AGATTGCGAGGTCTAGGTGCCGCAGATAAGCC-3' to replace both threonine 227 and serine 231 for alanines, 5'-GGTTCTAAAGGTCTGCTCCGAGACCTTCC-3' and 5'-GGAAGGTCTCGGAGCAGGACC TTTAGAACC-3' to replace threonine 286 for alanine, and 5'-GGTTCTAAAGGTCTGCTCC GAGACCTGCCAACTACGAAGAAG-3' and 5'-CTTCTTCGTAGTTGGCAGGTCTCGGAGCAGGACC TTTAGAACC-3' to replace threonine 286 and serine 290 for alanines at once.

The oligonucleotides used to introduce mutations in the *PIN1CLsv* cDNA were 5'-CGAATT CTACTCGAGACCTGCCAACTACGAAGAAGAC-3' and 5'-GTCTTCTTCGTAGTTGGCAGGTCTCGA GTAGAATTCG-3' to replace serine 290 for alanine.

RESULTS

The PIN1 cytoplasmic loop is a likely target for phosphorylation

The previous observations that PID activity affects PIN polar targeting (22), and that phosphorylation of transporters is a signal for endo- or exocytosis in animal cells (23, 26, 27, 35), led us to investigate whether PIN proteins are phosphorylation targets of the PID protein kinase. The fact that PINs contain transmembrane domains (Figure 1A), as predicted by Predictprotein (36), precludes the use of the complete proteins in *in vitro* phosphorylation assays. As an alternative approach we used the NetPhos program (37) to first identify putative phosphorylation sites in PIN1. This identified twenty-three possible phosphorylation sites, twenty-one of which are located in the large cytoplasmic loop of PIN1 (Figure 1B). Since trafficking-related phosphorylation of animal transporters is known to occur in the large cytoplasmic domain of these proteins (23, 26, 27, 35), we decided to focus our analysis on the cytoplasmic loop of PIN1 (PIN1CL).

PINOID does not show a strong interaction with the PIN1 cytoplasmic loop

First, we tested the physical interaction between PID and its putative phospho-target PIN1CL. Two yeast plasmids, the bait encoding PID fused to the GAL4 DNA binding domain (BD), and the prey encoding a fusion between PIN1CL and the GAL4 activation domain (AD), were co-introduced in the yeast strain PJ69-4A. A prey plasmid encoding the PID Binding Protein 2 (PBP2) GAL4 AD fusion was used as a positive control in this yeast two-hybrid experiment (Figure 1C). In a parallel approach, we tested *in vitro* pull down of an his-tagged shorter version of PIN1CL (PIN1CLsv) with GST-tagged PID (Figure 1D). Neither of the two approaches detected a direct interaction between PID and PIN1CL. The interaction between the PID protein serine/threonine kinase and its substrates may be very transient, and it could be that such weak interactions are not detected using the above-mentioned methods. Moreover, we can not exclude that PID interacts with other regions of PIN1 protein or that PID needs accessory proteins for its interaction with PIN1.

PID phosphorylates the cytoplasmic loop of PIN proteins *in vitro*

Next we co-incubated histidine-tagged PID with GST-tagged PIN1CL in an *in vitro* phosphorylation reaction. Following separation of the proteins on gel and autoradiography, clear PID-dependent phosphorylation of the PIN1CL was detected (Figure 1E). In order to map the PID substrates in PIN1CL, we synthesized seventeen PIN1CL-specific peptides containing all the twenty-one putative phosphorylation sites predicted by NetPhos (Figure 1B) (37). From these, only twelve peptides could be used in our assay, as the others could not be dissolved in the reaction buffer. The twelve soluble peptides represent seventeen of the putative

phosphorylation sites. *In vitro* phosphorylation reactions revealed that peptides 2, 6, 11 and 12, respectively corresponding to the sequences GLSATPRPS, TPRPSNYEE, VMPPTSVMT and RNPNSYSS, were most intensely phosphorylated by PID (Figure 1F).

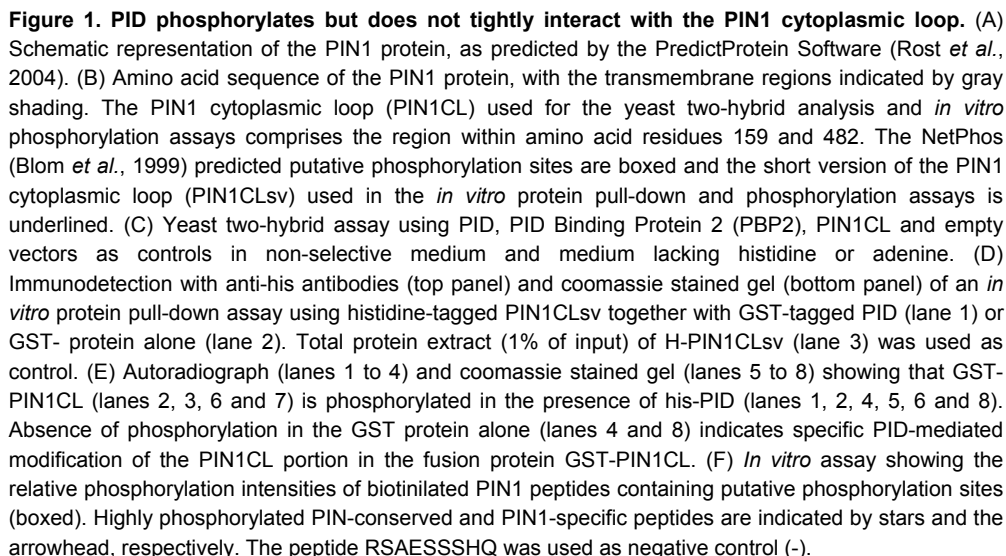
Since the PID-dependent switch in basal-to-apical polar targeting is not restricted to PIN1, but has also been observed for PIN2 and PIN4 (22), we aligned the cytoplasmic loops of PIN1, 2, 3, 4, 6 and 7 to identify the conserved serine- and threonine residues. Indeed several of such residues appeared to be fully conserved in the different CLs, although only five of them were predicted by the NetPhos program (37) to be putative phosphorylation sites (Figure 2). Interestingly, three of the five conserved and predicted phosphorylation sites are located in two TPRXSN motifs represented by peptides 2 (GSATPRPS) and 6 (TPRPSNYEE) that were highly phosphorylated by PID (Figure 1F and 2).

To test whether PID also phosphorylates the CLs of other PIN proteins, and to identify the phosphorylated residues, we performed new phosphorylation assays using his- or GST-tagged versions representing different portions of the CLs loops of PIN1 (PIN1CLsv), PIN2 (PIN2CL), PIN3 (PIN3CL), PIN4 (PIN4CL), PIN6 (PIN6CL) and PIN7 (PIN7CL) (Figure 3A). Notably, those PINCLs containing one or both of the conserved TPRXSN motifs were phosphorylated, whereas the PINCLs lacking these motifs showed much reduced phosphorylation levels (Figures 3B and 3C). These results suggested that the two conserved TPRXSN motifs represent the most significant targets in the PINCLs for post-translational modification by the PID protein kinase.

PID phosphorylates multiple conserved residues in the PINCL

In the view of the previous observations, we created the GST-tagged PIN1CL mutants PIN1CL^{S231A S290A}, PIN1CL^{T227A S231A S290A} and PIN1CL^{T227A S231A T286A S290A}, in which the serines and threonines in the two TPRXSN motifs were replaced by alanines. The mutations S231A and S290A resulted in a significant reduction in phosphorylation of PIN1CL (Figure 3D), whereas the mutations T227A and T286A did not cause a further reduction of the phosphorylation signal (Figure 3E). This result supports the previous conclusion that the conserved TPRXSN motifs represent important PID phospho-substrates in the PINCLs. However, the phosphorylation levels observed in the mutant PIN1CLs are still considerable (Figures 3D and 3E), suggesting that additional serine or threonine residues are phosphorylated by PID.

Considering that the GST-PIN1CL and GST-PIN1CL^{S231A S290A} proteins produce several breakdown products that are differentially phosphorylated (Figures 1E and 3D), we used these characteristics to estimate the position of other putative PID



				*		
PIN1CL	GAKLLISEQF	P.DTAGSIVS	IHVDSDIMSL	DGRQPLETEA	EIKEDGKLHV	
PIN2CL	GAKLLISEQF	P.ETAGSITS	FRVDSVISL	NGREPLQTD	EIGDDGKLHV	
PIN3CL	GAKMLIMEQF	P.ETAASIVS	FKVESDVVSL	DGHDFLETDA	EIGDDGKLHV	
PIN4CL	GAKLLIMEQF	P.ETGASIVS	FKVESDVVSL	DGHDFLETDA	EIGNDGKLHV	
PIN6CL	AARLLIRAEF	PGQAAGSI	IAKIQVDDVLSL	DGMDPLRTET	ETDVNGRIRL	
PIN7CL	GAKILIMEQF	P.ETGASIVS	FKVESDVVSL	DGHDFLETDA	QIGDDGKLHV	
	*	*		*		
PIN1CL	TVRRSNASRS	DIYSR....	.RSQGLSATP	RPSNLTNAEI	YSLQSSRN.P	
PIN2CL	VVRRSSAASS	MISSFNKSHG	GGLNSSMITP	RASNLTGVEI	YSVQSSRE.P	
PIN3CL	TVRKSNASRR	SFCG.....PNMT	RPSNLTGAEI	YSLST.....	
PIN4CL	TVRKSNASRR	SLM.....MTP	RPSNLTGAEI	YSLSS.....	
PIN6CL	RIRRSVSSVP	DSVMSS....SLCLTP	RASNLNAEI	FSVNTPNNR	
PIN7CL	TVRKSNASRR	SFYGG.....	.G..GTNMT	RPSNLTGAEI	YSLNT.....	
	*	*				
PIN1CL	TPRGSSFNHT	DFYSMMAS..GGGRNSNFG	PGEAVFG...	
PIN2CL	TPRASSFNQT	DFYAMFNASK	APSPRHGYTN	SYGGAGAGPG	.GDVYSLQS.	
PIN3CL	TPRGSNFNHS	DFYNMMGF..PGGRLSNFG	PADMYSVQS.	
PIN4CL	TPRGSNFNHS	DFYSVMGF..PGGRLSNFG	PADLYSVQS.	
PIN6CL	FHGGGSGTTL	QFYNGSNE..IM	FCNGDLGGFG	FTRPGLGASP	
PIN7CL	TPRGSNFNHS	DFYSMMGF..PGGRLSNFG	PADMYSVQS.	
		*	*			
PIN1CLSKGFTPRP	SNYEEDGGPA	KPTAAGTAAG	AGRFHYQSGG	
PIN2CLSKGVTPRT	SNFDEEVMT	AKKAGRGR.SM	
PIN3CLSRGFTPRP	SNFEENCAMA	SSPRFGY..	
PIN4CLSRGFTPRP	SNFEENNAV.	...KYGFYNN	T....NSSV	
PIN6CL	RRLSGYASSD	AYSLOFTPR	SNFNELDVN.	
PIN7CLSRGFTPRP	SNFEESCAMA	SSPRFGY..	
PIN1CL	SGGGGG....	AHYAPNPGM	FSPNTGGGG	TAAKGNAPVV	GGKRQD....	
PIN2CL	SGELYNNNSV	PSYPPNPMF	TGSTSGASGV	KKKESGGGGS	GGGVGVG...	
PIN3CL	PGGGA....	GSYPAPNPEF	SSTTTSTA.N	.KSVNKNPKD	VNTNQQTTL	
PIN4CL	PA..A....	GSYPAPNPEF	S...TGTGVS	TKP.NKIPKE	.N.QQQ..LQ	
PIN6CL	GN....G..	TPVWMKSPAA	GRIYRQS...	
PIN7CL	PGG.AP....	GSYPAPNPEF	S....TG.N	.KTGSKAPKE	.N.HHH..V.	
			*	*		
PIN1CLGN...	.GRDLHMFVW	SSSASPVSDV	FGG....GGGNHHADY	
PIN2CL	..GQ..N...	..KEMNMFVW	SSSASPVSEA	NAKNAMTRGS	
PIN3CL	TGGK..SN.SH	DAKELHMFVW	SSNGSPVSDR	A.GLVNFGGA	PDNDQGG..R	
PIN4CL	..EKDSKASH	DAKELHMFVW	SSSASPVSD.	VFG....GGA	..GDNVATEQ	
PIN6CLSPKMMW	E.....	
PIN7CL	..GK..SN.SN	DAKELHMFVW	GNGSPVSDR	A.GLQVDNGA	..NEQVG..K	
			▲	▲		
PIN1CL	STATNDHQKD	VKISVPQGN.	SNDNQ.....	
PIN2CL	S..T.DVSTD	PKVSIPPHDN	LATKAMQNLI	ENMSPGRKG.	
PIN3CL	SDQG.AKEIR	MLVPDQSHNG	ETKAVAHPAS	G.DFGG...	EQQFSFAGKE	
PIN4CL	SEQG.AKEIR	MVVSQDQPRK.	SN.ARG...G	GDDIGG...L	D...S..G..	
PIN6CL	SQGR.HAAKD	INGSVPEKEI	SFRDALKAAP	QATAAG....	
PIN7CL	SDQGGAKEIR	MLISDHTQNG	ENKA.G.PMN	G.DYGG....	E.....	
PIN1CL	.YVER..EEF	SFGNKDDDSK	VLATDGGN..	...NISNKT	QAK.VMPPTS	
PIN2CL	.HVEMD....	QDGNNGGKSP	YMGKKGS DVE	DG.GPG....	PRKQMPPAS	
PIN3CL	EEAER.PKDA	ENGLNKLAPN	STAALQSK..	TGLG.GAEAS	QRK.NMPPAS	
PIN4CL	.EGEREIEKA	TAGLNKMGSN	STAELEAAGG	DG.G.G.NNG	.T..HMPPTS	
PIN6CLGGASM	EEGAAGKDTT	PVAAIG....	.KQ.EMP	
PIN7CL	EESER.VKEV	PNGLHKLRCN	STAE LNPK..	EA IETG.ETV	PVK.HMP	
			*			
PIN1CL	VMTRLILIMV	WRKLIRNPNS	YSS			
PIN2CL	VMTRLILIMV	WRKLIRNPNT	YSS			
PIN3CL	VMTRLILIMV	WRKLIRNPNT	YSS			
PIN4CL	VMTRLILIMV	WRKLIRNPNT	YSS			
PIN6CL	VMMRLILITV	GRKLSRNPNT	YSS			
PIN7CL	VMTRLILIMV	WRKLIRNPNT	YSS			

Figure 2. Conserved putative phosphorylation sites in the cytoplasmic loops of PINs. Residues labeled with black (serines and threonines) and light gray (other amino acids) shading are completely conserved in the Arabidopsis PINCLs; Serines or threonines that are conserved in four or five of the six PINCLs are indicated by dark gray shading. Conserved serines or threonines that are predicted to be phosphorylated by NetPhos (Blom *et al.*, 1999) are marked with a star. Boxes highlight conserved TPRXSN motifs. The PKC-like and MAPK phosphorylation sites detected by Nushe and co-workers (Nuhse *et al.*, 2004) are indicated by empty (except for the methionine) and filled arrowheads, respectively.

phosphorylation sites. First we predicted the sizes of the phosphorylated breakdown products based on the protein size marker (not shown) and the known sizes of the full-length GST-PIN1CL (60 kDa) and his-PID (53 kDa). For this analysis we assumed that, based on their purification with glutathione beads, each GST-PIN1CL breakdown product should at least comprise the GST moiety (27 kDa). The smallest phosphorylated GST-PIN1CL breakdown product was estimated to be 35 kDa with an 8 kDa N-terminal part of PIN1CL containing the first conserved TPRXSN motif with serine 231. This was confirmed by the observation that the corresponding part of the GST-PIN1CL^{S231A S290A} mutant protein is not phosphorylated (Figure 3D). The next phosphorylated GST-PIN1CL breakdown product was estimated to be 43 kDa, and should comprise a 16 kDa N-terminal PIN1CL portion containing the serines 231 and 290 of the two conserved TPRXSN motifs, peptide 3 (YSLQSSRNP) that was weakly phosphorylated by PID (Figure 1F), and a third less well conserved TPRXS motif containing serine 252 (Figures 1B and 2). The fact that the corresponding GST-PIN1CL^{S231A S290A} mutant breakdown product is only weakly phosphorylated (Figure 3D), suggests that serines 231 and 290 are the main phosphorylation substrates of PID, and that the serines in YSLQSSRNP or TPRGSS are only weakly contributing to PID-mediated phosphorylation. The next two strongly phosphorylated GST-PIN1CL sub-products are respectively 47 and 50 kDa and include two additional conserved serines 377 and 380 that are putative weak phosphorylation targets of PID, based on the phosphorylation signal obtained with the corresponding peptide 8 (SSSASPVSD, Figure 1F). Interestingly, the same residues were shown to be *in vivo* phospho-substrates in PIN7 (38). Considering that the corresponding protein fragments derived from the mutant GST-PIN1CL^{S231A S290A} are efficiently phosphorylated (Figure 3D), it is likely that serines 377 and 380 are significantly modified by PID. Finally, the full length GST-PIN1CL and GST-PIN1CL^{S231A S290A} are efficiently modified by PID, but not more efficiently than the 47 and 50 kDa GST-PIN1CL break down products. The peptides 11 (VMPPTSVMT) and 12 (RNPNSYSS), which were observed to be very significantly phosphorylated by PID (Figure 1F), do not seem to significantly contribute to PID-mediated phosphorylation when in context of the full length cytoplasmic loop.

To narrow down the search for the other phospho-target sites of PID, further assays employed a shorter version of the PIN1CL (PIN1CLsv) and two of its mutant versions, PIN1CLsv^{S290A} in which serine 290 was replaced for an alanine, and PIN1CLsv^{ΔCT} lacking carboxy-terminal amino acids including serines-377 and -380 (Figure 3A). The results showed that PIN1CLsv and PIN1CLsv^{ΔCT} were still efficiently phosphorylated, but that PIN1CLsv^{S290A} was modified at a much reduced level (Figure 3F). In one hand, this confirmed that serine 290 is one of the most efficient targets of the PID kinase in the PIN1CLsv. On the other hand, the minor signal observed in PIN1CLsv^{S290A} indicates that other residues in this protein could still be phosphorylated at low levels. Based on the results obtained in the peptide experiments (Figure 1F), and on the analysis of the breakdown products of GST-PIN1CL, other putative phosphorylation targets of PID in PIN1CLsv^{S290A} could be the conserved serines 377 and 380. However, the significance of PID-mediated modification of these serines remains to be addressed.

DISCUSSION

Proper polar subcellular localization of PIN proteins in the plasma membrane of plant cells is essential for the correct directionality of PAT (12, 13, 17). Moreover, the apical-basal polar targeting of PINs has been demonstrated to be determined by the levels of activity of the serine/threonine kinase PID (22). PID belongs to the plant specific AGCVIII group of protein kinases (20, 21). Animal orthologs of these kinases are also known to play a role in regulating the membrane localization of transporter proteins by phosphorylation of their cytoplasmic loops (23, 26, 27). Therefore, it is conceivable that PID mediates its effect through phosphorylation of the cytoplasmic loop of PIN proteins.

PID-dependent phosphorylation of PINs may direct PIN apical targeting

Recently, several lines of evidence indicate that signals for the subcellular polar localization of PIN proteins are embedded in their amino acid sequence. For example, it has been shown that deployment of PIN1 to the correct cellular pole was affected by the position of the GFP insertion in the large cytoplasmic loop (13). Moreover, modification of a serine residue in one of the short cytoplasmic loops of PIN2 to a glycine resulted in failure of PIN2 deployment to the PM (11). Although these data do not clarify the particular signal responsible for PIN exocytosis, it is suggestive that protein modification, and possibly phosphorylation, events could be important for this process.

Accordingly, our own analysis shows that multiple putative phosphorylation sites are present in the large cytoplasmic loop that is present in six of the eight PINs, and that some of these sites are conserved among these proteins. Recently, Nuhse and co-

workers (38) showed that the cytoplasmic loop of the *Arabidopsis thaliana* PIN7 is phosphorylated *in vivo* in two conserved serines that were predicted as MAPK and PKC phosphorylation sites.

In the present work we show that PID is capable of phosphorylating different PINCLs *in vitro*. Our analysis suggests that PID modifies the serines 290 and 231

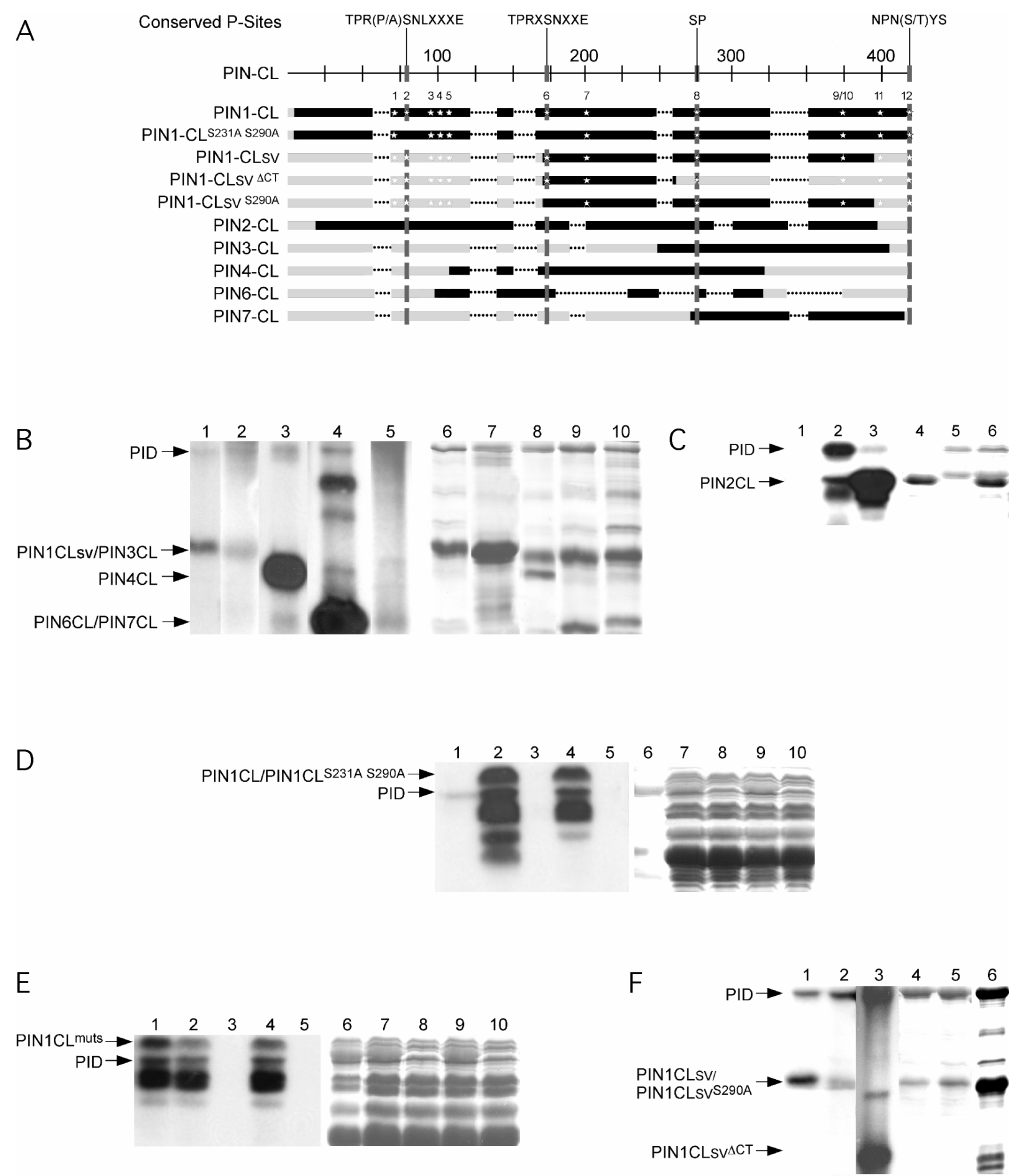


Figure 3. PID phosphorylates PINCLs in conserved sites. (A) Schematic alignment of the complete cytoplasmic loops of Arabidopsis PIN1, 2, 3, 4, 6 and 7. Thin punctuated lines indicate gaps in the alignment. The 100% conserved predicted phosphorylation sites are indicated with thin vertical dark gray bars. The parts of the CLs that were tested in the *in vitro* phosphorylation assays with PID are indicated with black bars. The positions of the peptides used in *in vitro* phosphorylation assays are indicated with stars in the PIN1CL. The corresponding numbers (see also Figure 1F) are provided above the alignment. (B) Autoradiograph (lanes 1 to 5) and coomassie stained gel (lanes 6 to 10) of an *in vitro* phosphorylation assay using his-PID (all lanes) together with his-PIN1CLsv (lanes 1 and 6), his-PIN3CL (lanes 2 and 7), his-PIN4CL (lanes 3 and 8), his-PIN6CL (lanes 4 and 9) or his-PIN7CL (lanes 5 and 10). (C) Autoradiograph (lanes 1 to 3) and coomassie stained gel (lanes 4 to 6) of an *in vitro* phosphorylation assay of GST-PID (lanes 2, 3, 5 and 6) together with GST-PIN2CL (lanes 1, 3, 4 and 6). (D) Autoradiograph (lanes 1 to 5) and coomassie stained gel (lanes 6 to 10) of an *in vitro* phosphorylation assay of his-PID (lanes 1, 2, 4, 6, 7 and 9) together with GST-PIN1CL (lanes 2, 3, 7 and 8) or GST-PIN1CL^{S231A S290A} (lanes 4, 5, 9 and 10). (E) Autoradiograph (lanes 1 to 5) and coomassie stained gel (lanes 6 to 10) of an *in vitro* phosphorylation assay of his-PID (lanes 1, 2, 4, 6, 7 and 9) together with the GST-PIN1CL mutants (PIN1CL^{mut}) GST-PIN1CL^{S231A S290A} (lanes 1 and 6), GST-PIN1CL^{T227A S231A S290A} (lanes 2, 3, 7 and 8) or GST-PIN1CL^{T227A S231A T286A S290A} (lanes 4, 5, 9 and 10). (F) Autoradiograph (lanes 1 to 3) and coomassie stained gel (lanes 4 to 6) of an *in vitro* phosphorylation assay of his-PID (all lanes) together with his-PIN1CLsv (lanes 1 and 4) or his-PIN1CLsv^{S290A} (lanes 2 and 5) or his-PIN1CLsv^{ΔCT} (lanes 3 and 6).

that are fully conserved in the different PINCLs. This could be an indication that PID is a common regulator of the different PINs, which could also explain the *in vivo* effect of altered PID activity on several of these proteins (22). The strong putative PID targets are other residues than the ones identified by Nushe and co-workers (corresponding PIN1 serines-377 and -380) (38), but we provide evidence that the latter may also be modified by the PID kinase, albeit at a much reduced level. Interestingly, if the *in vivo* PID phosphor-targets in the PIN proteins do correspond to the conserved serines 290 and 231 of PIN1, this implies that multiple pathways could be involved in regulating the subcellular localization of the PIN proteins. Several phosphorylation events may also lead to different effects on PINs such as modification in the activity and/or intracellular trafficking. For example, it has been observed that the kinase PKC mediates biphasic phosphorylation of the serotonin transporter (SERT), probably leading to SERT's inactivation and subsequent internalization (24).

PIN3 provides an exception in its response to elevated levels of PID. PIN3 contains all conserved phosphorylation sites present in other PIN proteins, including the ones that are putative phosphor-substrates of PID. However, its symmetric distribution in columella cells (5) is not responsive to PID overexpression (22). Preliminary data suggest that PIN3 is sensitive to the PID induced basal-to-apical switch in polar targeting when expressed in the root epidermis (Friml and co-workers, unpublished data). This suggests that there is a cell-type specific responsiveness to PID, which may be determined by the presence of PBPs that regulate PID activity (Chapters 2

and 3 of this thesis) (30, 31). Alternatively, the unresponsiveness of PIN3 in the columella could be explained by the existence of a PID-independent mechanism that determines a “pre-polar” distribution of PINs. In this framework PID action would determine the correct pole for the PINs which are predestined to have basal-apical subcellular localization. For example, PIN1, which is affected by PID, has been shown to be still polarly distributed at the basal side of epidermal cells in the shoot apex of the *pid* mutant (22). PIN3 may not be susceptible to PID signaling in columella cells due to the hypothetical fact that it does not undergo a “pre-polar” arrangement in these cells.

To further assess the significance of the putative *in vivo* PID-mediated phosphorylation of PINs, we are currently generating *pPIN1::PIN1-GFP* constructs harboring serine to alanine or serine to aspartic acid mutations in the *in vitro* identified PID phosphor-substrates. It is our expectation that such new plant lines will report the consequences of the hypothetical reduced or constitutive PID-mediated phosphorylation for the PIN1 protein.

Hypothetical molecular mechanisms of PID-dependent PIN regulation

Striking analogies have been found between the hypothetical PID-mediated regulation of PIN protein deployment in plant cells and the sub-cellular localization of membrane proteins in animal cells. In mammals, for example, PKC has been implicated in promoting endocytosis of the serotonin and dopamine transporters as well as exocytosis of the glucose transporter GLUT4 (23-25). In another example, it has been shown that PKA phosphorylates a cytoplasmic domain of the water transporter AQP2 in order to promote its exocytosis into the apical membrane of canine renal collecting duct cells (27). The latter situation seems to be more comparable to the PID-induced PINs polar switch, since it involves direct phosphorylation of the transporter leading to its targeting to the apical cell pole. The indications that PID could be directly involved in the mediation of endo- or exocytosis in plants, as well as our unpublished observations regarding the PID substrate preference (Galvan and Offringa, unpublished data), may be significant evidence that this kinase is the plant ortholog of PKA or PKC, as previously proposed by Benjamins and co-workers (21) and Bogre and co-workers (28).

Although very interesting, these analogies still lack considerable experimental evidence regarding what exactly could be the consequences of the hypothetical PID phosphorylation of PINs *in vivo* (does it lead to endo or exocytosis?), and what are the components acting prior to or after PID action that ultimately drive PINs to their polar localization at the PM. It is known, for example, that the ARF-GEF protein GNOM is required for the polar PIN1 localization at the PM (19, 39), but the connection between PID and GNOM remains obscure. It is believed that ARF-GEFs determine the destination of membrane trafficking vesicles by specifically recruiting

vesicle-coating proteins that define their cellular location, including COP1 and clathrin coats (40). Consequently, it is possible that GNOM is required for the migration of PIN1 from endosomal compartments to the apical or basal cell pole at the PM, although not necessarily the correct one, while PID activity could be required for the localization of PIN1 in the proper cellular pole. This assumption is corroborated by observations that in *gnom* loss-of-function embryos PIN1 is at the membrane, although in randomized polarities (18), and that in epidermal cells of inflorescence apices of *pid* loss-of-function plants PIN1 is localized at basal, instead of the apical, pole in the PM (22). Considering that PID probably phosphorylates PINs *in vivo*, three situations could possibly explain the relationship between PID, PINs and ARF-GEFs such as GNOM (Figure 4). PID could phosphorylate PINs following ARF-GEF action when they are already placed at the PM, and this modification could enable PINs to stay or go to a polar position (Figure 4A). Alternatively, PID could phosphorylate PINs in endosomal compartments prior to their ARF-GEF-dependent translocation to the PM. Subsequently, upon ARF-GEF-mediated transport of PIN vesicles, the phosphorylation would be an important informative signal for the polar deposition of these proteins in the PM (Figure 4B). A third possibility is that PID counteracts an hypothetical default basal localization of PINs determined by GNOM action (Figure 4B). The relationship between GNOM and PID-mediated PIN phosphorylation needs further investigation.

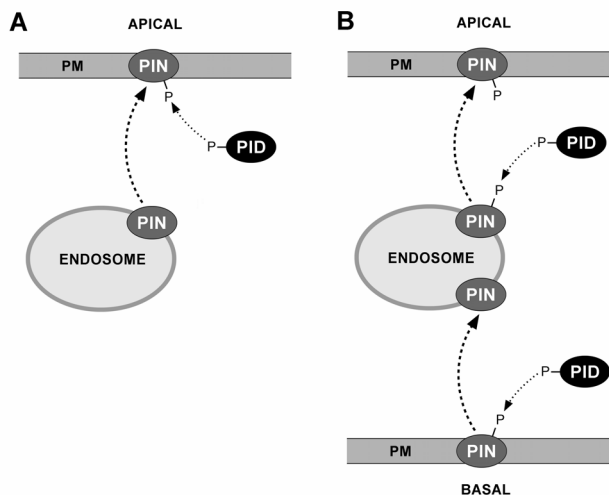


Figure 4. Models describing the molecular mechanism of PID action on PIN polar targeting. (A) PID-mediated phosphorylation of PIN proteins at the apical cell side could inhibit their endocytosis, thereby causing retention of these proteins at plasma membrane (PM). (B) PID-mediated phosphorylation of PIN proteins at the basal cell side could label these proteins for endocytosis and subsequent trafficking via endosomal compartments to the apical cell side. In parallel, PID could label endosomal PIN proteins for apical targeting.

Redundancy in PID function

Data shown in this chapter suggest that most PINs are susceptible to PID phosphorylation. However, acknowledged PID-sensitive PINs play a role in tissues such as roots (PIN1, PIN2 and PIN4) (4, 9, 32), hypocotyls (PIN1) (41), inflorescence meristem (PIN1) (3) and embryo (PIN1, PIN4) (1, 22, 32), whereas PID function is apparently limited to the latter two tissues (20-22, 42). Assuming that PID-like signaling is probably essential for PIN polarity throughout the whole plant, it is logical to assume that PID-related kinases likely regulate PINs in other tissues than in inflorescence meristems or embryos. Our previous analysis of the Arabidopsis genome identified twenty-two other members of the plant specific family of protein kinases to which PINOID belongs (21). Most likely, some of these members are also putative PINs regulators, and the comparative study of their function and activity will help to clarify their role in the regulation of the direction of PAT.

ACKNOWLEDGEMENTS

This work was funded by grant from CAPES (Brazilian Federal Agency for Post-Graduate Education, M.K.-Z.). The yeast two-hybrid plasmid pACT2-PIN1CL was kindly provided by Dr. Klaus Palme (Max-Delbruck-Laboratorium in der Max-Planck-Gesellschaft, Germany). The histidine tagged-PIN fusions pET-PIN1CLsv, pET-PIN3CL, pET-PIN4CL, pET-PIN6CL and pET-PIN7CL were kindly provided by Dr. Jiri Friml (University of Tübingen, Germany). The pGEX-PIN2CL was kindly provided by Drs. Christian Luschnig and Rene Benjamins (University of Natural Resources and Applied Life Sciences, Austria). We also thank Johan Memelink for providing pET16H, Rene Benjamins for the pGEX-PID, pAS2-PID and pACT2-PBP2 plasmids, Carlos Galvan for the plasmid encoding H-PID and for helpful comments on the manuscript, and Peter Hock for the art work.

REFERENCE LIST

1. Friml, J., Vieten, A., Sauer, M., Weijers, D., Schwarz, H., Hamann, T., Offringa, R. & Jurgens, G. (2003) *Nature* **426**, 147-153.
2. Sabatini, S., Beis, D., Wolkenfelt, H., Murfett, J., Guilfoyle, T., Malamy, J., Benfey, P., Leyser, O., Bechtold, N., Weisbeek, P. *et al.* (1999) *Cell* **99**, 463-472.
3. Reinhardt, D., Pesce, E. R., Stieger, P., Mandel, T., Baltensperger, K., Bennett, M., Traas, J., Friml, J. & Kuhlemeier, C. (2003) *Nature* **426**, 255-260.
4. Muller, A., Guan, C., Galweiler, L., Tanzler, P., Huijser, P., Marchant, A., Parry, G., Bennett, M., Wisman, E. & Palme, K. (1998) *EMBO J.* **17**, 6903-6911.
5. Friml, J., Wisniewska, J., Benkova, E., Mendgen, K. & Palme, K. (2002) *Nature* **415**, 806-809.
6. Luschnig, C., Gaxiola, R. A., Grisafi, P. & Fink, G. R. (1998) *Genes Dev.* **12**, 2175-2187.

7. Raven, J. (1975) *New Phytologist* **74**, 163-172.
8. Rubery, P. H. & Sheldrake, A. R. (1974) *Planta* **118**, 101-121.
9. Galweiler, L., Guan, C., Muller, A., Wisman, E., Mendgen, K., Yephremov, A. & Palme, K. (1998) *Science* **282**, 2226-2230.
10. Chen, R., Hillson, P., Sedbrook, J., Rosen, E., Caspar, T. & Masson, P. H. (1998) *Proc Natl. Acad. Sci. U S A* **95**, 15112-15117.
11. Petrasek, J., Mravec, J., Bouchard, R., Blakeslee, J. J., Abas, M., Seifertova, D., Wisniewska, J., Tadele, Z., Kubes, M., Covanova, M. *et al.* (2006) *Science*.
12. Benkova, E., Michniewicz, M., Sauer, M., Teichmann, T., Seifertova, D., Jurgens, G. & Friml, J. (2003) *Cell* **115**, 591-602.
13. Wisniewska, J., Xu, J., Seifertova, D., Brewer, P. B., Ruzicka, K., Blilou, I., Roquie, D., Benkova, E., Scheres, B. & Friml, J. (2006) *Science*.
14. Vieten, A., Vanneste, S., Wisniewska, J., Benkova, E., Benjamins, R., Beeckman, T., Luschig, C. & Friml, J. (2005) *Development* **132**, 4521-4531.
15. Blilou, I., Xu, J., Wildwater, M., Willemsen, V., Paponov, I., Friml, J., Heidstra, R., Aida, M., Palme, K. & Scheres, B. (2005) *Nature* **433**, 39-44.
16. Paponov, I. A., Teale, W. D., Trebar, M., Blilou, I. & Palme, K. (2005) *Trends Plant Sci.* **10**, 170-177.
17. Friml, J. (2003) *Curr. Opin. Plant Biol.* **6**, 7-12.
18. Steinmann, T., Geldner, N., Grebe, M., Mangold, S., Jackson, C. L., Paris, S., Galweiler, L., Palme, K. & Jurgens, G. (1999) *Science* **286**, 316-318.
19. Geldner, N., Anders, N., Wolters, H., Keicher, J., Kornberger, W., Muller, P., Delbarre, A., Ueda, T., Nakano, A. & Jurgens, G. (2003) *Cell* **112**, 219-230.
20. Christensen, S. K., Dagenais, N., Chory, J. & Weigel, D. (2000) *Cell* **100**, 469-478.
21. Benjamins, R., Quint, A., Weijers, D., Hooykaas, P. & Offringa, R. (2001) *Development* **128**, 4057-4067.
22. Friml, J., Yang, X., Michniewicz, M., Weijers, D., Quint, A., Tietz, O., Benjamins, R., Ouwerkerk, P. B., Ljung, K., Sandberg, G. *et al.* (2004) *Science* **306**, 862-865.
23. Ryu, J., Hah, J. S., Park, J. S., Lee, W., Rampal, A. L. & Jung, C. Y. (2002) *Arch. Biochem. Biophys.* **403**, 71-82.
24. Jayanthi, L. D., Samuvel, D. J., Blakely, R. D. & Ramamoorthy, S. (2005) *Mol. Pharmacol.* **67**, 2077-2087.
25. Loder, M. K. & Melikian, H. E. (2003) *J. Biol. Chem.* **278**, 22168-22174.
26. Fushimi, K., Sasaki, S. & Marumo, F. (1997) *J. Biol. Chem.* **272**, 14800-14804.

27. van Balkom, B. W., Savelkoul, P. J., Markovich, D., Hofman, E., Nielsen, S., van der, S. P. & Deen, P. M. (2002) *J. Biol. Chem.* **277**, 41473-41479.
28. Bogre, L., Okresz, L., Henriques, R. & Anthony, R. G. (2003) *Trends Plant Sci.* **8**, 424-431.
29. Sambrook, J., Fritsch, F. & Maniatis, T. (1989) *Molecular Cloning - A Laboratory Manual* (Cold Spring Harbour Laboratory Press, New York).
30. Benjamins, R., Ampudia, C. S., Hooykaas, P. J. & Offringa, R. (2003) *Plant Physiol* **132**, 1623-1630.
31. Benjamins, R. Functional analysis of the PINOID protein kinase in *Arabidopsis thaliana*. 2004. Leiden University.
32. Friml, J., Benkova, E., Blilou, I., Wisniewska, J., Hamann, T., Ljung, K., Woody, S., Sandberg, G., Scheres, B., Jurgens, G. *et al.* (2002) *Cell* **108**, 661-673.
33. Abas, L., Benjamins, R., Malenica, N., Paciorek, T., Wirniewska, J., Moulinier-Anzola, J. C., Sieberer, T., Friml, J. & Luschig, C. (2006) *Nat. Cell Biol.* **8**, 249-256.
34. Guan, K. L. & Dixon, J. E. (1991) *Anal. Biochem* **192**, 262-267.
35. Krantz, D. E., Waites, C., Oorschot, V., Liu, Y., Wilson, R. I., Tan, P. K., Klumperman, J. & Edwards, R. H. (2000) *J. Cell Biol.* **149**, 379-396.
36. Rost, B., Yachdav, G. & Liu, J. (2004) *Nucleic Acids Res.* **32**, W321-W326.
37. Blom, N., Gammeltoft, S. & Brunak, S. (1999) *J Mol Biol* **294**, 1351-1362.
38. Nuhse, T. S., Stensballe, A., Jensen, O. N. & Peck, S. C. (2004) *Plant Cell* **16**, 2394-2405.
39. Geldner, N., Friml, J., Stierhof, Y. D., Jurgens, G. & Palme, K. (2001) *Nature* **413**, 425-428.
40. Muday, G. K., Peer, W. A. & Murphy, A. S. (2003) *Trends Plant Sci.* **8**, 301-304.
41. Blakeslee, J. J., Bandyopadhyay, A., Peer, W. A., Makam, S. N. & Murphy, A. S. (2004) *Plant Physiol* **134**, 28-31.
42. Furutani, M., Vernoux, T., Traas, J., Kato, T., Tasaka, M. & Aida, M. (2004) *Development* **131**, 5021-5030.

PINOID is a potential COP9 signalosome-associated kinase that modulates auxin response

Marcelo Kemel Zago, Felipe Maraschin, Rene Benjamins, Ab Quint, Remko Offringa

SUMMARY

The protein serine/threonine kinase PINOID (PID) is a signaling component in the control of polar auxin transport (PAT), as it determines the apico-basal polarity of the PIN family of auxin efflux carriers. The polar transport of auxin results in differential distribution of this hormone, and the cellular auxin concentrations are subsequently translated into a primary gene expression response. This last step occurs through the complex and cell-specific interactions between ARF transcription factors and labile Aux/IAA repressors. Abundance of Aux/IAA repressors is controlled by their auxin-induced, SCF^{TIR1} E3 Ligase-dependent proteolysis, a process that is regulated by the COP9 Signalosome (CSN).

We identified CSN subunit CSN8/COP9 as interacting partner of PID, and found that not CSN8, but the linked subunit CSN7/COP15, is phosphorylated by PID *in vitro*. PID overexpressing plants were observed to share constitutive photomorphogenic characteristics with *csn* down-regulated mutant lines suggesting that PID may be a repressor of CSN activity. An alternative role for PID as a putative CSN-associated kinase could be to regulate the interaction between E3 ligase and their proteolysis targets. To this point, we identified the labile auxin response repressor BODENLOS (BDL)/IAA12 as an *in vitro* phosphorylation target of PID. The observation that PID-mediated phosphorylation possibly occurs in the PRXS motif close to the SCF^{TIR1}-interacting domain II of BDL/IAA12 suggests that this event plays a role in the stability of this repressor protein. Analysis of the *pid-bdl* double mutant and transient expression experiments provided important *in vivo* data concerning the role of PID as a negative regulator of BDL activity during embryogenesis. Considering that BDL has a functionally redundant paralog IAA13, and that IAA13 also contains the PRXS motif, it is plausible that PID affects the activity of both AUX/IAAs. Whether PID controls the stability of BDL and IAA13 together or their interaction with ARF5/MP remains to be determined.

Although the mechanisms and roles of PID-mediated regulation of BDL, IAA13 or CSN require further elucidation, our data finally indicates that the PID protein kinase provides a direct link between auxin transport and -signaling.

Abbreviations: ARF, auxin response factor; AuxRe, auxin responsive element; AXR, auxin resistant; BDL/IAA12, Bodenloss/IAA12 protein; COP, constitutive photomorphogenesis; CSN, COP9 Signalosome; IAA, indole-3-acetic acid; MP, ARF5/Monopteros; NPH4, ARF7/Nonphototropic hypocotyl 4; PAT, polar auxin transport; PID, pinoid; SCF, SKP1/Cullin/F-box

INTRODUCTION

The plant hormone auxin affects gene expression through the action of two types of transcriptional regulators: the auxin response factors (ARFs) and the Aux/IAA proteins. ARFs bind to promoters containing auxin responsive (AuxRE) elements and can either activate or repress transcription, depending on their domain structure (1). Aux/IAA proteins are short-lived nuclear proteins that function as repressors of auxin responsive gene expression. Most Aux/IAAs are encoded by auxin responsive genes themselves, and act in a feed-back loop to regulate their own expression (1). Aux/IAA proteins form a family of twenty-nine members in Arabidopsis that share four conserved domains (1). From amino- to carboxy-terminus, domain I has been shown to have transcription repression activity (2), domain II is involved in destabilization of Aux/IAA proteins, and may be target for ubiquitination (3), and domains III and IV have protein-protein interaction properties, allowing Aux/IAA proteins to homo- or heterodimerize with ARFs or other Aux/IAA proteins (4). The repression activity of Aux/IAA proteins is normally performed through their interaction with ARFs, that as a consequence can not dimerize to activate transcription (5). Several Arabidopsis *Aux/IAA* genes have been identified through gain-of-function mutations that stabilize the produced Aux/IAA protein. Usually, such gain-of-function mutations lead to reduced auxin response, as observed in the *bodenlos* (*bdl*) mutant, which apart from displaying auxin insensitivity lacks a primary root meristem and shows reduced hypocotyl growth and curled cotyledons (6). The phenotypes of *bdl* mutant seedlings imply that the BDL/IAA12 protein is involved in auxin-mediated apical-basal patterning of the Arabidopsis embryo.

In Arabidopsis, the stability of Aux/IAA proteins is regulated by the SCF^{TIR1} E3 Ubiquitin Ligase, a protein complex consisting of SKP1 (ASK1), CULLIN1 (CUL1), the RING protein RBX1 and the F-box protein TIR1 (7-9). High affinity binding of auxin to TIR1 was recently shown to enhance its affinity for Aux/IAA proteins, and to stimulate subsequent targeting of these proteins to the proteasome for degradation (10, 11). Mutants in components of this degradation pathway, such as *axr-1*, *tir-1* and *axr-6/cul1* were identified based on their impaired auxin response (7, 8, 12).

The activity of the SCF^{TIR1} E3 Ubiquitin Ligase is regulated by the COP9 Signalosome (CSN), a protein complex with homology to the lid of the 26S proteasome and an important regulator of photomorphogenesis in plants (13, 14). CSN interacts with the SCF^{TIR1} complex subunits CUL1 and RBX1 (15) and is involved in removal of RUB1, as part of the cyclic RUB modification of CUL1 that is essential for SCF activity (13, 16). Accordingly, mild loss-of-function mutants for the CSN5 subunit display phenotypes that are associated to defects in auxin response, and protein extracts from these plants do not degrade IAA6 from pea as efficiently as wild type plants extracts (15). More recently, it was shown that CSN, SCF^{TIR} and

26S proteasome components are recruited to nuclear bodies where Aux/IAA proteins are actively degraded (17). These findings place CSN, together with the proteolytic machinery, as a regulatory component of auxin signaling.

Apart from being translated into a primary gene expression response by the complex and cell-specific interaction of ARFs and Aux/IAA proteins, the auxin signal is primarily determined by its cellular concentration, which is again the result of biosynthesis and directional distribution through polar auxin transport (PAT). PAT-dependent differential distribution of auxin in young developing organs has been shown to be instrumental for a wide variety of developmental processes, such as embryogenesis (18), root development (19), shoot organogenesis (20), and tropisms (21-23). The chemiosmotic hypothesis proposed in 1970s suggested that the direction of PAT is determined by the polar subcellular localization of efflux carriers (24, 25). More recent molecular genetic studies with the model plant *Arabidopsis thaliana* have identified the PIN family of proteins to be essential for PAT. Analogous to the proposed efflux carriers in the chemiosmotic hypothesis, PIN proteins show auxin efflux activity and a polar subcellular localization that determines the direction of the auxin flow (18-21, 23, 26-31).

A substantial body of evidence from genetic and molecular approaches has determined that the serine/threonine kinase PINOID (PID) is a key component in the control of PAT. Recently, it was shown that the cellular levels of PID determine the apical-basal polarity of PINs. These observations explained the hypothesized changes in the auxin flow in PID loss and gain-of-function plant lines, implying that PID-mediated phosphorylation is essential for proper PAT and patterning processes (32, 33).

In addition to its central role as regulator of PAT, we identified two possible links between PID and auxin signaling. A screen for PID interacting proteins revealed that PID interacts with CSN8/COP9. *In vitro* phosphorylation assays indicated that PID does not phosphorylate CSN8/COP9, but instead phosphorylates CSN7/COP15, the subunit that is directly linked to CSN8/COP9 in the CSN complex (34). These results implicate that PID regulates the activity of the CSN. An alternative role for PID as a putative CSN-associated kinase could be to regulate the interaction between E3 ligase and their proteolysis targets. Moreover, we identified via *in vitro* assays that the labile auxin response repressor BODENLOS (BDL)/IAA12 is a phosphorylation target of PID. The observation that PID-mediated phosphorylation possibly occurs in the PRXS motif close to the SCF^{TIR1}-interacting domain II of BDL/IAA12 implicates that this changes the stability of this repressor protein. Intriguingly *pid-bdl* double mutants show an enhanced *pid* phenotype not present in either single mutant. Protoplast experiments provided further important indications for a role of PID as negative regulator of BDL. Together the data suggest that during embryogenesis PID inhibits specific IAA proteins that may include BDL/IAA12 and

IAA13, since IAA13 also has the potential phosphorylation site PRXS. The possible role of PID as modulator of auxin signaling will be discussed in light of its well-established role in directing PIN polar targeting.

MATERIALS AND METHODS

Molecular cloning and constructs

Molecular cloning was performed following standard procedures (35). The fusion GAL4BD (GAL4 Binding Domain)-PID was created as described by Benjamins (36). The construct GAL4AD (GAL4 Activation Domain)-COP9 was isolated from the yeast two-hybrid screen performed by Benjamins (36). The yeast two-hybrid bait plasmid pAS2-PBP2 was obtained by cloning a *PBP2* *Pst*/I/SalI-blunted fragment derived from pSDM6014 into pAS2 digested with *Pst*/XmaI-blunted. The histidine tagged PID construct was created by excising the *PID* cDNA with *Xmn*I-SalI from pSDM6005 (36) and cloning it into pET16H (pET16B derivative, J. Memelink, unpublished results) digested with *Bam*HI, blunted and subsequently digested with *Xho*I. *CSN7* cDNA was amplified by PCR using the primers 5'-ACGCAAGTCGACAAGATGGATATCGAGCAGAAGCAAGC-3' and 5'-GATAGATCTAACAGAGGATCTTATACAAGTTG-3', and subsequently digested with *Bgl*II to be ligated into the pBluescriptSK+ plasmid treated with *Eco*RV/*Bgl*II. His-CSN7 was obtained by cloning *CSN7* *Bam*HI/SalI fragment into the plasmid pET16B (Novagen) digested with *Xho*I/*Bam*HI. The construct encoding His-CSN8 was created by cloning *CSN8* fragment digested with *Sal*I into pET16H treated with *Xho*I/*Sma*I. The preparation of the plasmids encoding His-PBP1 and GST-PID fusions have been described previously (37). The plasmid containing 35S::BDL was obtained by cloning a partially digested *BDL* *Nco*I/*Bam*HI fragment from pET16H-BDL into the pRT104 vector treated with the same enzymes. The *DR5*::*GUS* construct has been previously described (33). The 35S::PID construct for protoplast transformation was generated as follows: initially the pEF-PID-FLAG plasmid was obtained, for which the overlapping oligos were designed: 3xFLAG#1 5'-GTACGCTTACTCCGCCGAGATTCTTCTTCCGTCGTCGAAGAAGCCGATGAAAT-3', 3xFLAG#2 5'-CGAAATGGATTATAAAGACCATGATGGAGATTAC-3', 3xFLAG#3 5'-P-AAAGATCATGACATTGATTA TAAGGATGACGATGACATTGTCGACTGAC-3', 3xFLAG#4 5'-TCGAGTCAGTCGACAATGTCATCGTC ATCCTTATAATCAATGTC-3', 3xFLAG#5 5'-ATGATCTTTGTAATCTCCATCATGGTCTTTATAATCCA TTT-3' and 3xFLAG#6 5'-AACGTCGCCGATTTCATCGGCTTCTTGACGACGGAAGAAGGAATCTCCGG CGGAGTAAGC-3'. The oligos 3xFLAG#1 and #6, 3xFLAG#2 and #5 and 3xFLAG#3 and #4 were annealed and ligated to create the FLAG fragment. FLAG *Bst*WI/*Xho*I fragment was subsequently cloned into pEF-PID (36) digested with the same enzymes. From the pEF-PID-FLAG plasmid, the PID-FLAG *Eco*RI/*Xba*I fragment was cloned into pART7 treated with the same enzymes.

Yeast two hybrid interaction

Using the Matchmaker II yeast two-hybrid system and *Saccharomyces cerevisiae* strain PJ69-4A (Clontech), COP9/CSN8 fused to the GAL4 activation domain (pACT2) was directly tested at 20°C for interaction with PID or PBP2 fused to the GAL4 DNA binding domain (pAS2).

In vitro pull down experiments

GST tagged PID or GST protein alone were used in pull down assays with histidine (his)-tagged CSN8, BDL and PBP1 (H-proteins). Cultures of *E. coli* strain BL21 containing one of the constructs were grown at 37°C to OD₆₀₀ 0,8 in 50 ml LC supplemented with antibiotics. The cultures were then induced for 4 hours with 1 mM IPTG at 30°C, after which cells were harvested by centrifugation (10 min. at 4.000 RPM in tabletop centrifuge) and frozen overnight at -20°C. Precipitated cells were re-suspended in 2 ml Extraction Buffer (EB: 1x PBS, 2 mM EDTA, 2 mM DTT, supplemented with 0,1 mM of the protease inhibitors PMSF - Phenylmethanesulfonyl Fluoride, Leupeptin and Aprotinin, all obtained from Sigma) for

the GST-tagged proteins or in 2 ml Binding Buffer (BB: 50 mM Tris-HCl pH 6.8, 100 mM NaCl, 10 mM CaCl_2 , supplemented with PMSF 0.1 mM, Leupeptin 0.1 mM and Aprotinin 0.1 mM) for the his-tagged proteins and sonicated for 2 min. on ice. From this point on, all steps were performed at 4°C. Eppendorf tubes containing the sonicated cells were centrifugated at full speed (14.000 RPM) for 20 min., and the supernatants were transferred to fresh 2 ml tubes. H-proteins supernatants were left on ice, while 100 μl pre-equilibrated Glutathione Sepharose resin (pre-equilibration performed with three washes of 10 resin volumes of 1x PBS followed by three washes of 10 resin volumes of 1x BB at 500 RCF for 5 min.) was added to the GST- fusion protein containing supernatants. Resin-containing mixtures were incubated with gentle agitation for 1 hour, subsequently centrifugated at 500 RCF for 3 min. and the precipitated resin was washed 3 times with 20 resin volumes of EB. Next, all H-proteins supernatants (approximately 2 ml per protein) were added to GST-fusions-containing resins, and the mixtures were incubated with gentle agitation for 1 hour. After incubation, supernatants containing GST resins were centrifugated at 500 RCF for 3 min., the new supernatants were discarded and the resins subsequently washed 3 times with 20 resin volumes of EB. Protein loading buffer was added to the resin samples, followed by denaturation by 5 min. incubation at 95°C. Proteins were subsequently separated on a 12% polyacrylamide gel prior to transfer to an Immobilon™-P PVDF (Sigma) membrane. Western blots were hybridized using a horse radish peroxidase (HRP)-conjugated anti-pentahistidine antibody (Quiagen) and detection followed the protocol described for the Phototope-HRP Western Blot Detection Kit (New England Biolabs).

***In vitro* phosphorylation assays**

All proteins used in *in vitro* phosphorylation assays were his-tagged for purification from several (usually five) aliquots of 50 ml cultures of *E. coli*. strain BL21 which were grown, induced, pelleted and frozen as described above for the *in vitro* pull down experiments. Each aliquot of frozen cells pellet was resuspended in 2 ml Lysis Buffer (25 mM Tris-HCl pH 8.0; 500 mM NaCl; 20 mM Imidazol; 0.1% Tween-20; supplemented with 0.1 mM of the protease inhibitors PMSF, Leupeptin and Aprotinin) and subsequently sonicated for 2 min. on ice. From this point on, all steps were performed at 4°C. Sonicated cells were centrifugated at full speed (14.000 RPM) for 20 min, the new pellets were discarded, and supernatants from all aliquots of the same construct were transferred to a 15 ml tube containing 100 μl of pre-equilibrated Ni-NTA resin (pre-equilibration performed with three washes of 10 resin volumes of Lysis Buffer at 500 RCF for 5 min.). Supernatant and resin were incubated with gentle agitation for 1 hour. After incubation, supernatant containing Ni-NTA resin was centrifuged at 500 RCF for 3 min., the new supernatant was discarded and the resin subsequently washed: 3 times with 20 resin volumes of Lysis Buffer, once with 20 resin volumes of Wash Buffer 1 (25 mM Tris.Cl pH 8.0; 500 mM NaCl; 40 mM Imidazol; 0.05% Tween-20) and once with 20 resin volumes of Wash Buffer 2 (25 mM Tris-HCl pH 8.0; 600 mM NaCl; 80 mM Imidazol). In between the washes, the resin was centrifugated for 5 min. at 500 RCF. After the washing steps, 20 resin volumes of Elution Buffer (25 mM Tris.HCl pH 8.0; 500 mM NaCl; 500 mM Imidazol) was added to the resin and incubated for 15 min. with gentle agitation. The resin was centrifugated for 3 min. at 500 RCF, and the supernatant containing the desired protein was diluted a 1000-fold in Tris Buffer (25 mM Tris.HCl pH7.5; 1 mM DTT) and concentrated to a workable volume (usually 50 μl) using Vivaspin microconcentrators (10 kDa cut off, maximum capacity 600 μl , manufacturer: Vivascience). Glycerol was added as preservative to a final concentration of 10% and samples were stored at -80°C.

Approximately 1 μg of each purified his-tag protein (PID and substrates) in maximal volumes of 10 μl were added to 20 μl kinase reaction mix, containing 1x kinase buffer (25 mM Tris-HCl pH 7.5; 1 mM DTT; 5 mM MgCl_2) and 1 x ATP solution (100 μM MgCl_2/ATP ; 1 μCi ^{32}P - γ -ATP). Reactions were incubated at 30°C for 30 min. and stopped by the addition of 5 μl of 5 x protein loading buffer (310 mM Tris-HCl pH 6.8; 10 % SDS; 50% Glycerol; 750 mM β -Mercaptoethanol; 0.125% Bromophenol Blue) and 5 min. boiling. Reactions were subsequently separated over 12.5% acrylamide gels, which were washed 3 times for 30 min. with kinase gel wash buffer (5% TCA – Trichloroacetic Acid; 1% $\text{Na}_2\text{H}_2\text{P}_2\text{O}_7$), coomassie stained, destained, dried and exposed to X-ray films for 24 to 48 hours at -80°C using intensifier screens.

For the peptides assays, 1 µg of purified PID was incubated with 4 nmol of 9^{mer} biotinylated peptides (Pepscan) in a phosphorylation reaction as described above. Reaction processing, spotting and washing of the SAM² Biotin Capture Membrane (Promega) were performed as described in the corresponding protocol. Following washing, the membranes were wrapped in plastic film and exposed to X-ray films for 24 to 48 hours at -80°C using intensifier screens. The phosphorylation intensities of each peptide were determined by densitometry analysis of the autoradiographs using the ImageQuant software (Molecular Dynamics).

Protoplast transformations

Protoplasts were obtained from *Arabidopsis thaliana* Col-0 cell suspension cultures that were propagated as described by Schirawski and co-workers (38). Protoplast isolation and PEG-mediated transformation followed the protocol described originally by Axelos and co-workers (39) and adapted by Schirawski and co-workers (38). The transformations were performed with 10 µg of the constructs *DR5::GUS* and *35S::PID*, 1 µg of *35S::BDL*, and 2 µg of a plasmid expressing Renilla luciferase for signal normalization, after which the protoplasts were incubated for at least 16h. Subsequent treatments of the prepared protoplasts employed IAA 1 µM for a period of 8 hours.

Plant growth

Seeds were germinated and seedlings grown *in vitro* on MA medium (40) supplemented with antibiotics or other compounds when required, at 21°C, 50% relative humidity and a 16 hours photoperiod of 2500 lux. Flowering Arabidopsis plants were grown on substrate soil, in growth rooms at 20°C, 40% relative humidity and a 16 hours photoperiod of 2500 lux.

RESULTS

PINOID interacts with CSN8/COP9 and phosphorylates CSN7/COP15 *in vitro*

One of the PID interacting proteins identified using the yeast two-hybrid system (36) was the subunit 8 of the CSN (CSN8/COP9). This interaction was confirmed by re-transformation of the respective bait and prey vectors into the yeast strain PJ69-4A (Figure 1A) and by *in vitro* protein pull-down assays (Figure 1B).

Only few kinases have been shown to associate with the CSN. For example, Uhle and co-workers (41) demonstrated that the proteins CK2 and PKD bind CSN Subunit 3 and phosphorylate CSN Subunits 2, 5 and 7. Based on this information, we hypothesized that PID phosphorylates CSN8/COP9 or another subunit of the CSN complex. Our initial *in vitro* phosphorylation assays did not show any evidence that PID phosphorylates CSN8/COP9 (Figure 1C). Since it has been shown that CSN8/COP9 interacts with the phosphoprotein CSN7 (34, 41, 42), we directly tested if CSN7 could be phosphorylated by PID *in vitro*. Indeed, CSN7 was efficiently phosphorylated by PID and in our assays CSN7 phosphorylation occurred independently of CSN8/COP9 (Figure 1C). Most likely the excess of PID and CSN7 used in these experiments overruled the requirement for CSN8/COP9-mediated PID anchoring.

The NetPhos program (43) was used to identify putative amino acids in CSN7 that are targets for PID phosphorylation, and this *in silico* analysis identified eight potential CSN7 phosphorylation sites (Figure 1D). To test each of these residues we synthesized eight biotinylated peptides, only six of which could be used in phosphorylation reactions as the other two were insoluble (Figure 1E). The two peptides with the amino acid sequence core KRASTCKS, which starts at position 16 in the CSN7 protein, were most efficiently phosphorylated by PID (Figure 1E). More detailed analysis of these peptides in the ScanProsite database (44) indicated that they share characteristics of phosphorylation substrates of cyclic AMP dependent Protein Kinase (PKA: R/K-R/K-X-S/T) and of Protein Kinase C (PKC: S/T-X-R/K). Pep-Chip experiments have shown that PID efficiently phosphorylates PKA and PKC substrates (Galvan-Ampudia and Offringa, unpublished data), therefore either CSN7 serine 19 or threonine 20 are interesting putative PID phosphorylation targets. These results suggest that PID possibly regulates CSN activity through phosphorylation of subunit CSN7.

35S::PID lines show weak constitutive photomorphogenesis

The possible role of PID as regulator of the CSN, and the fact that the CSN complex has been discovered as repressor of photomorphogenesis (45), suggested that plant lines with altered *PID* expression may develop photomorphogenesis-related seedling phenotypes. The fact that no such phenotypes were observed in *pid* mutant seedlings may be explained by the specific role of PID in organogenesis in the embryo and inflorescence (33, 46, 47) and that other related kinases may be functionally redundant with PID. The mutant phenotypes of the 35S::PID gain-of-function lines, however, are strongest in the seedling stage. Several of the strong auxin related features such as the collapse of the main root meristem and agravitropic growth are well-accounted for by the changes in PIN polar targeting (32, 33). However, 35S::PID plants show a delay in lateral root formation, a phenotype that is also observed in *csn5* reduction-of-function lines (15). Furthermore, 35S::PID seedlings present mild constitutive photomorphogenic characteristics that are observed in the *cop/fus* mutants (14). These phenotypes include lack of an apical hook and opening of cotyledons when grown in the dark and enhanced accumulation of anthocyanins when grown under light are also observed in 35S::PID (Figure 2). Although these observations suggest that the role of PID as CSN-associated kinase is to repress CSN activity, further *in vivo* studies are required to clarify the functional relationship between PID and the CSN.

bodenlos is an enhancer of *pinoid*

The CSN has been shown to regulate proteolysis of AUX/IAA proteins through its interaction with the SCF^{TIR} E3 ligase (13, 15, 17, 48). The interaction of PID with

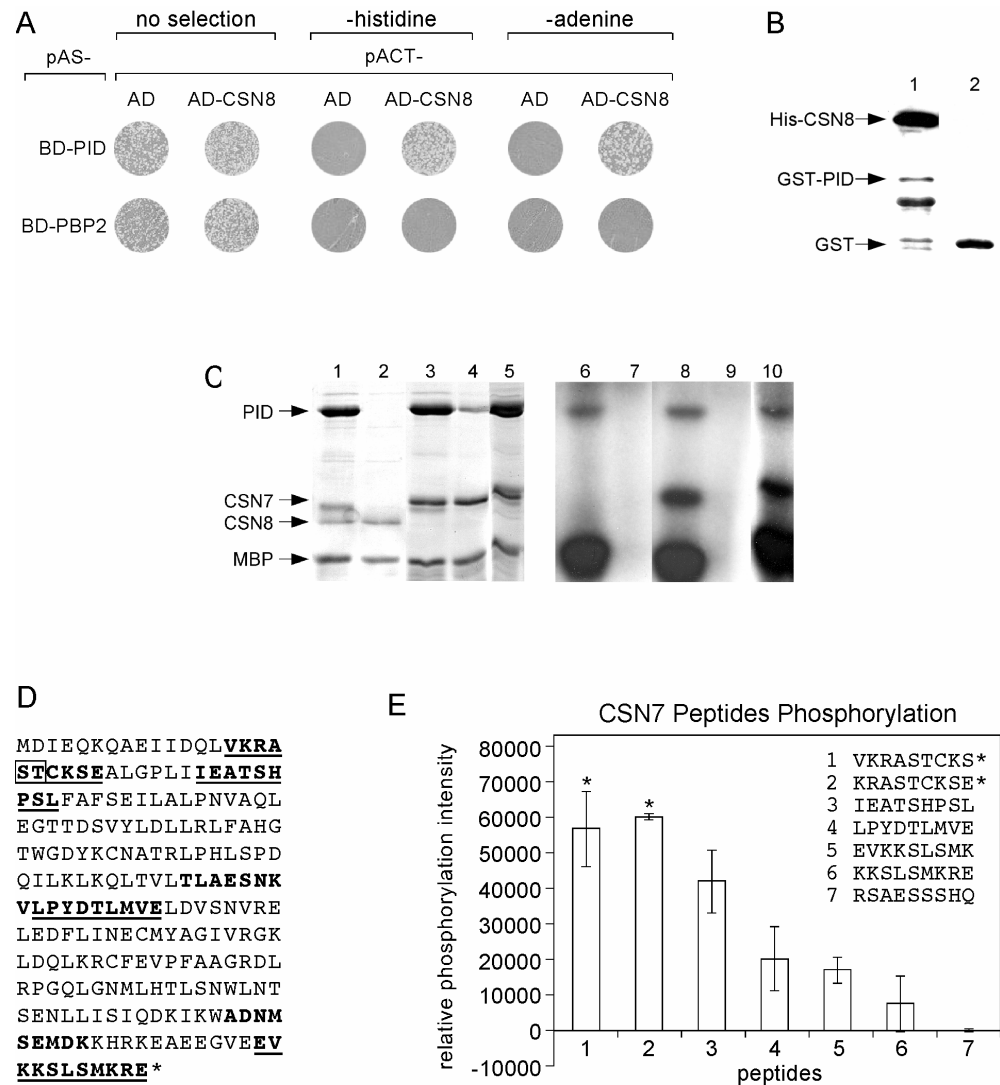


Figure 1. PID interacts with CSN8/COP9 and phosphorylates CSN7/COP15. (A) Yeast two-hybrid assay with PID and PBP2 fused to the GAL4 DNA binding domain (BD; pAS vector), and CSN8/COP9 fused to the GAL4 activation domain (AD) or the AD alone (pACT vector) in non-selective medium or in medium lacking either histidine or adenine. (B) *In vitro* pull-down of his-tagged CSN8/COP9 with GST-tagged PID (lane 1) and not with GST (lane 2), as shown by immunodetection with anti-his antibodies (top panel). The comassie stained gel is shown in the bottom panel. (C) Autoradiograph (right panel) and coomassie stained gel (left panel) of *in vitro* phosphorylation assay using MBP (all lanes), his-CSN8 (lanes 1, 2, 5, 6, 7 and 10) and his-CSN7 (lanes 3, 4, 5, 8, 9 and 10) as substrates and PID (lanes 1, 3, 5, 6, 8 and 10) as protein kinase. (D) Amino acid sequence of CSN7, with the eight putative phosphorylation sites identified by NetPhos (Blom *et al.*, 1999) as central residues within nine aminoacids peptides indicated in bold. The peptides tested in the *in vitro* phosphorylation assay (E) are underlined and the putative PID phosphorylation substrates are boxed in (D). BDL peptide RSAESSSHQ (7) was used as a negative control.

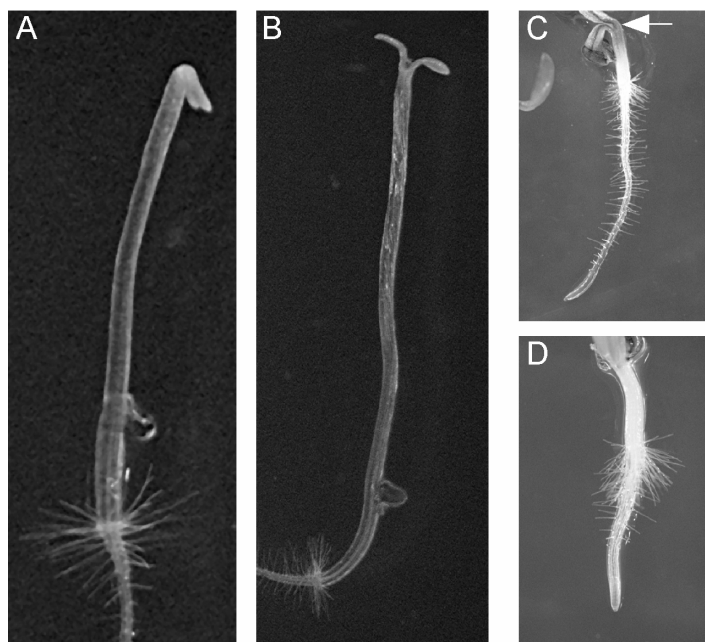


Figure 2. PID overexpression plants display mild constitutive photomorphogenic characteristics. Three-day-old seedlings of Columbia WT (A and D) and *35S::PID* (B and C) grown in dark (A and B) and light (C and D). The area in the upper-hypocotyl with high accumulation of anthocyanin in a *35S::PID* seedling is indicated with an arrow (C).

CSN entertained the possibility that PID may be involved in regulating the stability of Aux/IAA proteins (5). Since PID is expressed in the embryo and is essential for proper embryonic patterning (33, 46, 49), we decided to test whether PID could alter the activity of the embryonic Aux/IAA protein BODENLOS (BDL)/IAA12.

A *pid* loss-of-function mutant allele was crossed with the *bdl* gain-of-function mutant. F2 seedlings from this cross displayed a range of phenotypes, varying from wild type and typical *pid* and *bdl* seedlings to seedlings that lack or only develop rudimentary cotyledons (no-cot), or no-cot seedlings that even lack a primary root (Figure 3A to 3D). As the latter seedlings phenocopied the previously identified *gurke* mutants (50), their phenotype was referred to as *gurke*-like. The frequency of no-cot or *gurke*-like seedlings matched the expected numbers for respectively *BDL/bdl pid/pid* and *bdl/bdl pid/pid* progeny (Table 1). Few seedlings of the no-cot and *gurke*-like class were able to grow beyond the seedling stage, but showed a completely disorganized phyllotaxis and formed early pin-like inflorescences (Figure 3E). The no-cot phenotype was also observed in *pid-pin1* double mutants (49), and since we know now that PID regulates PIN polar targeting (32), these results suggest that a functional interaction may also exist between PID and BDL.

PID reduces BDL-mediated repression of auxin responsive gene expression

Considering the possible effect of PID on BDL action, we decided to test whether this interaction could be directly observed on the gene expression level in *Arabidopsis* protoplasts. In this system, expression of the auxin responsive *DR5::GUS* reporter gene was significantly induced by 8 hours treatment with 1 μ M IAA. Co-transformation of the *DR5::GUS* reporter with the *35S::BDL* construct resulted in a 50% reduction of the IAA-induced reporter gene activity (Figure 3F). When the *DR5::GUS* and *35S::BDL* constructs were co-introduced together with the *35S::PID* plasmid, auxin-induced GUS expression was restored to approximately 90% of the activity in the control transformation with the reporter gene alone (Figure 3F). The *35S::PID* construct itself did not significantly alter *DR5::GUS* activity (Figure 3F). In these assays the amount of plasmid DNA transformed for each construct was variable, meaning that the different transformed protoplast samples contained different amounts of total plasmid. Therefore, we cannot fully exclude that this influenced the data obtained. In spite of this, our results appear to indicate that PID can antagonize the repression of auxin responsive gene expression by BDL. Together with the observed synergistic phenotypes in the *pid-bdl* double mutants, these results suggest that PID activity represses BDL.

PID phosphorylates, but does not interact directly with BDL *in vitro*

To find more evidence for the putative functional interaction between PID and BDL, we tested whether PID phosphorylates or binds to BDL *in vitro*. Although we did not observe a clear interaction between the two proteins in pull down assays (Figure 4A), we did detect a strong PID-dependent phosphorylation of BDL (Figure 4B).

By using the NetPhos software (43), thirteen putative phosphorylation sites were mapped in the BDL protein (Figure 4C). Biotinylated peptides corresponding to these sites were synthesized and ten soluble peptides were used in *in vitro* phosphorylation reactions. The peptides with the amino acid sequences MRGVSELEV (Peptide 1), PPRSSQVVG (Peptide 5) and LKDVS MKVN (Peptide 6) in BDL were strongly phosphorylated by PID (Figure 4D), and phosphorylation of peptide 9 was rather variable. Further analysis of the amino acid sequences of the consistently phosphorylated peptides by the ScanProsite (44) and NetPhos software (43) indicated that Peptide 1 comprises the phosphorylation consensus of Casein Kinase 2 (CK2: S/T-X-X-D/E), Peptide 5 contains the consensus of DNA-Dependent Protein Kinase (DNAPK: S/T-Q) and Peptide 6 shows the consensus of Protein Kinase C (PKC: S/T-X-R/K). Interestingly, peptide 5 comprises the PRXS motif that was also present in the two major PID target sites identified in PIN1 (Figure 4E and Chapter 4). The fact that the serine residue of this motif is located close to the

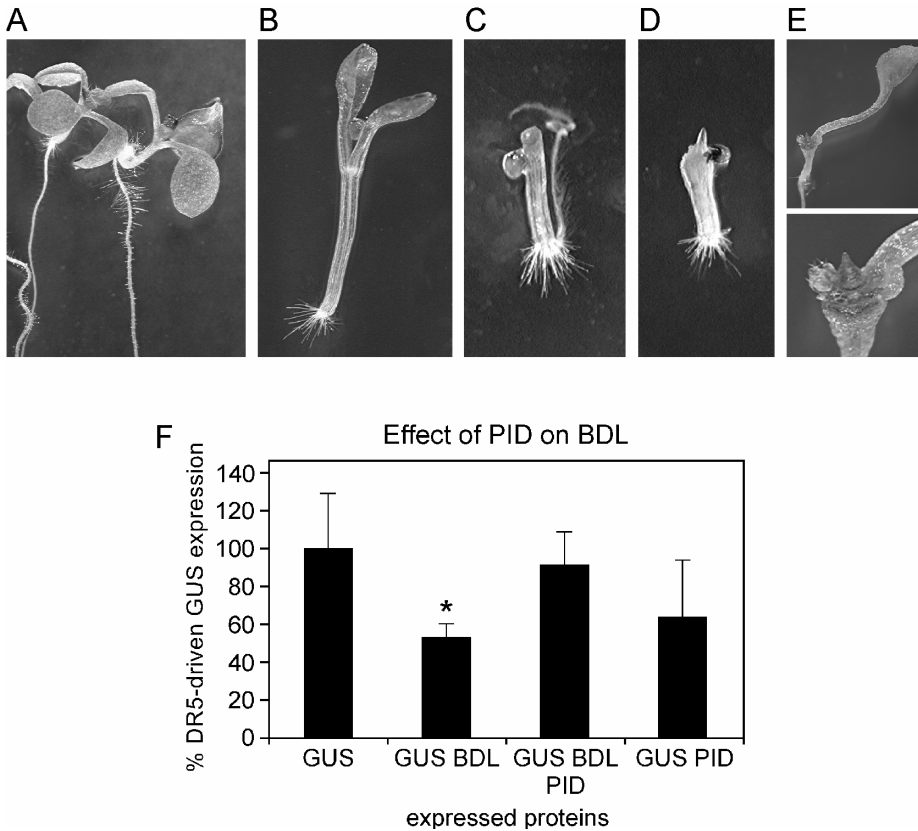


Figure 3. PID antagonizes the transcriptional repressor activity of BDL. The *bdl* gain-of-function mutation enhances the cotyledon defects of the *pid* loss-of-function mutant (A-E). The phenotypes of the *pid* (A) and *bdl* (B) parental lines and the synergistic no-cot (C) and *gurke*-like (D) phenotypes observed in the *pid* x *bdl* F2 population. Older no-cot and *gurke*-like seedlings display disorganized phyllotactic pattern and early formation of pin structures (E). (F) Auxin-induced *DR5::GUS* expression in Arabidopsis cell suspension-derived protoplasts is repressed by *35S::BDL* and this repression is alleviated by co-transformation of *35S::PID*. Co-transformation of *35S::PID* alone does not significantly affect *DR5::GUS* activity. The protoplasts were treated for 8 hours with 1 μ M IAA. The star indicates a significant difference with the *DR5::GUS* control transformation using Student's t-test ($t=3,75$; $p>0,05$; 7 GUS and 6 GUS BDL samples were analyzed).

conserved part of domain II makes it tempting to speculate that PID-mediated phosphorylation at this specific position enhances the SCF^{TIR1}-dependent proteolysis of BDL.

An alignment of 27 Arabidopsis Aux/IAA proteins showed that, although several other Aux/IAAs have a serine or threonine at the same domain II-linked position, the PRXS motif is only found in IAA12/BDL and IAA13 (Figure 4E). This, together with the recently identified functional redundancy between IAA12/BDL and IAA13 (51),

suggests that PID controls the proteolysis of both proteins during embryo development. The synergistic phenotypes observed in *bdl-pid* double mutants could be explained by the enhanced IAA13 stability as a consequence of the absence of PID regulatory activity during cotyledon development.

Table 1. Segregation analysis of phenotypes observed in a <i>pid</i> x <i>bdl</i> F2 population						
	Total	Phenotypic classes				
		kans [‡]	tricot ^{†,*}	<i>bdl</i> [*]	no-cot. [*]	<i>gurke-l</i> [*]
Observed number of seedlings (%)	198 (100)	50 (25)	6 (3)	17 (8,5)	13 (6)	4 (2)
Expected number of seedlings (%)	198 (100)	50 (25)	6 (3)	25 (12,5)	12 (6)	6 (3)

‡ Seedlings homozygous for the wild type *PID* gene and kanamycin sensitive, as seeds were germinated on MA medium containing 25µg/ml of kanamycin, to select for the T-DNA insertion causing the *pid* loss-of-function mutation.

† The three cotyledon phenotype of this *pid* mutant allele shows a penetrance of 50%, indicating that it is a complete loss-of-function allele (Bennett *et al.*, 1995; Christensen *et al.*, 2000).

*The expected number of kanamycin resistant three cotyledon, *bdl*, no-cotyledon and “*gurke-like*” seedlings, based on 1:16 (*BDL/BDL pid/pid*), 1:8 (*bdl/bdl PID/pid*), 1:8 (*BDL/bdl pid/pid*) and 1:16 (*bdl/bdl pid/pid*) segregation ratios, respectively, and a 50% penetrance of the phenotypic changes induced by the homozygote *pid* mutation. The numbers between brackets indicate percentages. The observed numbers did not significantly differ from the expected ones in the χ^2 test ($\chi^2=3,69$, $p<0,05$).

DISCUSSION

Several lines of evidence indicate that at several steps auxin controls its own polar transport. For example, auxin was found to inhibit the endocytosis step in the cyclic trafficking of PIN vesicles between PM and endosomal compartments, thereby increasing the levels of PM localized PINs to promote its own efflux (52). In gravistimulated roots, the redistributed auxin was shown to affect both PIN2 localization and protein levels (53). Moreover, the directionality of PAT is regulated by the PID protein kinase that controls the polar subcellular localization of the PIN auxin efflux carriers (32). The observation that auxin controls cellular PID levels (33), suggests that PID is involved in a feedback mechanism by which auxin directs its own efflux. Overall, the three observations suggest that auxin signaling and -transport processes are tightly linked by regulatory feedback loops.

In this chapter we present preliminary data suggesting that the PID protein kinase, next to its auxin-enhanced cellular levels, also provides a direct link between auxin transport and -signaling. Firstly, we obtained evidence that PID interacts with and phosphorylates the CSN, a central component in E3-ligase-dependent degradation of proteins such as the Aux/IAA repressors of auxin responsive gene expression. Secondly, our results suggest that PID antagonizes the action of IAA12/BDL and

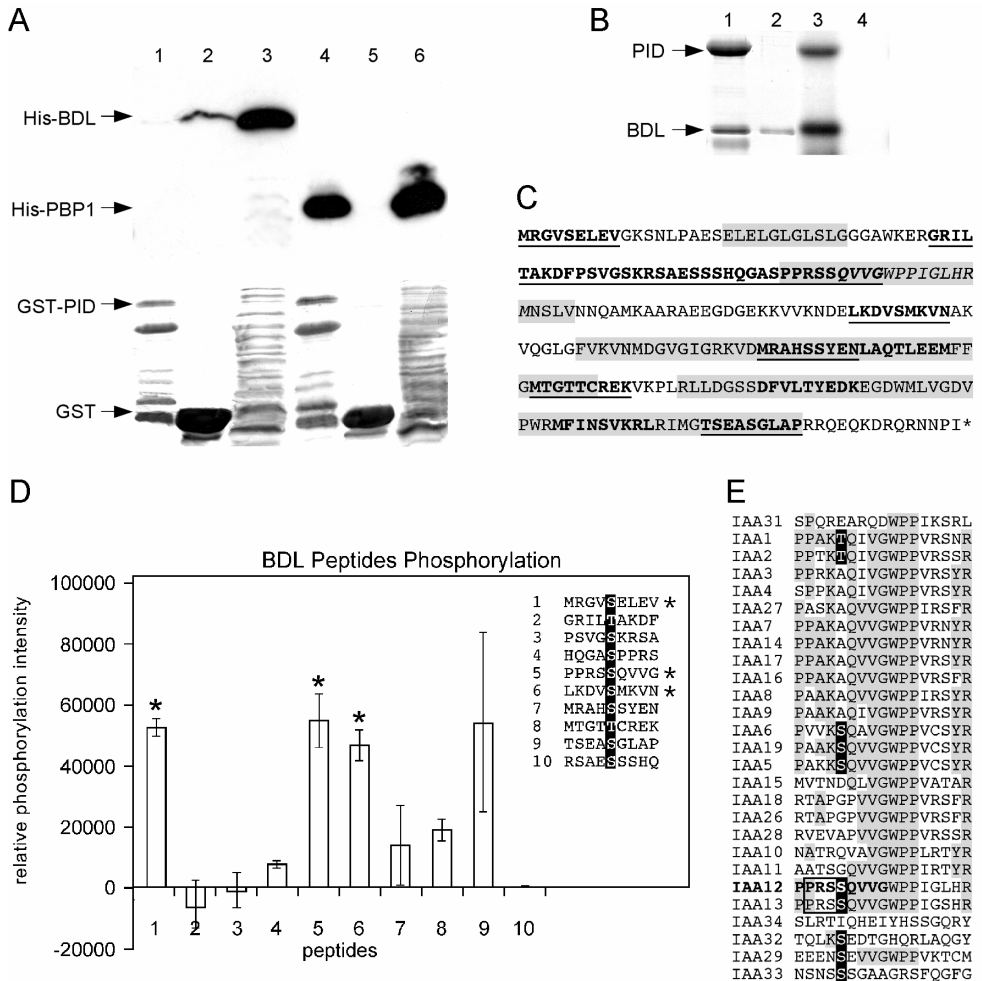


Figure 4. PID does not interact with, but phosphorylates BDL. (A) An *in vitro* protein pull-down assay showing that his-tagged BDL (lanes 1 to 3) is not pulled down with GST-PID (lane 1) nor with GST alone (lane 2), whereas his-tagged PBP1 (lanes 4 to 6) is specifically pulled down with GST-tagged PID (lane 4) and not with GST alone (lane 5). Total protein extracts (1% of input) of *E. coli* cells expressing his-BDL (lane 3) or his-PBP1 (lane 6) are loaded as controls. The top panel shows immunodetection of his-tagged proteins, and the coomassie stained gel is shown in the bottom panel. (B) Coomassie stained gel (lanes 1 and 2) and autoradiograph (lanes 3 and 4) of an *in vitro* phosphorylation reaction with PID (lanes 1 and 3) and BDL (all lanes). (C) BDL protein sequence with domains I, II, III and IV shaded, all putative phosphorylation residues identified by NetPhos (Blom *et al.*, 1999) within nine aminoacids peptides indicated in bold, and the peptides used in *in vitro* phosphorylation assays underlined. The highly conserved portion of domain II is in italics. (D) Relative radioactive labeling intensities of different BDL-derived peptides by PID in *in vitro* phosphorylation reactions. The BDL-derived peptides that are highly phosphorylated by PID are indicated with a star. (E) Alignment of the conserved part of domain II of 27 Arabidopsis Aux/IAAs. Gray shading shows conserved residues. Putative phosphorylation sites at position 5 are shaded in black and the PRXS motif that is unique for BDL/IAA12 and IAA13 is boxed.

IAA13 during embryogenesis as a direct result of phosphorylation on these repressors at a site close to the conserved domain II. Below we will discuss the implications of our findings, which are rather surprising in light of the well-established role of PID in directing the subcellular trafficking of PIN proteins.

PID as a possible CSN-associated kinase

Our observations provide the first clues that a plant protein kinase is associated with the CSN. CSN-associated kinases have been identified in bovine and human cells; inositol 1,3,4 triphosphate 5/6 kinase was shown to physically interact with CSN subunit CSN1 (54), and the kinases CK2 and PKD were shown to interact with CSN subunit CSN3 and to phosphorylate CSN2, CSN5 and CSN7 (41). The three CSN-associated kinases were also shown to phosphorylate and thereby control the stability of the regulatory proteins p53 and c-JUN (41, 54-56).

The role of PID as CSN-associated kinase is as yet unclear. *35S::PID* seedlings phenocopy some of the constitutive photomorphogenesis aspects of *csn* down-regulated mutants or lines overexpressing the photomorphogenesis promoting transcription factor HY5, a target of the CSN-dependent COP1 E3 ligase (15, 57, 58). This suggests that PID acts as a negative regulator of CSN activity. Interestingly, HY5 phosphorylation at a CK2 consensus site in the COP1 interacting domain was shown to lower the affinity for COP1 and to stabilize this transcription factor (58). It seems most likely, however, that HY5 phosphorylation is not performed by PID, but by the plant CK2 that is possibly associated with CSN, and that has been implied in promoting light regulated plant growth in Arabidopsis (59).

What would then be the role of PID in association with CSN? PID could regulate the stability of other targets of the CSN-E3 ligase proteolysis pathway. This second hypothesis is supported by our observation that the CSN-SCF^{TIR1} E3 ligase target IAA12/BDL is phosphorylated by PID *in vitro*. The alternative role of PID as CSN-associated kinase could be to regulate the activity or stability of the CSN complex itself by phosphorylating CSN7. To test this option, we would have to reevaluate the putative PID phosphorylation sites through site directed mutagenesis of CSN7 and subsequent testing of the mutant forms in *in vitro* phosphorylation assays. Based on the conclusive identification of the amino acids phosphorylated by PID, mutant forms of CSN7 that miss the phosphorylation site or that mimic constitutive phosphorylation should then be expressed in a *csn7* loss-of-function mutant background, to identify the *in vivo* significance of PID-mediated phosphorylation of CSN7.

The role of PID as CSN-associated kinase could also relate to its function in directing the polar subcellular targeting of PIN proteins. Previously, we have shown that enhanced cellular PID levels can redirect PIN proteins from a basal (bottom) to an apical (top) subcellular localization within a 12 to 16 hours time frame (32). This

polarity switch could involve proteolytic degradation of the basally localized PIN1 proteins, and PID-mediated phosphorylation of PINs (see Chapter 4 of this thesis) could enhance the affinity of these proteins for the corresponding E3-ligase. In yeast and mammalian cells, ubiquitination of membrane proteins, a step that is often preceded by phosphorylation, provides a key signal for endosomal sorting of membrane proteins (60). Interestingly, for PIN2 it has recently been shown that cellular levels and intracellular relocation of this protein are dependent on endosomal cycling and proteasome activity (53). The involvement of PID and PID-like kinases in these processes clearly requires further study.

PID possibly modulates auxin responses during embryogenesis

The crucial role of the CSN in auxin-induced, SCF^{TIR1} E3 ligase-dependent proteolysis of Aux/IAA proteins is well established (13, 15, 17). Until now, however, it was not known whether CSN-associated kinases were involved in this process, even though several protein kinases have been proposed as regulators of Aux/IAA stability (5). In this chapter we do not only provide data on a possible role of PID as CSN-associated kinase, but our results also suggest that PID reduces IAA12/BDL activity by phosphorylation of this labile transcriptional repressor close to its SCF^{TIR1}-interacting domain II (3, 61, 62). The double mutant analysis and transient protoplast expression experiments provide important *in vivo* indications for a role of PID as negative regulator of BDL activity during embryogenesis.

It remains to be determined however, whether PID-mediated BDL inhibition is due to protein degradation. In fact, the more severe *pid-bdl* phenotypes can not easily be explained in terms of reduced *iaa12/bdl* degradation, since the gain-of-function mutations in Aux/IAA proteins have been shown to disrupt the interaction with SCF^{TIR1}, thereby preventing their subsequent proteolysis (61). In the embryo, however, IAA12/BDL is known to act redundantly with IAA13 to regulate MONOPTEROS (MP)/ARF5, and possibly also NONPHOTOTROPIC HYPOCOTYL 4 (NPH4)/ARF7, -dependent embryonic organ formation (51, 63). Since IAA13, like BDL, has the PRXS motif in domain II, PID phosphorylation at this position could lead to reduced IAA13 stability. Conversely, in the *pid-bdl* double mutant, IAA13 stability would be increased, leading to a greater reduction in auxin responsive gene expression. Alternatively, PID-mediated phosphorylation could negatively interfere with the interaction between IAA12/BDL or IAA13 and ARF5/MP or ARF7/NPH4 (51, 63), thereby weakening IAA12/IAA13-mediated repression of auxin responsive genes. In this case, the moderate defects observed in *bdl* mutants could be due to the presence of PID-mediated repression of BDL/IAA13 interaction with ARF5/ARF7. In *pid-bdl* double mutants, on the other hand, absence of PID could result in enhanced repression of ARF5 or ARF7 by BDL and IAA13, thereby causing the more severe phenotypes observed in these plants.

Although the first hypothesis implies that PID phosphorylation is necessary for efficient SCF-dependent recruitment of BDL and IAA13 for proteolysis, it has been recently reported that IAA7 does not require phosphorylation in order to be degraded (10). By contrast, IAA7 does not have the PRXS motif in domain II. In fact, this motif is specific for IAA12 and IAA13, and it could very well be that the possible role of PID as modulator of auxin responses is specific for these two Aux/IAA proteins. PID is encoded by an auxin responsive gene, and as a regulator of auxin responsive gene expression it may provide a strong positive feedback on its own expression. In context to embryogenesis this may be important in allowing proper cotyledon primordia development.

A functional interaction between PID, BDL and IAA13 requires that the spatio-temporal expression of the corresponding genes overlap and that the proteins co-localize to the same subcellular compartments. Detailed expression analysis and subcellular localization studies will be important steps in future research, but currently we are testing the expression of a mutant BDL version that lacks the putative PID phosphorylation site, under control of its own promoter.

ACKNOWLEDGEMENTS

This work was financially supported by CAPES (Brazilian Federal Agency for Post-Graduate Education, M.K.-Z.). We thank Dolf Weijers for providing the plasmid pET16H-BDL, Carlos Galvan for the plasmid pET16H-PID and for the pictures of wild type and 35S::PID seedlings, Helene Robert for the plasmid pEF-PID-FLAG, Johan Memelink for plasmid pET16H, Adam Vivian-Smith for helpful comments on the manuscript, and Peter Hock for the art work.

REFERENCE LIST

1. Liscum, E. & Reed, J. W. (2002) *Plant Mol. Biol.* **49**, 387-400.
2. Tiwari, S. B., Hagen, G. & Guilfoyle, T. J. (2004) *Plant Cell* **16**, 533-543.
3. Ramos, J. A., Zenser, N., Leyser, O. & Callis, J. (2001) *Plant Cell* **13**, 2349-2360.
4. Ulmasov, T., Hagen, G. & Guilfoyle, T. J. (1999) *Plant J.* **19**, 309-319.
5. Reed, J. W. (2001) *TRENDS in Plant Science* **Vol.6**, 420-425.
6. Hamann, T., Mayer, U. & Jurgens, G. (1999) *Development* **126**, 1387-1395.
7. Hellmann, H., Hobbie, L., Chapman, A., Dharmasiri, S., Dharmasiri, N., del Pozo, C., Reinhardt, D. & Estelle, M. (2003) *EMBO J.* **22**, 3314-3325.

8. Gray, W. M., del Pozo, J. C., Walker, L., Hobbie, L., Risseuw, E., Banks, T., Crosby, W. L., Yang, M., Ma, H. & Estelle, M. (1999) *Genes Dev.* **13**, 1678-1691.
9. Gray, W. M., Hellmann, H., Dharmasiri, S. & Estelle, M. (2002) *Plant Cell* **14**, 2137-2144.
10. Dharmasiri, N., Dharmasiri, S. & Estelle, M. (2005) *Nature* **435**, 441-445.
11. Kepinski, S. & Leyser, O. (2005) *Nature* **435**, 446-451.
12. Pozo, J. C., Timpote, C., Tan, S., Callis, J. & Estelle, M. (1998) *Science* **280**, 1760-1763.
13. Lyapina, S., Cope, G., Shevchenko, A., Serino, G., Tsuge, T., Zhou, C., Wolf, D. A., Wei, N., Shevchenko, A. & Deshaies, R. J. (2001) *Science* **292**, 1382-1385.
14. Castle, L. A. & Meinke, D. W. (1994) *Plant Cell* **6**, 25-41.
15. Schwechheimer, C., Serino, G., Callis, J., Crosby, W. L., Lyapina, S., Deshaies, R. J., Gray, W. M., Estelle, M. & Deng, X. W. (2001) *Science* **292**, 1379-1382.
16. Bostick, M., Lochhead, S. R., Honda, A., Palmer, S. & Callis, J. (2004) *Plant Cell* **16**, 2418-2432.
17. Tao, L. Z., Cheung, A. Y., Nibau, C. & Wu, H. M. (2005) *Plant Cell* **17**, 2369-2383.
18. Friml, J., Vieten, A., Sauer, M., Weijers, D., Schwarz, H., Hamann, T., Offringa, R. & Jurgens, G. (2003) *Nature* **426**, 147-153.
19. Sabatini, S., Beis, D., Wolkenfelt, H., Murfett, J., Guilfoyle, T., Malamy, J., Benfey, P., Leyser, O., Bechtold, N., Weisbeek, P. *et al.* (1999) *Cell* **99**, 463-472.
20. Reinhardt, D., Pesce, E. R., Stieger, P., Mandel, T., Baltensperger, K., Bennett, M., Traas, J., Friml, J. & Kuhlemeier, C. (2003) *Nature* **426**, 255-260.
21. Muller, A., Guan, C., Galweiler, L., Tanzler, P., Huijser, P., Marchant, A., Parry, G., Bennett, M., Wisman, E. & Palme, K. (1998) *EMBO J.* **17**, 6903-6911.
22. Friml, J., Wisniewska, J., Benkova, E., Mendgen, K. & Palme, K. (2002) *Nature* **415**, 806-809.
23. Luschnig, C., Gaxiola, R. A., Grisafi, P. & Fink, G. R. (1998) *Genes Dev.* **12**, 2175-2187.
24. Raven, J. (1975) *New Phytologist* **74**, 163-172.
25. Rubery, P. H. & Sheldrake, A. R. (1974) *Planta* **118**, 101-121.
26. Okada, K., Ueda, J., Komaki, M. K., Bell, C. J. & Shimura, Y. (1991) *Plant Cell* **3**, 677-684.
27. Galweiler, L., Guan, C., Muller, A., Wisman, E., Mendgen, K., Yephremov, A. & Palme, K. (1998) *Science* **282**, 2226-2230.
28. Friml, J., Benkova, E., Blilou, I., Wisniewska, J., Hamann, T., Ljung, K., Woody, S., Sandberg, G., Scheres, B., Jurgens, G. *et al.* (2002) *Cell* **108**, 661-673.
29. Petrasek, J., Mravec, J., Bouchard, R., Blakeslee, J. J., Abas, M., Seifertova, D., Wisniewska, J., Tadele, Z., Kubes, M., Covanova, M. *et al.* (2006) *Science*.

30. Wisniewska, J., Xu, J., Seifertova, D., Brewer, P. B., Ruzicka, K., Blilou, I., Roquie, D., Benkova, E., Scheres, B. & Friml, J. (2006) *Science*.
31. Chen, R., Hilson, P., Sedbrook, J., Rosen, E., Caspar, T. & Masson, P. H. (1998) *Proc Natl. Acad. Sci. U S A* **95**, 15112-15117.
32. Friml, J., Yang, X., Michniewicz, M., Weijers, D., Quint, A., Tietz, O., Benjamins, R., Ouwerkerk, P. B., Ljung, K., Sandberg, G. *et al.* (2004) *Science* **306**, 862-865.
33. Benjamins, R., Quint, A., Weijers, D., Hooykaas, P. & Offringa, R. (2001) *Development* **128**, 4057-4067.
34. Serino, G., Su, H., Peng, Z., Tsuge, T., Wei, N., Gu, H. & Deng, X. W. (2003) *The Plant Cell* **15**, 719-731.
35. Sambrook, J., Fritsch, F. & Maniatis, T. (1989) *Molecular Cloning - A Laboratory Manual* (Cold Spring Harbour Laboratory Press, New York).
36. Benjamins, R. Functional analysis of the PINOID protein kinase in *Arabidopsis thaliana*. 2004. Leiden University.
37. Benjamins, R., Ampudia, C. S., Hooykaas, P. J. & Offringa, R. (2003) *Plant Physiol* **132**, 1623-1630.
38. Schirawski, J., Planchais, S. & Haenni, A. L. (2000) *J Virol. Methods* **86**, 85-94.
39. Axelos, M., Curie, C., Mazzolini, L., Bardet, C. & Lescure, B. (1992) *Plant Physiol Biochem* **30**, 123-128.
40. Masson, J. & Paszkowski, J. (1992) *Plant J* **2**, 208-218.
41. Uhle, S., Medalia, O., Waldron, R., Dumdey, R., Henklein, P., Bech-Otschir, D., Huang, X., Berse, M., Sperling, J., Schade, R. *et al.* (2003) *EMBO J.* **22**, 1302-1312.
42. Bech-Otschir, D., Seeger, M. & Dubiel, W. (2002) *J. Cell Sci.* **115**, 467-473.
43. Blom, N., Gammeltoft, S. & Brunak, S. (1999) *J Mol Biol* **294**, 1351-1362.
44. Gattiker, A., Gasteiger, E. & Bairoch, A. (2002) *Appl. Bioinformatics.* **1**, 107-108.
45. Schwechheimer, C. (2004) *Biochim. Biophys. Acta* **1695**, 45-54.
46. Bennett, S., Alvarez, J., Bossinger, G. & Smyth, D. (1995) *Plant J.* **8**, 505.
47. Christensen, S. K., Dagenais, N., Chory, J. & Weigel, D. (2000) *Cell* **100**, 469-478.
48. Chamovitz, D. A., Wei, N., Osterlund, M. T., von Arnim, A. G., Staub, J. M., Matsui, M. & Deng, X. W. (1996) *Cell* **86**, 115-121.
49. Furutani, M., Vernoux, T., Traas, J., Kato, T., Tasaka, M. & Aida, M. (2004) *Development* **131**, 5021-5030.
50. Torres-Ruiz, R. A., Lohner, A. & Jurgens, G. (1996) *Plant J.* **10**, 1005-1016.

51. Weijers, D., Benkova, E., Jager, K. E., Schlereth, A., Hamann, T., Kientz, M., Wilmoth, J. C., Reed, J. W. & Jurgens, G. (2005) *EMBO J.* **24**, 1874-1885.
52. Paciorek, T., Zazimalova, E., Ruthardt, N., Petrasek, J., Stierhof, Y. D., Kleine-Vehn, J., Morris, D. A., Emans, N., Jurgens, G., Geldner, N. *et al.* (2005) *Nature* **435**, 1251-1256.
53. Abas, L., Benjamins, R., Malenica, N., Paciorek, T., Wirniewska, J., Moulinier-Anzola, J. C., Sieberer, T., Friml, J. & Luschnig, C. (2006) *Nat. Cell Biol.* **8**, 249-256.
54. Sun, Y., Wilson, M. P. & Majerus, P. W. (2002) *J. Biol. Chem.* **277**, 45759-45764.
55. Seeger, M., Kraft, R., Ferrell, K., Bech-Otschir, D., Dumdey, R., Schade, R., Gordon, C., Naumann, M. & Dubiel, W. (1998) *FASEB J* **12**, 469-478.
56. Wilson, M. P., Sun, Y., Cao, L. & Majerus, P. W. (2001) *J. Biol. Chem.* **276**, 40998-41004.
57. Ang, L. H., Chattopadhyay, S., Wei, N., Oyama, T., Okada, K., Batschauer, A. & Deng, X. W. (1998) *Mol. Cell* **1**, 213-222.
58. Hardtke, C. S., Gohda, K., Osterlund, M. T., Oyama, T., Okada, K. & Deng, X. W. (2000) *EMBO J.* **19**, 4997-5006.
59. Lee, Y., Lloyd, A. M. & Roux, S. J. (1999) *Plant Physiol* **119**, 989-1000.
60. Bonifacino, J. S. & Traub, L. M. (2003) *Annu. Rev. Biochem* **72**, 395-447.
61. Gray, W. M., Kepinski, S., Rouse, D., Leyser, O. & Estelle, M. (2001) *Nature* **414**, 271-276.
62. Kepinski, S. & Leyser, O. (2002) *Plant Cell* **14 Suppl**, S81-S95.
63. Hardtke, C. S., Ckurshumova, W., Vidaurre, D. P., Singh, S. A., Stamatiou, G., Tiwari, S. B., Hagen, G., Guilfoyle, T. J. & Berleth, T. (2004) *Development* **131**, 1089-1100.

Summary

The phytohormone auxin - or indole-3-acetic acid (IAA) - is a major determinant in a wide array of plant developmental processes, such as photo- and gravitropism, apical dominance, embryogenesis and phyllotaxis. Although IAA was the first plant hormone to be isolated and characterized, it was only recently that the mechanisms underlying auxin's action began to be unraveled. Molecular and genetic studies - mostly using the model plant *Arabidopsis thaliana* - have revealed the unique dynamics of auxin and have identified several components that play an essential role in this hormone's functionality. Auxin action was found to depend on dynamic gradients of this hormone generated by PIN protein-facilitated polar auxin transport (PAT). These PIN proteins possess auxin efflux activity and direct PAT through their asymmetric subcellular localization. The polar PIN localization is dynamically maintained and regulated through cyclic trafficking of PIN loaded vesicles along the actin cytoskeleton between endosomal compartments and the plasma membrane (PM).

Previously, the protein kinase PINOID (PID) was identified as regulator of the apico-basal polar localization of PIN proteins, as above-threshold levels of this signaling enzyme direct PIN trafficking to the upper (apical) side of plant cells. A yeast two-hybrid screen identified four PID Binding Proteins (PBPs): the two calcium binding proteins PBP1 and TCH3, PBP2 and the COP9 signalosome subunit CSN8 (Figure 1). This thesis describes a more detailed study of several components and the identification of putative targets of the PID signaling complex.

Chapter 2 focuses on PBP2, a likely scaffold protein that - based on its possible localization at the cytoskeleton in onion cells - was considered as a promising link between PID and PIN vesicle trafficking. The presumed scaffold function of PBP2 was apparent, since the protein consists of two domains that are known to mediate protein-protein interactions: an amino-terminal Bric-a-brac, Tramtrack and Broad Complex/Pox virus and Zinc finger (BTB/POZ) domain, and a carboxy-terminal Transcriptional Adaptor putative Zinc Finger (TAZ) domain. In contrast to previous results, *in vitro* phosphorylation assays showed that PBP2 is not a phosphorylation target of PID, but that instead PID activity is repressed by PBP2. *In vitro* pull down assays suggested that PID interacts with the BTB/POZ domain, and transient expression of both proteins fused to GFP in *Arabidopsis* protoplasts suggested that this interaction occurs in the cytoplasm.

The likely scaffold function of PBP2 indicated that other PBP2 interacting proteins (PBP2IPs) play a role in the PID signaling pathway. In an yeast two-hybrid screen sixteen putative PBP2IPs were identified that classified as cytoskeletal proteins, transcription factor-like proteins or proteins with an enzymatic function in primary metabolism. Three PBP2IPs, the putative microtubule-associated PBP2 BINDING MYOSIN-LIKE PROTEIN (PBMP), the transcription factor-like PBP2 BINDING MYB PROTEIN (PBMYP), and an uncharacterized AUXIN-INDUCIBLE PBP2 BINDING

PROTEIN (APBP), are analyzed in more detail. *In vitro* pull down assays showed that PBMP and PBMYP interact with the C-terminal TAZ domain containing portion, whereas APBP interacts with the N-terminal part of PBP2. *In vitro* phosphorylation assays did not show any evidence that these PBP2 partners are phosphorylated by PID, implying that PBP2 is not a scaffold for PID substrates. Further analysis did not provide evidence that PBMYP and PBMP are part of the PID signaling complex. In contrast, for APBP we concluded that it may be involved in modulating flowering time, and that it possibly competes with PID for the interaction with PBP2, and as a consequence activates the kinase by relieving it from PBP2-mediated repression. Overall, the data presented in Chapter 2 indicate that PBP2 is a scaffold protein with multiple functions, one of which is to be recruited to the PID signaling complex to regulate PIN polar targeting.

Chapter 3 describes the more detailed analysis of the interaction of PBP2 with two paralogous plant-specific microtubule motor proteins, PBP2 BINDING KINESIN 1 (PBK1) and 2 (PBK2). *In vitro* pull down and phosphorylation assays corroborated the scaffold function of PBP2, since the PBKs bind the C-terminal TAZ domain portion and the PID kinase binds the N-terminal BTB/POZ domain portion of PBP2. The possible existence of such a protein complex at the cytoplasm-plasma membrane boundary was corroborated by the overlapping spatio-temporal expression of *PID*, *PBP2* and the *PBKs*, and by the fact that the proteins - when fused to GFP - co-localize in the cytoplasm of Arabidopsis protoplasts. Analysis of *pbk1/pbk2* mutant plants and *35S::PBK1* overexpression lines showed phenotypes that were also observed in mutants defective in *PAT* and in *pid* loss-of-function seedlings, respectively. These observations suggest that the PBKs are involved in the suppression of PID kinase activity. As PBP2 was shown to inhibit PID activity *in vitro*, we propose that PBK1 and PBK2 transport PBP2 to suppress PID and PID-like activity at specific subcellular locations, thereby providing polarity to the signaling of these kinases (Figure 1A).

The subcellular localization of animal transporters is known to be regulated by direct phosphorylation, often in a large cytoplasmic domain of these membrane proteins. In **Chapter 4** the possibility is addressed that PIN proteins are direct phosphorylation targets of PID. *In silico* analysis of PIN1 revealed twenty-three putative phosphorylation sites, twenty-one of which are localized at the large cytoplasmic loop (CL) of this protein, and five of which are 100% conserved among the CL-containing PINs in Arabidopsis. *In vitro* assays using PID and synthetic PIN1 peptides containing most of the predicted phosphorylation sites identified four highly phosphorylated peptides comprising three of the predicted phosphorylated residues that are 100% conserved in the CL containing PINs. Notably, two of the strongly phosphorylated peptides comprise the T-P-R-X-S-N motif. By testing CLs of different PIN proteins and through site directed mutagenesis we deduced that the

serines 231 and 290, both positioned in the conserved T-P-R-X-S-N motifs, are the major substrates for PID-mediated phosphorylation, and that the serines 377 and 380, that were previously shown to be phosphor-substrates in PIN7 *in vivo*, may also be modified by PID. Our results suggest that the PID kinase affects PIN polarity through direct modification of multiple conserved serine residues in the large cytoplasmic loop of these auxin efflux facilitators.

Polar transport-mediated distribution of auxin results in differential distribution of this hormone, and the cellular auxin concentrations are subsequently translated into a primary gene expression response by the complex and cell-specific interactions between ARF transcription factors and labile Aux/IAA repressors. The abundance of Aux/IAA repressors is controlled by their auxin-induced, SCF^{TIR1} E3 Ligase-dependent proteolysis, a process that is regulated by the COP9 Signalosome (CSN).

Chapter 5 describes the identification of CSN subunit CSN8/COP9 as interacting partner of PID, and that not CSN8, but the linked subunit CSN7/COP15 is phosphorylated by PID *in vitro*. The observation that PID overexpressing plants share constitutive photomorphogenic characteristics with *csn* down-regulated mutant lines suggests that PID may be a repressor of CSN activity. An alternative role for PID as a putative CSN-associated kinase could be to regulate the interaction between E3 ligases and their proteolysis targets. Interestingly, we identified the labile auxin response repressor BODENLOS (BDL)/IAA12 as *in vitro* phosphorylation target of PID. The observation that PID-mediated phosphorylation possibly occurs in the PRXS motif close to the SCF^{TIR1}-interacting domain II of BDL/IAA12, suggests that this event plays a role in the stability of this repressor protein. Analysis of the *pid-bdl* double mutant and transient expression experiments provided important *in vivo* clues for a role of PID as negative regulator of BDL activity during embryogenesis. Considering that BDL is functionally redundant with IAA13, and that IAA13 also contains the PRXS motif, it is plausible that PID affects the activity of both AUX/IAAs. Whether PID controls the stability of BDL and IAA13 or their interaction with ARF5/MP remains to be determined.

Although the mechanisms and roles of PID-mediated regulation of BDL, IAA13 or CSN require further elucidation, our data suggest that the PID protein kinase provides a direct link between auxin transport and -signaling.

Conclusions

The results described in this thesis suggest a duality in the function of the PID kinase, which leads us to propose the following working model (Figure 1). On one hand PINOID functions in the cytosol, where its activity - to mark endosomal PIN proteins for apical targeting (Figure 1A, region 1) or to signal apical-localized PINs to stay in this position (Figure 1A, region 2) - is regulated in sub-cellular manner

through a PBP2-kinesin complex (Chapter 3), and through the calcium binding proteins PBP1 and TCH3 (Figure 1A). On the other hand, PID functions in the nucleus as a CSN-associated kinase that may regulate the activity of the CSN itself, or that regulates the proteolytic degradation of targets of the E3 ligase-CSN complex, such as BDL/IAA12 and IAA13, by phosphorylation (Figure 1B). In this subcellular compartment, it is possible that PID function is again controlled by PBP2. It is likely, however, that PBP2 is also involved in other - PID-unrelated – processes, such as the regulation of gene transcription by the transcription factor PBMYB (Figure 1B).

Interestingly, none of the possible phosphorylation targets of PID identified thus far, namely PIN1 (Chapter 4) BDL or CSN7 (Chapter 5), show a strong interaction with PID. Conversely, none of the PID interactors obtained in a yeast two-hybrid screen are phosphorylation targets of this protein kinase, but instead three of the PBPs seem to regulate PID kinase activity (Chapter 2). All together, these results indicate that PID interacts very transiently with its substrates. This is in contrast to what has been observed for mitogen activated protein kinases that need to stably interact with their substrates for efficient phosphorylation. It could be, however, that PID uses non-substrate proteins in order to be anchored to and efficiently modify its phosphotargets. The use of CSN8 as an adaptor protein for PID-mediated phosphorylation of CSN7 may be an example of such a behavior. However, the true relationship between PID and its putative phosphor-substrates remains to be established.

The results presented in this thesis provide interesting new insights into putative molecular mechanisms of PID action, the most important of which is the direct PID-mediated phosphorylation of PIN proteins in their cytoplasmic loop. Acknowledged PID-sensitive PINs direct auxin transport in roots (PIN1, PIN2 and PIN4), hypocotyls (PIN1), inflorescence meristems (PIN1) and embryos (PIN1, PIN4), whereas PID function is limited to the latter two tissues. Assuming that PID-like signaling is essential for PIN polarity throughout the whole plant, it is logical to assume that other PID-related kinases regulate PINs in other tissues than in inflorescence meristems or embryos. Our previous analysis of the Arabidopsis genome identified twenty-two other members of the plant specific family of protein kinases to which PINOID belongs. Most likely, some of these members are also putative PINs regulators, and the comparative study of their function and activity will help to clarify their role in regulating the direction of PAT.

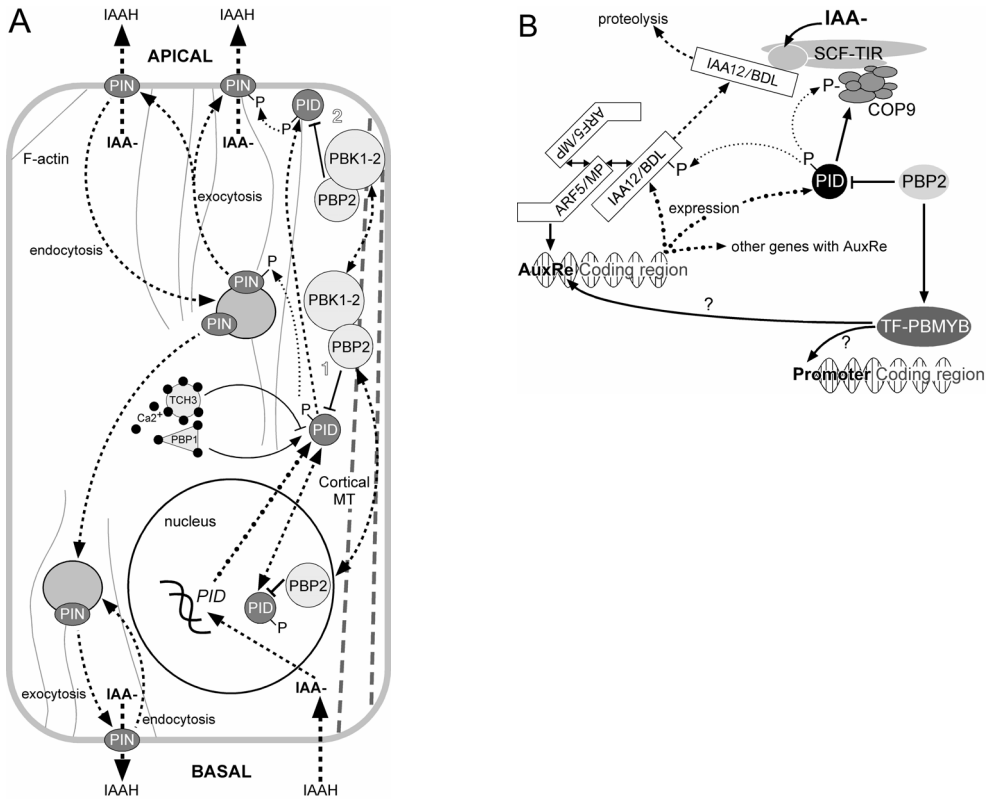


Figure 1. Model for the mechanisms of PID-mediated regulation of PAT. (A) Protonated (non-charged) auxin enters the cell by passive diffusion or by active carrier-mediated uptake and induces expression of auxin responsive genes, such as *PID*. In response to cytosolic calcium levels, PID activity is enhanced by the calcium binding protein PBP1 or repressed by the calmodulin TCH3. The PBK-PBP2 complex moves along cortical microtubuli to repress PID activity in different cellular locations: 1) at the endosomes where PID-mediated phosphorylation of PINs marks them for exocytosis to the apical cell pole, or 2) at the plasma membrane where PID-mediated phosphorylation prevents endocytosis, thereby signaling PINs to stay at their current apical position. Controlled PID-mediated PIN phosphorylation ultimately results in modulation of cellular auxin efflux. (B) In the nucleus, auxin induces the expression of genes containing auxin responsive elements (AuxRe) such as *PID* and *IAA12/BDL*. This induction is enabled by initial auxin binding to TIR1, which enhances SCF^{TIR1}-Aux/IAA interaction, leading to enhanced proteolysis of Aux/IAA proteins. The degradation of the Aux/IAA protein BDL releases its repression upon ARF5/MP, therefore enabling ARF5 activation of auxin responsive genes. BDL phosphorylation by CSN-associated kinase PID could stimulate BDL binding to TIR1, and enhance BDL degradation. Alternatively, PID phosphorylation could weaken the BDL-ARF5 interaction. PID-CSN interaction could also result in CSN repression upon phosphorylation. Continuous lines indicate protein-protein or protein-DNA interactions; thick punctuated lines indicate mobility; thin punctuated lines indicate phosphorylation; thick punctuated lines with dots indicate gene expression.

Samenvatting

Het plantenhormoon auxine, ofwel indol-3-azijnzuur (IAA), speelt een centrale rol bij de ontwikkeling van planten. Ontwikkelingsprocessen zoals embryogenese, phyllotaxis en de geo- of fototrope groei worden gestuurd door dynamische auxine gradiënten, die gegenereerd worden middels polair transport van dit hormoon door de PIN familie van membraan eiwitten. PIN eiwitten vertonen auxine efflux activiteit en bepalen de richting van het transport door hun asymmetrische subcellulaire lokalisatie. Deze wordt in stand gehouden en gereguleerd door cyclisch transport - langs het actine cytoskelet - van PIN bevattende membraanblaasjes tussen endosomale celcompartimenten en het plasmamembraan.

Het PINOID (PID) proteïne kinase is geïdentificeerd als een regulator van de polaire lokalisatie van PIN eiwitten. Daarbij is gevonden dat het PID kinase de PIN eiwitten naar de apicale (boven-) celpool stuurt. Hoe dit kinase de lokalisatie van PIN eiwitten precies beïnvloedt, is nog niet duidelijk. Wel zijn via een twee-hybride screen in gist een viertal PID Bindende eiwitten (PBPs) geïdentificeerd. Het in dit proefschrift beschreven onderzoek richtte zich op de verdere functionele analyse van twee van deze PBPs, en op de mogelijkheid dat de PIN eiwitten zelf fosforylatiesubstraten van het PID kinase zijn.

Hoofdstuk 2 beschrijft een nadere analyse van de interactie tussen PID en PBP2, een eiwit met een BTB/POZ (Bric-a-brac, Tramtrack and Broad Complex/Pox virus and Zinc finger) domein in de amino(N)-terminale regio en een TAZ (Transcriptional Adaptor putative Zinc Finger) domein aan de carboxy(C)-terminale zijde. Van beide domeinen is bekend dat ze eiwit-eiwit interacties verzorgen, en PINOID bleek specifiek aan de BTB/POZ bevattende N-terminus van PBP2 te binden. Tevens bleek dat PBP2 geen fosforylatiesubstraat van PID is, maar dat dit eiwit de activiteit van het kinase onderdrukt. In een daaropvolgende twee-hybride screen in gist werden 16 PBP2 bindende eiwitten geïdentificeerd. De functies van deze eiwitten varieerden van transcriptiefactoren en cytoskeleteiwitten tot eiwitten met een enzymatische functie in het primaire metabolisme. Voor de meeste PBP2 bindende eiwitten kon niet eenduidig worden aangetoond dat ze een rol spelen in de signaaltransductieroute van het PID kinase. Dit suggereert dat PBP2 een multifunctioneel “scaffold” eiwit is, dat - als component van het PID signaaltransductiecomplex - betrokken is bij de regulatie van PIN polariteit.

Hoofdstuk 3 beschrijft een verdere analyse van de interactie van PBP2 met twee paraloge plant-specifieke microtubule motoreiwitten, PBP2 Bindend Kinesine 1 en -2 (PBK1 en -2). De PBKs bleken specifiek aan de TAZ bevattende C-terminus van PBP2 te binden. Een belangrijk onderdeel van de analyses betrof het aannemelijk maken dat PID, PBP2 en de PBKs een complex kunnen vormen. De drie eiwitten bleken inderdaad in dezelfde weefsels tot expressie te komen, en protoplasttransformaties met GFP-eiwitfusies toonden aan dat de drie eiwitten co-lokaliseren in het cytoplasma. Overexpressie van PBK1 leidde tot een significante

verhoging van het aantal zaailingen met drie zaadlobben, een fenotype dat kenmerkend is voor *pid* verlies-van-functie mutanten. Op basis van de eerdere observatie dat PBP2 werkt als een negatieve regulator van PID activiteit, veronderstellen we dat de PBKs betrokken zijn bij het transport van PBP2, om daarmee de PID activiteit op subcellulair niveau te onderdrukken, en daarmee polariteit te geven aan de signaaltransductie van dit kinase.

Voor een aantal dierlijke transporters is bekend dat hun subcellulaire lokalisatie gereguleerd wordt door fosforylering van aminozuurresiduen in een cytoplasmatisch domein van deze membraaneiwitten. In **hoofdstuk 4** is de mogelijkheid onderzocht dat fosforylering van de PINs zelf deze eiwitten markeert voor lokalisatie aan de apicale celpool. Zes van de acht Arabidopsis PIN eiwitten bevatten een groot cytoplasmatisch domein dat aan weerszijde geflankeerd wordt door de transmembraanregio's. Door middel van *in silico* analyse en *in vitro* fosforylatie-assays kon achterhaald worden, dat PIN eiwitten waarschijnlijk door PID op een viertal geconserveerde serine residuen in dit cytoplasmatische domein gefosforyleerd worden. Opmerkelijk was dat de twee serines die *in vitro* de sterkste fosforylering laten zien, zich bevinden in twee TPRXSN motieven die geconserveerd zijn tussen de zes Arabidopsis PIN eiwitten met een grote cytoplasmatische loop. Op dit moment worden mutante *PIN1::PIN1-GFP* fusieconstructen gegenereerd waarin de specifieke serine residuen vervangen zijn door een alanine of een glutaminezuur, waarmee fosforyleren voorkomen of juist nagebootst wordt. Door transgene Arabidopsis lijnen met deze constructen te maken, kan *in planta* worden getest wat het effect van fosforylering is op de subcellulaire lokalisatie van PIN eiwitten. Hopelijk wordt daarmee een belangrijk aspect van het moleculaire mechanisme achter de PID-afhankelijke PIN polariteit opgehelderd.

Polair auxine transport zorgt voor een differentiële verdeling van dit hormoon in weefsels en organen, en de cellulaire auxine concentraties worden vervolgens door een complexe en celspecifieke interactie tussen de ARF transcriptiefactoren en de labiele Aux/IAA repressoreiwitten vertaald in een primaire respons in genexpressie. De cellulaire niveaus van de labiele Aux/IAA repressoreiwitten worden daarbij onderdrukt door auxine geïnduceerde, SCF^{TIR1} E3-ligase-afhankelijke proteolyse, een proces dat positief gereguleerd wordt door het COP9 signalosoom (CSN).

Hoofdstuk 5 beschrijft de identificatie van CSN subeenheid CSN8/COP9 als interacterende partner van PID. Een opmerkelijke vinding daarbij was dat niet CSN8, maar de daarmee interacterende subeenheid CSN7/COP15 *in vitro* door PID gefosforyleerd wordt. De observatie dat Arabidopsis zaailingen waarin PID tot overexpressie is gebracht een aantal fenotypes vertonen die vergelijkbaar zijn met de constitutieve fotomorfogenese fenotypes van *csn* mutanten, suggereert dat PID mogelijk als een negatieve regulator van het CSN complex functioneert. Als CSN-

geassocieerd kinase zou PID echter ook de interactie tussen en het E3 ligase en een proteolyse target kunnen reguleren. In *in vitro* reacties kon inderdaad worden aangetoond, dat de Aux/IAA repressor BODENLOS(BDL)/IAA12 door PID gefosforyleerd wordt, waarschijnlijk op de serine in het PRXS motief dat zich vlak naast het SCF^{TIR1} interacterende domein II bevindt. Analyse van de *pid/bdl* dubbelmutant en transiënte expressie-experimenten in Arabidopsis protoplasten gaven belangrijke *in vivo* aanwijzingen dat PID waarschijnlijk de stabiliteit van zowel BDL/IAA12 als de paraloog IAA13 negatief reguleert, en daarmee de auxine responsieve genexpressie gedurende embryogenese stimuleert.

De rol van PID als CSN-geassocieerd kinase en als negatieve regulator van BDL/IAA12 en IAA13 behoeft verder onderzoek. Onze resultaten suggereren dat het PID kinase een schakel vormt tussen het polaire transport en de signaaltransductie van het belangrijke plantenhormoon auxine.

Curriculum vitae

Marcelo Kemel Zago was born on November 19th 1976 in Porto Alegre, State of Rio Grande do Sul (RS), Brazil. He attended high school at the Instituto Educacional João XXIII in Porto Alegre. In 1995 he started the study of Biological Sciences at the Federal University of Rio Grande do Sul (UFRGS) in Porto Alegre. From April 1996 until April 1997, he dedicated himself to a research training in molecular biology and mutagenesis in yeast in the Biophysics Department at UFRGS under the supervision of Dr. João Antônio Pêgas Henriques. From July 1997 until March 1999 he was involved in research related to molecular biology of *Eucalyptus spp.* as a research trainee at the Molecular Biology and Biotechnology Department at UFRGS under the supervision of Dr. Giancarlo Pasquali. In April 1999 he obtained his BSc degree in Biology. As a MSc student he was involved in the project "Isolation and characterization of the gene encoding the Cinnamoyl CoA Reductase (CCR) enzyme from *Eucalyptus saligna*" at the Post-Graduation Program in Cellular and Molecular Biology at UFRGS under the supervision of Dr. Giancarlo Pasquali. In March 2001 he obtained his MSc degree in Cellular and Molecular Biology. In August 2001 he was awarded with a grant from CAPES (Brazilian Federal Agency for Post-Graduate Education) for his PhD project and in March 2002 he started his PhD research under the supervision of Dr. Remko Offringa and Prof. Dr. Paul Hooykaas at the Institute of Biology at Leiden University, Leiden, The Netherlands.

Publications

Endt, D. V., Costa, P., Zago, M. K., Bodanese-Zanettini, M. H., Pasquali, G. Genes de lignificação: em busca do eucalipto transgênico com reduzidos teores de ligninas (Lignification genes: looking for the transgenic eucalypt with reduced lignin content, article in Portuguese). *Biotecnologia Ciência & Desenvolvimento*, year 3, number 15, july/august 2000.

Zago, M. K., de Felippes, F. F., Perini, P. , Endt, D. V., Lopes, O. R., Colodette, J. L., Bodanese-Zanettini, M. H., Pasquali, G. The cinnamoyl-CoA reductase gene (CCR) from *Eucalyptus saligna*: cloning, characterization and transgenic expression in *Nicotiana tabacum*. *Plant Science*, Submitted.

Acknowledgements

or

Thank you! – Valeu!

This acknowledgement section was written as the very final portion of this thesis, which is the result of more than four years of research that was only feasible with the help of many people.

I am very grateful to all people at Clusius that somehow participated in my research. In special, I would like to thank the “auxin group” – Ab, Adam, Carlos, Fang, Helene, Werner and students – for helping me with all kinds of things in the lab and for the fruitful scientific discussions. It was a lot of fun to work with you. My student Douwe, for the great help with important experiments and the opportunity you gave me to learn more about the job of teaching. Peter Hock, for the excellent art work, in spite of all the “final” modifications I asked you to do. My very special Spanish speaking friends Esmeralda and Fernando, for the help with my initial adaptation to this strange country, and also for all the fun we could have and for the assistance with all sort of lab-related and -unrelated things. Joy & Carlos, for the nice chats and moments we spent (and still spend) playing sports. Felipe, for the special occasions when we could finally speak “Brazilian” and talk about the things we miss from Brazil and also for the southern-Brazilian – and nicely familiar - atmosphere you bring to the lab and outside the lab. Valeu, tchê!

Although all these people crucially contributed to the development of this thesis, this accomplishment would have not been possible without the essential support of all people that are in Brazil. Giancarlo, thank you for opening the door that allowed me to do my research in Holland. Tua sempre inspiradora orientação teve um peso enorme nessa conquista! Debora, thanks for making my adaptation to this new culture so much easier. Se não fosse por ti, aqueles primeiros meses em Leiden teriam sido tão mais complicados! Tio Neron and Tia Sirlei, thanks for always being there! Vocês sempre serão muito especiais pra mim. Pai, mãe, Maninho, Déia, Coroa and Nara, thanks for being so supportive and present in spite of all the distance that separated us. You are a wonderful family! Não dá nem pra descrever a saudade que eu senti de vocês! Finally, but most importantly, Sheilinha, without you nothing of this would have been possible. You were the one who kept me going. Tu sempre serás a minha maior inspiração!

